

FEDERAL UNIVERSITY OF TECHNOLOGY OF PARANÁ  
GRADUATE SCHOOL OF ELECTRICAL ENGINEERING AND INDUSTRIAL  
COMPUTER SCIENCE

EDUARDO MUSSOI ESSER

**DESIGN AND DEVELOPMENT OF AN ELECTRONIC SYSTEM FOR THE  
SELECTIVE STIMULATION AND SIMULTANEOUS MEASUREMENT OF  
THE SKIN IMPEDANCE**

DISSERTATION

CURITIBA

2011



EDUARDO MUSSOI ESSER

**DESIGN AND DEVELOPMENT OF AN ELECTRONIC SYSTEM FOR THE  
SELECTIVE STIMULATION AND SIMULTANEOUS MEASUREMENT OF  
THE SKIN IMPEDANCE**

This dissertation was presented to the Graduate School of Electrical Engineering and Industrial Computer Science (CPGEI) at the Federal University of Technology of Paraná as a requirement for obtaining the title of Master of Science – Biomedical Engineering.

Supervisor: Prof. Ph.D. Humberto Gamba  
Co-supervisor: Dr. Dipl.-Ing. Phuc Nguyen

CURITIBA

2011

---

Dados Internacionais de Catalogação na Publicação

---

E78 Esser, Eduardo Mussoi  
Design and development of an electronic system for the selective stimulation and simultaneous measurement of the skin impedance / Eduardo Mussoi Esser. — 2010.  
145 p. : ill. ; 30 cm

Orientador: Humberto Remígio Gamba

Co-orientador: Phuc Nguyen

Dissertação (Mestrado) – Universidade Tecnológica Federal do Paraná. Programa de Pós-graduação em Engenharia Elétrica e Informática Industrial. Área de concentração: Engenharia Biomédica, Curitiba, 2010.

Bibliografia: p. 143-145

1. Estimulação elétrica transcutânea do nervo. 2. Estimulação neural. 3. Impedância bioelétrica. 4. Eletrofisiologia 5. Tecidos (anatomia e fisiologia) – Análise. 5. Engenharia elétrica – Dissertações. I. Gamba, Humberto Remígio, orient. II. Nguyen, Phuc, co-orient. Universidade Tecnológica Federal do Paraná. Programa de Pós-graduação em Engenharia Elétrica e Informática Industrial. III. Título.

CDD (22. ed.) 621.3

---

Biblioteca Central da UTFPR, Campus Curitiba

**Dissertação Nº 550**

**Double Master's Degree Dissertation #01**

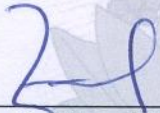
**Agreement of Cooperation with Mannheim University of Applied Sciences**

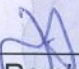
**“Design and development of an electronic system  
for the selective stimulation and simultaneous  
measurement of the skin impedance”**

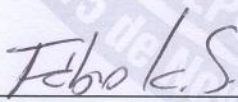
por

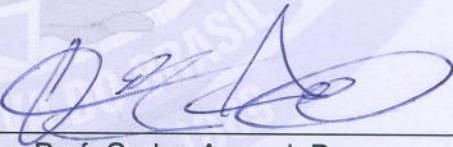
**Eduardo Mussoi Esser**

Esta dissertação foi aprovada como requisito parcial para a obtenção do grau de MESTRE EM CIÊNCIAS – Área de Concentração: Engenharia Biomédica, pelo Programa de Pós-Graduação em Engenharia Elétrica e Informática Industrial da Universidade Tecnológica Federal do Paraná, no dia 11 de fevereiro de 2011.

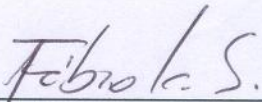
  
\_\_\_\_\_  
Prof. Albrecht Zwick, Dr.  
(University of Applied Science of  
Mannheim)

  
\_\_\_\_\_  
Prof. Humberto Remigio Gamba, Dr.  
(Presidente – UTFPR)

  
\_\_\_\_\_  
Prof. Fábio Kurt Schneider, Dr.  
(UTFPR)

  
\_\_\_\_\_  
Prof. Carlos Amaral, Dr.  
(UTFPR)

Visto da coordenação:

  
\_\_\_\_\_  
Prof. Fábio Kurt Schneider, Dr.  
(Coordenador do CPGEI)



## ACKNOWLEDGEMENT

I would like to thank all the people that somehow helped me to carry out this project and that encouraged and supported me during my studies in Germany. Especially I would like to name:

My family in Brazil for all the personal support, which despite the distance was essential for me;

Phuc Ngyen, my supervisor in Germany, for all the attention and technical orientation during the development of this project;

Humberto Gamba, my supervisor in Brazil, and professor Zwick from the *Hochschule Mannheim*, for having the great idea and initiative of starting the double degree program and the partnership between Brazil and Germany. Thank you for giving me the opportunity to be the first student to participate and graduate on this program;

Paola Luparelli, for all patience she had reviewing this text;

All my colleagues and friends from the master course and from the laboratory, which helped me discussing ideas or participating on the tests.





## ABSTRACT

ESSER, Eduardo Mussoi. **Design and development of an electronic system for the selective stimulation and simultaneous measurement of the skin impedance.** 2011. 145f. Master's dissertation in Biomedical Engineering – Graduate School of Electrical Engineering and Applied Computer Sciences, Federal University of Technology of Paraná. Curitiba, 2011.

It has been found that electrical current applied to the human skin stimulates some of the peripheral nerves and fibers of the human body, causing several reactions such as the increase of sweat production. Moreover the analyses of such reactions can be used to diagnose some diseases, for example diabetes. Nevertheless, most of the electrical stimulation devices, which use mostly square wave signals, are not optimal since they stimulate not only the desired glands (C-fiber) but also the A $\delta$ -fibers of the body, responsible for the fast pain sensation. In this context, this work presents the development of a microcontroller based electronic system for controlling the electrical stimulation of human skin. The objective of the system was to make it possible to test different patterns of electric current pulses, in order to obtain the ideal shape for maximizing the desired stimulation effects with minimal pain. The result of the project was an electronic device that generates electrical pulses based on pre-programmed signals, which are received through a USB interface from a PC. Moreover the system was able to measure the skin impedance value during the electrical stimulation, complementing the diagnosis. The results of the tests carried out with the system showed that the pain intensity during the stimulation could be minimized according to the pulse shape not changing the amplitude and energy of the signal. Moreover a slight difference in the skin impedance was observed when different shapes were applied.

**Keywords:** Electrical Skin Stimulation. Skin Impedance Measurement. Signal Generation and Acquisition. Biomedical Diagnosis Systems.



## RESUMO

ESSER, Eduardo Mussoi. **Projeto e desenvolvimento de um sistema eletrônico para estimulação seletiva e medição simultânea da impedância da pele.** 2011. 145f. Dissertação de mestrado em Engenharia Biomédica – Programa de Pós-Graduação em Engenharia Elétrica e Informática Industrial, Universidade Tecnológica Federal do Paraná. Curitiba, 2011.

A aplicação de corrente elétrica na pele humana estimula alguns dos nervos periféricos e fibras do corpo humano, causando diversas reações tais como o aumento da produção de suor. Além disso, a análise dessas reações pode ser usada para diagnosticar doenças como diabetes. No entanto, grande parte dos aparelhos de estimulação elétrica comerciais utilizam sinais de onda quadrada. Esses sinais não são ideais uma vez que estimulam não somente as glândulas desejadas (fibras C), mas também as fibras A-delta do corpo, responsáveis pela sensação rápida de dor. Neste contexto, este trabalho apresenta o desenvolvimento de um sistema eletrônico para controlar a estimulação elétrica da pele humana. O objetivo do sistema é tornar possível o teste diferentes padrões de pulsos de corrente elétrica, a fim de obter a forma ideal para maximizar os efeitos desejados com um mínimo de dor. Como resultado do projeto tem-se o desenvolvimento de um dispositivo eletrônico microcontrolado que gera pulsos elétricos baseados em sinais pré-programados recebidos de um PC via USB. Além disso, o sistema é capaz de medir o valor da impedância da pele durante a estimulação elétrica, o que pode complementar o processo de diagnóstico. Os resultados dos testes realizados com o sistema mostraram que a intensidade da dor durante a estimulação pode ser minimizada apenas com a forma do pulso, sem a alteração da amplitude e da energia do sinal. Além disso, uma pequena diferença na impedância da pele foi observada quando diferentes formas de onda foram aplicadas.

**Palavras-Chave:** Estimulação elétrica da pele. Medição da impedância da pele. Geração e aquisição de sinais. Sistemas de diagnóstico.



## LIST OF FIGURES

|   |    |
|---|----|
| Figure 1 – Simplified Block Diagram of the Stimulation System .....   | 18 |
| Figure 2 – Representation of the A $\delta$ and C fibers and the pain intensity. ....   | 20 |
| Figure 3 – Typical QTsignal for selective stimulation used by SEIF (2001).....  | 22 |
| Figure 4 – (a) Debye circuit with ideal components. (b) Cole circuit with the ideal capacitor replaced by a CPE with frequency-dependent components. .... | 23 |
| Figure 5 – Variations of electric skin resistance on forearm using conductive paste with different concentrations of NaCl .....                           | 25 |
| Figure 6 – Example of commercial Silver-silver chloride (Ag/AgCl) electrode .....   | 27 |
| Figure 7 – Skin surface electrode geometry and its equivalent electric model at 10 Hz....   | 28 |
| Figure 8 – Hardware development process .....   | 38 |
| Figure 9 – Firmware development process based on the V-model process. ....  | 39 |
| Figure 10 – Block overview of the stimulation system architecture.....  | 42 |
| Figure 11 – Picture of the microcontroller.....   | 43 |
| Figure 12 – Block diagram of the SAM3U4E.....   | 43 |
| Figure 13 – Core pins, JTAG and power supply of the microcontroller. ....   | 46 |
| Figure 14 – USB and ADC pins.....   | 47 |
| Figure 15 – Pins and connector to the analog board as well as power supply connectors. ....   | 47 |
| Figure 16 – Top layer of the digital board layout .....   | 48 |
| Figure 17 – Bottom layer of the digital board layout.....   | 49 |
| Figure 18 – Settling time of a digital-to-analog converter. ....  | 52 |
| Figure 19 – Block diagram of the LTC1666 internal circuit.....  | 53 |
| Figure 20 – Differential output current of the LTC1666 as a function of the DAC code. ....  | 54 |
| Figure 21 – Example circuit for an arbitrary waveform generator with $\pm 10V$ output.....  | 55 |
| Figure 22 – Differential current to voltage amplifier with 2 <sup>nd</sup> order low pass filter. ....  | 56 |
| Figure 23 – Output voltage for a DAC sinusoidal differential output current .....   | 57 |
| Figure 24 – Frequency response of the low-pass filter.....  | 58 |
| Figure 25 – DAC Schematic and current to voltage converter .....  | 58 |
| Figure 26 – Low-pass filter and output buffers schematics .....   | 59 |
| Figure 27 – Block diagram of the signal conditioning circuit. ....  | 60 |
| Figure 28 – High-impedance voltage divider and shunt resistor for sampling the skin (Load) stimulation signals (voltage and current). ....                | 61 |
| Figure 29 – High input-impedance voltage follower and pre-amplifier. ....   | 62 |
| Figure 30 – PGA simulation schematic and internal block diagram. ....   | 64 |
| Figure 31 – Low-pass Bessel filter. ....  | 66 |
| Figure 32 – Frequency response before (red) after (green) the low-pass filter.....  | 67 |
| Figure 33 – Adder for offset compensation. ....   | 68 |
| Figure 34 – Effect of the protection Schottky diodes.....   | 69 |
| Figure 35 – Frequency response of the entire signal conditioning circuit .....  | 69 |
| Figure 36 – Buffer and pre amplifier .....  | 70 |
| Figure 37 – PGA and low pass filter .....   | 71 |
| Figure 38 – Offset compensation and Schottky diodes for protection.....   | 71 |
| Figure 39 – Functional block diagram of the AD5933 .....  | 72 |
| Figure 40 – Pin configuration of the AD5933.....  | 73 |
| Figure 41 – Schematic of the AD5933.....  | 75 |
| Figure 42 – 3.3V Linear Voltage Regulator .....   | 76 |

|  |     |
|--|-----|
| Figure 43 – Switching mode power supply to generate -5V from +5V .....   | 77  |
| Figure 44 – Top layer and top overlay of the analog board. ....  | 78  |
| Figure 45 – Bottom layer of the analog board. ....   | 78  |
| Figure 46 – Use case diagram of the firmware .....   | 80  |
| Figure 47 – General state chart of the firmware.....   | 81  |
| Figure 48 – State flow of the Setup state. ....  | 82  |
| Figure 49 – State chart of the system initialization.....  | 84  |
| Figure 50 – State chart of the impedance measurement state .....   | 85  |
| Figure 51 – Flow chart of the impedance measurement.....   | 87  |
| Figure 52 – Example of received buffers and how they are used to generate a pulse .....                                    | 89  |
| Figure 53 – Input DAC code and output current.....   | 89  |
| Figure 54 – State chart of the interrupt sources .....   | 92  |
| Figure 55 – State chart representing the signal generation task.....   | 93  |
| Figure 56 – Representation of the transmit buffer: in every cycle four bytes are saved in the buffer until it is full..... | 94  |
| Figure 57 – State chart of the signal acquisition .....  | 95  |
| Figure 58 – USB Received Data interrupt handler state diagram .....  | 95  |
| Figure 59 – Signal buffer with the samples of the skin signals.....  | 97  |
| Figure 60 – Structures of the data buffers.....  | 99  |
| Figure 61 – Sequence diagram of the entire system.....   | 100 |
| Figure 62 – State chart of the HMI .....   | 107 |
| Figure 63 – Main menu of the skin stimulator HMI.....  | 108 |
| Figure 64 – Setup connection window.....   | 109 |
| Figure 65 – Main menu after connecting to the microcontroller. ....  | 109 |
| Figure 66 – Single frequency impedance measurement.....  | 110 |
| Figure 67 – Interface after a sweep frequency measurement.....   | 111 |
| Figure 68 – Set signal window with the QT-Signal signal loaded.....  | 112 |
| Figure 69 – Main menu after during the idle state.....   | 113 |
| Figure 70 – Stimulation window for stimulation control .....   | 114 |
| Figure 71 – Example of the stimulation window during a stimulation process. ....   | 115 |
| Figure 72 – Front panel of the Digitmer DS5.....   | 117 |
| Figure 73 – Picture of the DS5 used on the experiments.....  | 117 |
| Figure 74 – Ag/AgCl electrodes used on the experiments .....   | 118 |
| Figure 75 – Back view of the Digitmer DS5.....   | 118 |
| Figure 76 – Digital board .....  | 119 |
| Figure 77 – Analog board .....   | 120 |
| Figure 78 – Digital board, analog board and connections.....   | 120 |
| Figure 79 – Impedance measurement of a 10K resistor from 5KHz to 100KHz. ....  | 122 |
| Figure 80 – Forearm front skin impedance measurement (5KHz to 100KHz) .....  | 123 |
| Figure 81 – 1KHz square wave before (red) and after (blue) the filter. ....  | 125 |
| Figure 82 – Square wave in details. ....   | 125 |
| Figure 83 – Pulsed square wave before (red) and after (blue) the filter.....   | 126 |
| Figure 84 – Pulsed square wave in details.....   | 126 |
| Figure 85 – 20 Hz pulsed square wave.....  | 127 |
| Figure 86 – QT-signal before (red) and after (blue) the filter.....  | 128 |
| Figure 87 – QT-signal in details.....  | 128 |
| Figure 88 – 20Hz QT-signal. ....   | 129 |
| Figure 89 – Input signal (red) and after the unitary gain pre-amplifier and 8V/V gain PGA (yellow). ....                   | 130 |
| Figure 90 – Signal before (red) and after (yellow) the low-pass filter.....  | 130 |
| Figure 91 – Signal before the filter (red) and after the 1.65V offset compensation (yellow).                               |     |

|   |     |
|---|-----|
| .....   | 131 |
| Figure 92 – Signal at the input (red) and output (yellow) of the signal measurement block   | 131 |
| .....   | 131 |
| Figure 93 – Skin current (red) and voltage (yellow) signals during the stimulation process. | 132 |
| .....   | 132 |
| Figure 94 – Picture of the system operation during the tests.....                           | 133 |
| Figure 95 – Average of the human body sensibility for the square and QT pulses .....        | 136 |
| Figure 96 – Skin impedance value measured during the stimulation.....                       | 138 |

## LIST OF TABLES

|  |     |
|--|-----|
| Table 1 – Site dependence of skin impedance ( $k\Omega cm^2$ ) at 10 Hz for 12cm <sup>2</sup> electrodes.<br>Initial values and values obtained after two intervals of 2 hours ..... | 24  |
| Table 2 – Initial impedance dependence on frequency for different skin sites .....   | 24  |
| Table 3 – Electrodes conductor materials .....   | 26  |
| Table 4 – Two experiments showing the problems of resolution when using constant gain.<br>.....  | 35  |
| Table 5 – Summary of the most relevant requirements of the stimulation system .....  | 41  |
| Table 6 – Pin map of the digital – analog board connector.....   | 45  |
| Table 7 – Maximal gain for each measuring circuit considering a constant 50k $\Omega$ load and<br>maximum final amplitude of 3.3Vpp. ....  | 64  |
| Table 8 – Gain settings and properties of the LTC6910-2 PGA. ....  | 65  |
| Table 9 – Description of the AD5933's pins. ....   | 74  |
| Table 10 – IO Configuration Table .....  | 83  |
| Table 11 – Registers to be configured in the initialization state.....   | 86  |
| Table 12 – Control Register Map (D15 to D12) of the AD5933 .....   | 86  |
| Table 13 – Relationship between the absolute skin maximal voltage and current levels and<br>the PGA's gains. ....  | 90  |
| Table 14 – Headers and commands of the communication protocol.....   | 98  |
| Table 15 – Impedance measurement for a 10kHz single frequency point measurement. ....  | 122 |
| Table 16 – Skin impedance measurement for a 10kHz single frequency point<br>measurement. ....  | 124 |
| Table 17 – Results of the pain intensity measurement.....  | 135 |
| Table 18 – Results of the impedance variation test.....  | 137 |



# TABLE OF CONTENTS

|          |  |           |
|----------|--|-----------|
| <b>1</b> | <b>INTRODUCTION.....</b>                         | <b>15</b> |
| 1.1      | MOTIVATION .....                                 | 15        |
| 1.2      | OBJECTIVES .....                                 | 16        |
| 1.3      | SYSTEM BLOCK DIAGRAM .....                       | 17        |
| 1.4      | STRUCTURE OF THE DISSERTATION.....               | 18        |
| <b>2</b> | <b>THEORETICAL FOUNDATIONS.....</b>              | <b>19</b> |
| 2.1      | INTRODUCTION .....                               | 19        |
| 2.2      | ELECTRICAL SKIN STIMULATION .....                | 19        |
| 2.2.1    | Parameters of the Stimulation .....              | 19        |
| 2.2.2    | Electrical Features of Human Skin .....          | 22        |
| 2.2.3    | Electrodes.....                                  | 26        |
| 2.3      | MICROCONTROLLERS.....                            | 29        |
| 2.3.1    | Important Features .....                         | 29        |
| 2.3.2    | Requirements for Digital Signal Processing ..... | 30        |
| 2.4      | LARGE VOLTAGE RANGE SIGNAL CONDITIONING .....    | 33        |
| 2.4.1    | Issues of the Fixed Gain Amplifier .....         | 34        |
| 2.4.2    | Programmable Gain Amplifier (PGA).....           | 35        |
| <b>3</b> | <b>THE STIMULATION SYSTEM DESIGN .....</b>       | <b>37</b> |
| 3.1      | INTRODUCTION .....                               | 37        |
| 3.2      | TOOLS AND METHODS .....                          | 37        |
| 3.2.1    | Hardware development .....                       | 37        |
| 3.2.2    | Firmware development .....                       | 38        |
| 3.3      | SYSTEM REQUIREMENTS .....                        | 40        |
| 3.4      | SYSTEM ARCHITECTURE .....                        | 41        |
| 3.5      | THE MICROCONTROLLER BOARD.....                   | 42        |
| 3.5.1    | Microcontroller Overview .....                   | 42        |
| 3.5.2    | Digital Board Description .....                  | 44        |
| 3.5.3    | Schematics .....                                 | 46        |
| 3.5.4    | Digital Board Layout .....                       | 48        |
| 3.6      | THE ANALOGUE BOARD .....                         | 50        |
| 3.6.1    | The D/A Converter .....                          | 50        |
| 3.6.2    | Signal Measurement Circuit .....                 | 59        |
| 3.6.3    | Impedance Measurement.....                       | 72        |
| 3.6.4    | The Power Supply .....                           | 75        |
| 3.6.5    | Layout of the Analog Board .....                 | 77        |

|       |  |     |
|-------|--|-----|
| 3.7   | FIRMWARE OF THE STIMULATION SYSTEM .....       | 79  |
| 3.7.1 | Requirements Definition .....                  | 79  |
| 3.7.2 | Firmware Design .....                          | 80  |
| 3.7.3 | Implementation .....                           | 101 |
| 3.8   | HUMAN MACHINE INTERFACE (HMI) .....            | 107 |
| 3.8.1 | Setup Connection .....                         | 108 |
| 3.8.2 | Impedance Measurement.....                     | 110 |
| 3.8.3 | Set signal.....                                | 112 |
| 3.8.4 | Idle.....                                      | 113 |
| 3.8.5 | Stimulation.....                               | 113 |
| 4     | <b>SYSTEM INTEGRATION AND VALIDATION</b> ..... | 116 |
| 4.1   | HARDWARE INTEGRATION .....                     | 116 |
| 4.1.1 | The external source.....                       | 116 |
| 4.1.2 | Prototype .....                                | 119 |
| 4.2   | SYSTEM VALIDATION .....                        | 121 |
| 4.2.1 | Impedance Measurement.....                     | 121 |
| 4.2.2 | Signal Generation.....                         | 124 |
| 4.2.3 | Signal Measurement.....                        | 129 |
| 4.2.4 | Stimulation.....                               | 132 |
| 5     | <b>TESTS AND RESULTS</b> .....                 | 133 |
| 5.1   | PAIN INTENSITY TEST .....                      | 134 |
| 5.1.1 | Methods.....                                   | 134 |
| 5.1.2 | Results of the Pain Intensity Test .....       | 135 |
| 5.2   | IMPEDANCE VARIATION TEST .....                 | 136 |
| 5.2.1 | Methods.....                                   | 136 |
| 5.2.2 | Results of the Impedance Variation Test .....  | 137 |
| 5.3   | DISCUSSION.....                                | 138 |
| 6     | <b>CONCLUSIONS</b> .....                       | 140 |
| 6.1   | FUTURE WORK .....                              | 141 |
|       | <b>REFERENCES</b> .....                        | 143 |

# CHAPTER 1

## INTRODUCTION

This project was developed at the Institute for Biomedical Engineering at the *Hochschule Mannheim* in Germany, in partnership with the Graduate School of Electrical Engineering and Industrial Computer Science (CPGEI) at the Federal University of Technology – Paraná, Brazil. It is part of a research in the area of electrical skin stimulation for purpose of diagnosing diseases and studying the human neuronal system.

### 1.1 MOTIVATION

The study of the human body reactions to electrical stimulation of the skin and the peripheral nerves has a promising future in the medicine field, mainly for diagnosing and preventing diseases in a fast and non-invasive way.

The diagnosis of several diseases that affect the population worldwide is nowadays based on invasive methods such as blood tests. Diabetes, for example, is characterized by recurrent or persistent hyperglycemia (excessive amount of glucose in the blood plasma), which can be detected through different methods of blood analyses (WHO, 1999). However, a positive result, in the absence of unequivocal hyperglycemia should be confirmed by repeating any of the methods on a different day. All these processes make the diagnosis not only time consuming but also invasive for the patient. Hence there is a need for a fast non-invasive method for diagnosing diseases such as diabetes. Moreover it has been found that the stimulation of human skin by faradic current pulses causes secretion of sweat in the vicinity of the applied signal (WILKINS, 1938). Furthermore, it is known that diabetes can damage sympathetic nerves and sweat glands. The release of neurotransmitters facilitating vasodilatation at the blood vessel or the sweat glands is also impaired and if they are not released effectively, the production of nitric oxide (NO) is diminished, vasodilatation is impacted and sweat responses are also reduced. Thus, patients with

diabetes have lowered sweat rates and with moderate fiber damage the sweat response may be lost (PETROFSKY, 2008). As a result, the analysis of the sweat response to electrical stimulation can be used to diagnose diabetes.

Nevertheless most of the usual electrical stimulation devices use symmetrical pulse shapes, mostly generating either sine or square waves, which are not optimal signals to stimulate the human skin (SEIF, 2001). These signals stimulate not only the C-fibers of the body, responsible for the sweat production among other functions, but also the A $\delta$ -fibers, which are responsible for the fast pain sensation (QUATTRINI, 2004). Therefore, other signal shapes could be applied to obtain a selective stimulation of those fibers.

Furthermore, an arbitrary signal generation for skin stimulation can be also applied for many other medical applications beyond diagnosing diabetes. A stimulation device with such features can be applied for diagnosing and also for treating several neuropathies, which are usually called Clinical Nerve Excitability Tests (cNET). As example of neuropathies one may list: carpal tunnel syndrome (CTS), amyotrophic lateral sclerosis (ALS), multifocal motor neuropathy (MMN), motor neuron disease (MND), Neuromyotonia (NMT) among others. Another possible application is detecting neuronal response in human brain after an electrical stimulation, such as evoked potentials, using electroencephalogram (EEG) devices. This study is important in neuronal sciences for better understanding how electrical signals propagate and which effects they might cause on the human body.

In this context, the need for a stimulation system able to generate several signal patterns in order to find out the ideal pulse shape that maximizes the desired stimulation effects with minimal pain is therefore the major motivation for this project.

## 1.2 OBJECTIVES

The main purpose of this work was to develop a microcontroller based electronic system for controlling the electrical stimulation of the human skin. This device should be able to generate arbitrary signals loaded from a host computer to stimulate the skin with help of external current sources. Moreover the system should measure the current and voltage levels of the skin during the stimulation. The

measurement of the skin impedance value is also an important step of the project.

More specifically the objective of this work can be divided in five topics:

1. Implement the firmware for a microcontroller to generate signals based on the data received from a host computer, acquire analog signals and transmit them back to the host;
2. Design and develop an electronic circuit to convert the stimulation digital pulse from the microcontroller to analog and transmit it to a current source for further stimulation of the human skin;
3. Design and develop an electronic circuit to measure the skin voltage and current signals during the stimulation;
4. Measure the skin impedance.
5. Compare pulse shapes in order to obtain the ideal pattern for selective stimulation of the skin;

### 1.3 SYSTEM BLOCK DIAGRAM

In this topic a block diagram of the entire system is shown for better comprehension of the objectives. The system can be divided in three major blocks, which are:

- Remote host computer: responsible for the remote control of the system and the communication between the user and the stimulation device;
- Microcontroller board: consists of a microcontroller that generates and acquires signals among other controlling and monitoring tasks;
- Analog signal board: consists of a DAC circuit that controls a voltage controlled current source to stimulate the skin and of circuits for measuring the skin current and voltage levels during the stimulation. In addition this board contains a circuit for measuring unknown impedances.

A simplified diagram of the project representing the blocks above is shown in Figure1. Details of the system architecture are presented in Chapter 3.

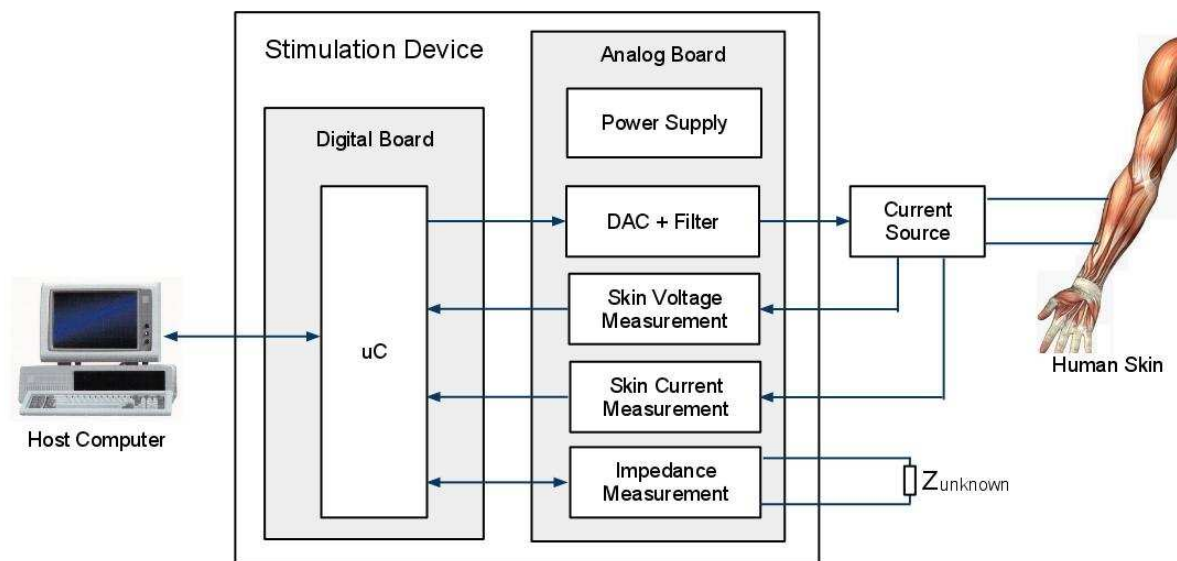


**Figure 1 – Simplified Block Diagram of the Stimulation System**

#### 1.4 STRUCTURE OF THE DISSERTATION

This document is divided into six chapters. In this first chapter an introduction to the project was presented, including the motivation, objectives and the system block diagram. Chapter 2 contains a theoretical foundation that addresses the basic theory applied in this work, reviewing some issues related to selective skin stimulation. In the third chapter the design and the implementation of the proposed device are presented, detailing the development steps for each block of the system. Furthermore, the integration of the blocks in a final solution and their validation are shown in Chapter 4. In Chapter 5 the results of some tests carried out with the system are presented as well as a discussion about them. Finally the conclusions and proposals for continued research are presented in Chapter 6.

## **CHAPTER 2**

### **THEORETICAL FOUNDATIONS**

#### **2.1 INTRODUCTION**

This chapter presents the theoretical foundations of the main topics addressed in this project. In addition it describes the most relevant aspects of some methods concerning electrical skin stimulation found in the literature. First one discusses the electrical skin stimulation, including its basic parameters, the electrical features of human skin and the different kinds of electrodes applied in biomedical applications. The following topic covers the microcontrollers, their technologies and applications, including the requirements for digital signal generation. Finally one shows the methods for measuring signals with large voltage range and their issues in analog-to-digital conversions.

#### **2.2 ELECTRICAL SKIN STIMULATION**

The electrical skin stimulation consists in applying an electric current signal in the human skin in order to stimulate certain muscles or nerves. Electrical pulse stimulation has been applied in the medical fields since the 18th century (MCNEAL, 1977). Among the many applications one can cite the treatment of several disorders such as inflammations, bleeding and nausea as well as for nerves and muscles contraction. Although different techniques have been developed for different purposes and effects on the human body, the basic principles and instruments applied are still very similar.

##### **2.2.1 Parameters of the Stimulation**

The most relevant parameters of stimulation refer to the properties of the

electric current signal. More specifically: current type (direct, alternating or pulsed current), amplitude, frequency, shape and pulse width. These parameters should be chosen according to the application and the desired stimulation effects.

It is known that direct or unidirectional pulsed current injection in the human skin can damage or irritate the tissues due to the electric charge applied on it. For this reason it is recommended the use of alternating or bidirectional pulsed current, so that all the electric charge injected during the first phase of the stimulus is completely recovered by the following phase (SCHUETTLER, 2008).

The signal frequency depends on the purpose of the stimulation. The optimal frequency for electrical stimulation is determined by the conduction velocity of the fibers to be stimulated, which means how quickly the impulses pass through the nerve (PURVES, 2004). C-fibers are unmyelinated unlike most other fibers in the nervous system and are on average 0.2-1.5  $\mu\text{m}$  in diameter. This lack of myelination is the cause of their slow conduction velocity, which is on the order of no more than 2 m/s. On the other hand, A $\delta$ -fibers have axons that are larger (1-5  $\mu\text{m}$ ) in diameter, are myelinated and have a higher conduction velocity, which is about 20 m/s (PURVES, 2004). A representation of these fibers with the relationship to the subjective pain intensity can be seen in Figure 2. The pain sensation caused by an abrupt current stimulus on the skin is mostly conducted by fast A $\delta$ -fibers.

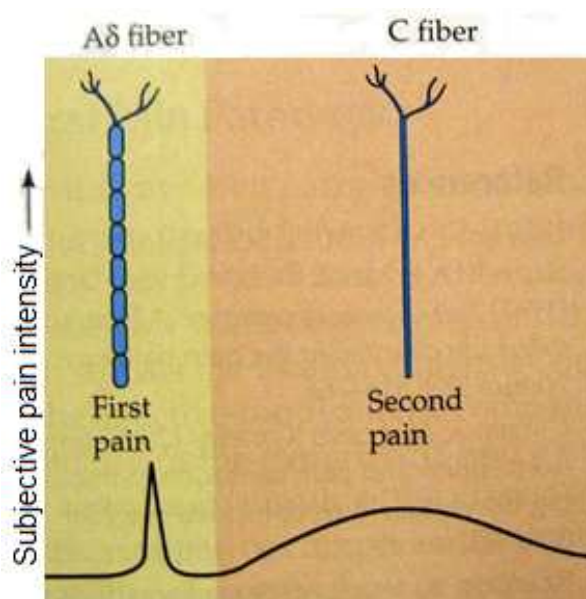


Figure 2 – Representation of the A $\delta$  and C fibers and the pain intensity.



An experiment made by QUATTRINI (2004) based on studies carried on by the American Association of Electrodiagnostic Medicine, used small electrical stimuli (max 9.99 mA) via skin surface electrodes at different frequencies to selectively quantify the response to stimulation of different-sized sensory nerve populations. It was applied 5Hz for stimulating the C-fibers, 250Hz for A $\delta$ -fibers, and 2kHz for A $\beta$ -fibers.

Considering this information most applications of electrical skin stimulation concerning muscles or nerves make use of relatively low frequency signals. More specifically for selective stimulation of C-fibers, minimizing the pain sensation, frequencies not higher than 200Hz are applied. The most usual values are either 20Hz or 50Hz (SCHUETTLER, 2008 and SEIF, 2001).

Not only the frequency but also the pulse shape has a great relevance for the final results of the fiber stimulation. This shape includes also the pulse width and amplitude levels of the current signal. The determination of these parameters is one of the main purposes of this project. Previous stimulation experiments have already been carried out to find the best combination of these features for several medical applications. Moreover most of them focus only on the pulse width and amplitude, using sine or square waves, but not on the pulse shape itself (CHRONI, 2006).

A study about the ideal pulse pattern for selective neuronal stimulation of C-fibers aiming urinary bladder stimulation was successfully carried out by SEIF (2001). Different pulse patterns were tested at 20Hz, varying also the maximum amplitude (0-2mA), in order to determine the most suitable parameters. According to the experiments, the best pulse shape for blocking A $\delta$ -fibers stimulation was a quasi-trapezoidal signal (QT-signal) which is represented in Figure 3. As a normal square pulse it has an abrupt level transition from 0 to a negative maximum value and holds this value for about 500 $\mu$ s to 2ms. This transition is responsible for the fibers stimulation. After that, instead of suddenly rising, the signal should rise slowly for another 500 $\mu$ s to 2ms until it comes back to zero. This gradual rise is responsible for blocking the fast A $\delta$ -fibers that cause the first pain sensation. Moreover, in order to recover the charge applied during the negative phase, a very low positive trapezoidal pulse should be applied in the sequence. Both rising and falling time are 100 $\mu$ s and the current value should be no more than 100 $\mu$ A, not to stimulate any fiber. The duration of the positive pulse must be calculated based on the peak negative value so that the total negative and positive signal area (negative and positive charges) are

always the same.

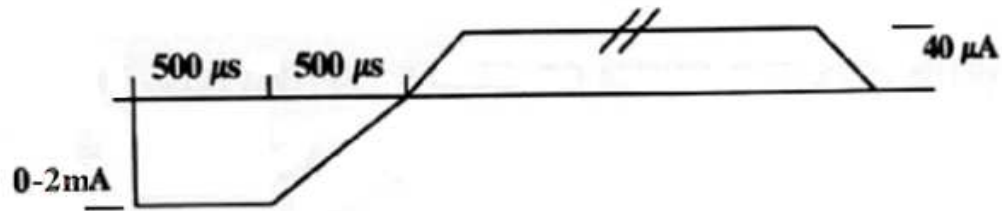
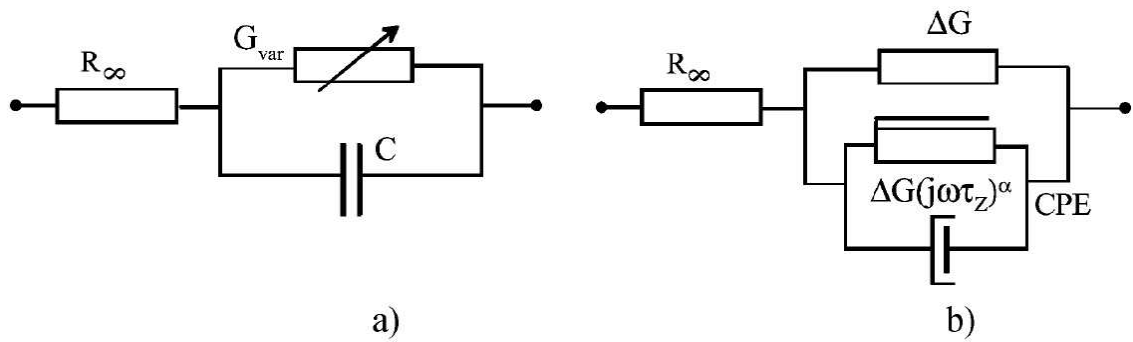


Figure 3 – Typical QTsignal for selective stimulation used by SEIF (2001).

### 2.2.2 Electrical Features of Human Skin

In an electrical stimulation circuit the skin plays the role of load. Therefore, an important step for designing the stimulator's electronic circuit is to determine some electrical features of the human skin such as the impedance value range. Nevertheless the skin impedance is known to be non-linear and is a function of many factors including the intensity, duration, and frequency of the applied stimulus (LOCHNER, 2003). Moreover the skin impedance is affected by the electrode type and coupling medium and can also vary according to the skin site, temperature and humidity.

Many studies attempted to develop an electrical model for the human skin and one of the most well known is the Cole impedance model, proposed in its final form by Kenneth Cole in 1940 (COLE, 1940). It consists of an improvement to the Debye model, applying a constant phase element (CPE) with frequency-dependent components instead of an ideal capacitor (GRIMNES, 2005). These two models are shown in Figure 4.



**Figure 4 – (a) Debye circuit with ideal components. (b) Cole circuit with the ideal capacitor replaced by a CPE with frequency-dependent components.**

Font: GRIMNES, 2005

The determination of each component depends on many experimental issues already mentioned in this topic. Therefore the model can't give an absolute value for the skin impedance. However it is important to help understanding how the dispersion of ions in the human skins occurs and which behavior is expected when applying current stimuli on it.

An example of the impedance dependence on the skin site and stimulus duration is shown in Table 1. Impedance measurements were made at 10 Hz on different skin sites with a 12cm<sup>2</sup> ECG dry metal plate electrode positioned directly on the skin site after a short breath had been applied to the skin surface (GRIMNES, 1983).

The first column of Table 1 presents measurements intervals immediately after the electrode had been applied, and the two subsequent columns give the values after 2 and 4 hours respectively. The first column shows a large variation in the control impedance, which was interpreted as unstable sweat duct filling during the measurement. The two other columns show stable results at two different levels of control. These values clearly demonstrate the large variability of skin impedance on different sites (GRIMNES, 2008).

The impedance dependence on the frequency of the stimulation signal was also evaluated by GRIMNES (1983) using a 1cm<sup>2</sup> plate electrode to stimulate different sites of the human body with 10Hz and 1kHz, as shown in Table 2. The results show much higher impedance values for low frequencies. Moreover the use of a smaller electrode (1cm<sup>2</sup> instead 12cm<sup>2</sup>) made the impedance lower than the previous results, indicating a relation between skin impedance and electrode size.

**Table 1 – Site dependence of skin impedance ( $k\Omega cm^2$ ) at 10 Hz for  $12cm^2$  electrodes. Initial values and values obtained after two intervals of 2 hours**

|                               | $k\Omega cm^2/k\Omega$ |        |        |
|-------------------------------|------------------------|--------|--------|
|                               | Start                  | 2 hour | 4 hour |
| Hand: – dorsal side           | 720/80                 | 210/17 | 300/33 |
| Forearm: – ventral – distal   | 250/80                 | 240/17 | 190/35 |
| Forearm: – ventral – middle   | 840/80                 | 230/17 | 360/36 |
| Forearm: – ventral – proximal | 560/80                 | 180/17 | 260/36 |
| Upper arm: – dorsal           | 840/75                 | 260/16 | 660/36 |
| Upper arm: – ventral          | 1000/70                | 300/16 | 780/34 |
| Forehead                      | 60/70                  | 36/16  | 48/35  |
| Calf                          | 325/45                 | 375/17 | 325/16 |
| Thorax                        | 130/17                 | 110/16 | 130/35 |
| Palm                          | 200/80                 | 150/17 | 200/33 |
| Heel                          | 120/60                 | 180/15 | 120/35 |

Font: GRIMNES, 1983.

Further experiments proved that the impedance value decreases with higher frequencies (ROSELL, 1988). At low frequencies (1 – 100Hz) it varies from  $10k\Omega$  to  $1M\Omega$  depending on the skin site and conditions, while at high frequencies (100kHz – 1Mz) the impedance range is between  $100\Omega$  and  $1k\Omega$ .

**Table 2 – Initial impedance dependence on frequency for different skin sites**

| Skin site                | $k\Omega cm^2$ (10Hz) | $k\Omega cm^2$ (1000Hz) |
|--------------------------|-----------------------|-------------------------|
| Hand: – dorsal side      | 320                   | 31                      |
| Forearm: – ventral side  | 550                   | 29                      |
| Upper arm: – dorsal side | 700                   | 33                      |
| Forehead                 | 40                    | 7                       |
| Calf                     | 650                   | 28                      |
| Thorax                   | 600                   | 16                      |
| Palm                     | 190                   | 25                      |
| Heel                     | 500                   | 25                      |

Font: GRIMNES, 1983.

Besides the electrode size, another parameter that must be considered when estimating the skin impedance is the coupling mode. It is known that the use of

conductive paste can reduce the impedance value depending on the concentration of NaCl in it (TAKAGI, 1962). Experiments were made using two silver plate electrodes, 2cm<sup>2</sup> and 3cm apart from each other. The values of electric skin resistance on the forearm using conductive paste with 0.2%, 10% and 18% NaCl are shown in Figure 5 (TAKAGI, 1962). It can be clearly seen that the concentration of NaCl in the coupling paste has a great influence on the measured values.

Since an absolute skin impedance value is uncertain, it is important to define the methods to be used, such as signal frequency, skin site, type, size and distance between the electrodes among others before designing the electronic circuit. In addition the impedance measurement is crucial for configuring the system properly.

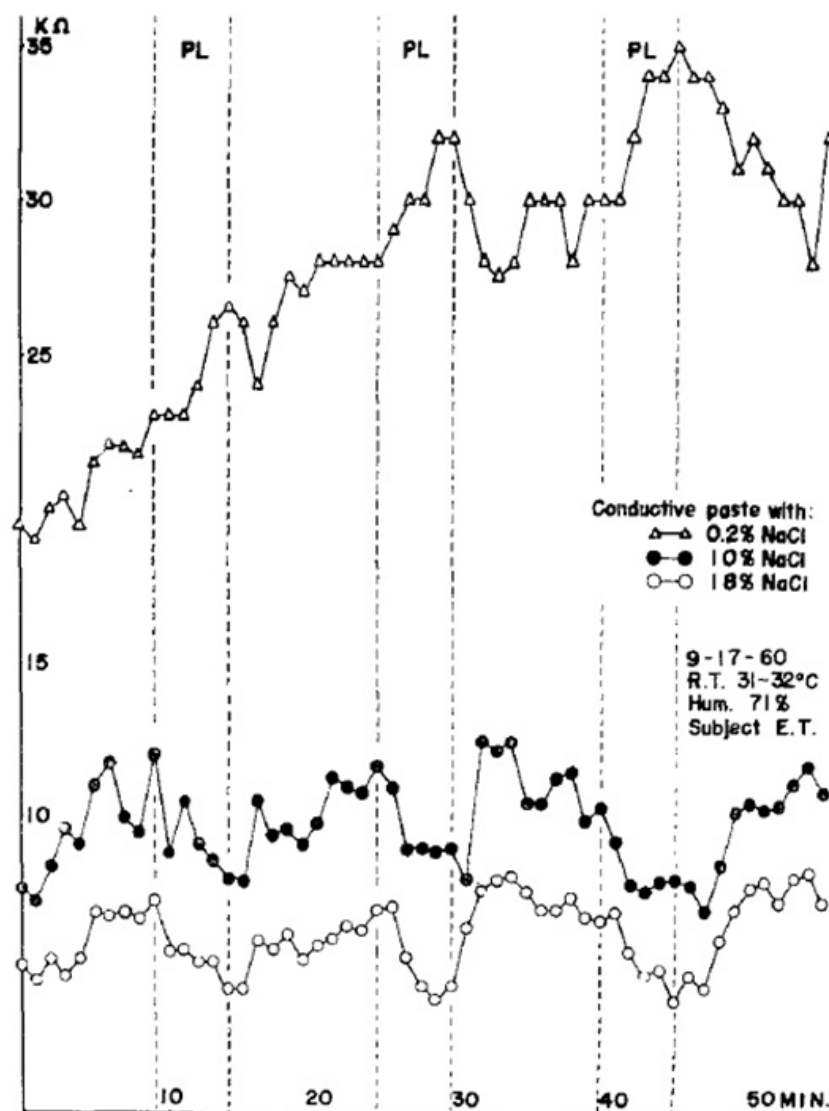


Figure 5 – Variations of electric skin resistance on forearm using conductive paste with different concentrations of NaCl

Font: TAKAGI, 1962.

### 2.2.3 Electrodes

The word electrode was first coined by Michael Faraday to represent an electrical conductor used to make contact between nonmetallic parts of a circuit. In medical applications, an electrode can be defined as the site of shift from electronic (metallic conductor) to ionic conduction (human body). In the case of carrying an electric current from a circuit through the skin, two electrodes are necessary (GRIMNES, 2008).

According to GRIMNES (2008) there are many types of electrodes suitable for different medical applications, as can be seen in Table 3. The most common surface electrodes for non invasive current carrying through the skin are made of silver-silver chloride (Ag/AgCl). It is very simple and has a low well defined DC potential but can be toxic for the skin when used for long-term contact. Therefore it is often used with a salt bridge to prevent the electrode metal from direct tissue contact.

**Table 3 – Electrodes conductor materials**

| <b>Metal</b>                 | <b>Properties</b>  | <b>Use</b>                        |
|------------------------------|--|-----------------------------------|
| Silver-silver chloride       | Stable DC reference, low DC polarization, not biocompatible                              | Skin surface ECG, EMG             |
| Platinum metals              | Non-corrosive, biocompatible, polarizable  | Needles, implants                 |
| Gold                         | Non-corrosive, less biocompatible than platinum  | Needles                           |
| Titanium                     | Highly biocompatible   | Implants                          |
| Stainless steel              | Mechanically strong, noncorrosive, highly DC polarizable and noisy, very alloy dependent | Needles                           |
| Tin, lead                    | Low noise, soft and moldable   | EEG                               |
| Nickel                       | Thin flexible plates, skin allergic reactions  | Skin surface                      |
| Silver, zinc, iron, aluminum | Pharmaceutical or bactericidal properties  | DC therapy and skin iontophoresis |
| Carbon                       | X-ray translucent, soft and flexible multiuse rubber plates                              | Skin surface ECG, EMG             |
| Polymers                     | Special consideration must be taken for the ionic contact medium                         | Skin surface                      |

Font: GRIMNES, 2008.



**Figure 6 – Example of commercial Silver-silver chloride (Ag/AgCl) electrode**

Another important feature concerning the electrodes is the use of contact electrolytes. The contact medium is an ionic conductor positioned between the electronic conductor and the tissue. Since the *stratum corneum* layer of non-wetted human skin is strongly variable and may be very poorly conductive, the use of contact electrolyte can help to moisten a poorly conducting skin with electrolytes. It can also form a high conductance salt bridge from the metal to the skin or tissue among other functions such as ensuring small junction potentials and filling out spaces between the electrode plate and tissues (GRIMNES, 2008).

Ionic contact media of special interest are:

- Wet gel or paste with electrolytes;
- Solid gel (hydrogel) with electrolytic conductance, with or without adhesive properties;
- Saline (e.g. physiological 0.9%) or salt bridge electrolytes;
- Body fluids;
- Tap water;
- Ionic polymers.

The most common skin surface contact electrolytes are wet gel with NaCl. This kind of contact medium represents an electrolytic volume DC resistance in series with the polarization and tissue impedances. An equivalent electric model of the complete system (electrode, contact electrolyte, skin) can be seen in Figure 7 (GRIMNES, 2008). Usually the electrode polarization impedance is about 1kΩ and

the gel resistance  $30\Omega$ . When compared to the skin impedance without moisture at 10Hz for the given electrode size and signal parameters (up to  $300k\Omega$ ), these values are irrelevant in most cases.

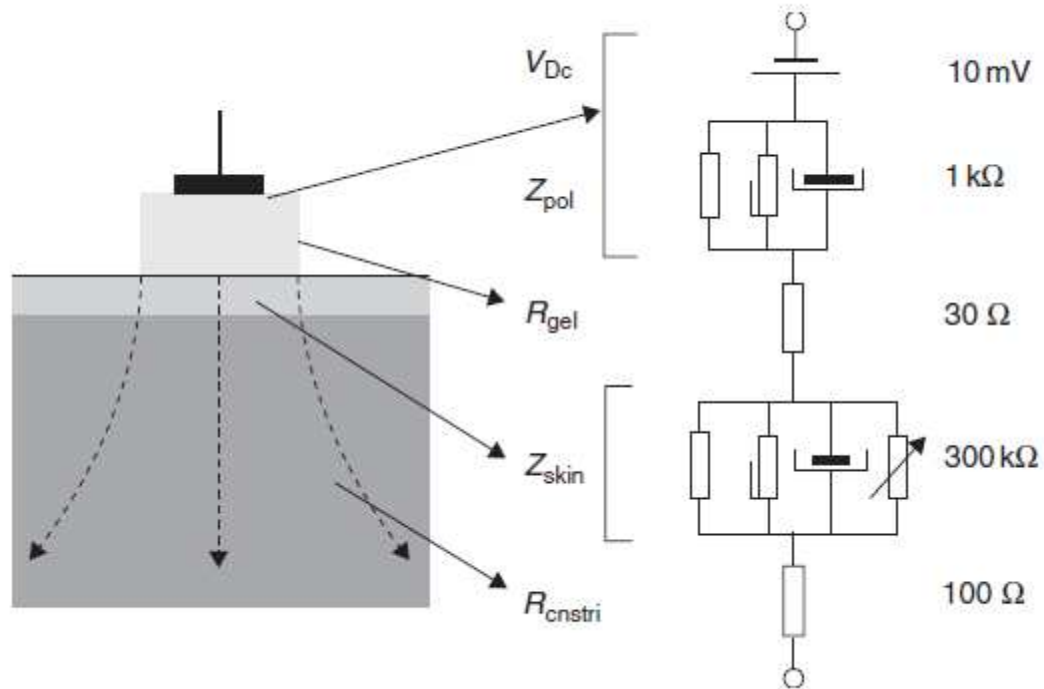


**Figure 7 – Skin surface electrode geometry and its equivalent electric model at 10 Hz for a commercial wet gel ECG electrode**

Font: GRIMNES, 2008.

It is important here to report that the DC potential  $V_{Dc}$  that arises in the electrode is actually due to the accumulation of electrons in the border electrode/skin (electric/ionic conduction). This is one of the reasons to use a current instead of a voltage source for the stimulation. The advantage of the current source is that any DC voltage source in series with it can be seen as a short circuit given that the current is always being controlled from the current source.

The analysis of the electrodes includes not only choosing the material, shape and contact media but also their size and the distance between them. The larger the electrode area, the lower the impedance value and also the noise because of the averaging effect (GRIMNES, 2008). It is affirmed that the skin impedance (on average conditions) varies from  $200k\Omega/cm^2$  at 1Hz to  $200\Omega/cm^2$  at 1MHz. These values depend also on the electrodes material and distance, skin site, among other



factors as already discussed and it is hence difficult to estimate. This parameter should be then measured before any experiment is performed for obtaining more accurate results.

## 2.3 MICROCONTROLLERS

A microcontroller, also called embedded microprocessor, can be defined as a computer on a single chip. It consists mainly of a processor core, memory (both for data and program) and peripherals, including general purpose input/output pins (GPIO). The most common peripherals included in a microcontroller are: analog-to-digital converters (ADC) for external data acquisition and less often digital-to-analog converter (DAC) for analog signal generation. In addition to the converters, many embedded microprocessors include hardware for communication interfaces such as Universal Asynchronous Receiver/Transceiver (UART), Serial Peripheral Interface (SPI) or even Universal Serial Bus (USB), timers, dedicated Pulse Width Modulation blocks (PWM) among others (VERLE, 2008).

### 2.3.1 Important Features

When analyzing a microcontroller for a project it is important to analyze not only its architecture and peripherals but also other important features in order to obtain the desired performance (VAGLICA, 1990). The most relevant parameters are:

#### 1. Core features

- Processor clock: speed of the processor clock, usually in MHz, is one factor to determine how fast instructions can be executed;
- Word length: defines the size (in bits) of the registers and data that can be manipulated. Most usual are: 4, 8, 16 and 32-bits processors;
- Architecture and Instructions set: Harvard or Von Newman, RISC or CISC;
- Other features: Memory Protect Unit (MPU) and Memory management Unit (MMU) to run an operational system, for example;

## 2. On-chip memories features

- The size of the memories included in the microcontroller is important to define, for example, the amount of data that can be stored and manipulated during execution time or the maximum code size. The most relevant are:
  - a) RAM: volatile memory for data storage;
  - b) FLASH/ROM: static memory for program and operating parameters storage.

## 3. Power consumption

- Important are the supply voltage levels and current consumption during active mode. A good reference is the relative consumption, given in mW/MHz;
- Low power modes, such as sleep and back up mode, can help to reduce power consumption.

## 4. On-chip debug and test capabilities

- Allows debugging of the firmware with a remote debugging tool;
- Serial Wire/JTAG Debug Ports.

## 5. GPIO lines

- The number of I/O lines available for external interface is also important, for example, when connecting peripheral circuits to a motherboard.

All these features must be carefully analyzed based on the application requirements when choosing a microcontroller. In the following topic it is made an analysis of the most important microcontroller requirement for this project, which should be able to generate, acquire and transmit signals.

### 2.3.2 Requirements for Digital Signal Processing

As already reported in the item 1.3, the objectives of this project include generating analog signals from the microcontroller, reading the preprocessed skin voltage and current signals and transmitting them to a remote computer. Based on these requirements it is possible to define some fundamental features that must be

included in the chosen microcontroller.

One point that should be considered is if the system must perform critical calculations. Critical calculations are those that if not completed within a specified period of time cause the system to lose synchronization, create a dangerous situation or generate wrong results (VAGLICA, 1990). The following example illustrates this analysis: if a simple timer is to generate a square wave of a given frequency, the central processing unit (CPU) must be fast enough to calculate the time at which each edge should occur and to program the timer appropriately. Moreover it must have a word length big enough to guarantee the desired precision. Peripherals such as timers and an ADC are also required in this case.

More specifically to this work, the following microcontroller requirements for signal processing should be met.

#### 2.3.2.1 Processor performance

The CPU must be fast enough to generate, read and transmit the signals with a minimal rate that still ensures good signal quality. Furthermore, while executing these tasks, the microcontroller must process the acquired data and transfer it to a computer, among other monitoring functions. Assuming a signal pattern as shown in Figure 3, typical for selective stimulation applications, it is possible to see that to generate or read this signal with reasonable quality, a good rate would be higher than 50 kHz. Based on the number of clocks cycles that each instruction takes to be executed, which are defined by the architecture and instruction set, it is possible to define a minimum CPU clock rate in order to perform all the tasks.

#### 2.3.2.2 Word length

The word length of the CPU determines the precision of the calculations to be executed by the processor. With regard to signal processing, when synchronization and high precision requirements are needed, it is recommended to have a large word

length such as 16 or even 32 bits for example when floating point operations are demanded.

#### 2.3.2.3 Memory features

Another relevant parameter for generating and reading external signal is the amount of memory available for data storage during execution time. This feature is really important when the acquired signal data must be transferred to a remote system, which usually is not deterministic such as a PC. This would typically occur when the sample rate is faster than the data transfer rate or when the host computer is running a multi-task operating system, where there are inherent interrupt latencies or a large number of other tasks being performed causing a delay on the reading process. A solution for this issue is implementing a data buffer, usually a FIFO (First In First Out), to store data before transferring it to the computer.

In this project, for example, when acquiring the skin voltage and current signals it is possible to calculate how much RAM would be required in order to implement a buffer to store the data before it can be transferred without losing information. This is done based on the required sampling rate, data size and average transfer rate from the USB interface to the remote computer.

#### 2.3.2.4 Peripherals

The most common peripheral used in signal processing applications are timers, analog-to-digital converters and external communication interfaces. Digital-to-analog converters are also sometimes required but are often not included in many microcontrollers. For this reason DACs are usually applied in an external circuit when necessary.

Timers are crucial peripherals for synchronization purposes when generating signals with time constraints or when sampling external signals. It is important to analyze not only the number of channels and their sizes but also the several

functionalities that can be programmed with them, such as frequency measurement, event counting, interval measurement, pulse generation, delay timing or pulse width modulation.

Analog-to-digital converters are fundamental when dealing with external signal acquisition, hence several microcontrollers already include an ADC on the chip. The main features to be evaluated when choosing the ADC are the resolution, speed and number of available channels. The resolution can be defined through the number of bits used to represent the converted data. Usually internal ADCs support 8, 10, 12 or 16-bits of resolution. This parameter should be chosen based on the desired precision of the conversion. For example, a 12-bits ADC uses 4096 levels to represent a signal. Considering a 3.3V full scale voltage, it leads to a 0.8mV/level, what means that any signal variation lower than 0.8mV can't be detected. Furthermore the conversion speed, also called the maximum sampling rate, defines the possible maximum signal frequency that can be read without distortion. This relation is defined as *Nyquist rate*, which says that the minimum rate to sample a signal to avoid aliasing (effect that causes different signals to become indistinguishable when sampled) is equal to twice the highest frequency contained within the signal. Another common feature of ADCs converters is the number of channels that can be internally multiplexed. It is relevant when more than one signal source need to be read.

Internal hardware for communication interfaces such as UART, SPI or USB are also important peripheral when data transfer between the microcontroller and a remote system is required. To define this interface it is necessary to evaluate some features such as data transfer rate, external compatibility and protocol complexity. When the host system is a personal computer it is recommended to use standard interfaces that can be easily found in almost all of them, as USB for example.

## 2.4 LARGE VOLTAGE RANGE SIGNAL CONDITIONING

The acquisition of analog signals is very often required in many electronic engineering applications and most of them make use of analog-to-digital converters (A/D). These converters have a limited power supply, from which it is possible to

calculate the maximum signal amplitude that can be acquired. Moreover, each ADC has a resolution that gives the minimum detectable amplitude variation. Consequently, in most of these applications a signal conditioning step is first required so that the signal level is suitable for the A/D conversion. This signal conditioning can be amplification, filtering, attenuation, offset compensation among others.

In the case that the input signal has a large voltage range this task can be much harder. For example, when sampling the skin voltage level after the stimulation, the signal can vary from less than 1V to values much higher than the A/D reference voltage such as 100V. This is because the skin impedance varies a lot with many parameters, as already described in this chapter, and because the stimulation current signal also varies widely. The design of a signal conditioning circuit for such a large range of amplitude values is not trivial since the attenuation needed for high-voltage signals to be sampled makes low voltage signals almost undetectable. That means that predefined gains can lead to losses of data precision.

#### 2.4.1 Issues of the Fixed Gain Amplifier

The problem of using a fixed gain signal conditioning, when dealing with large range signal amplitudes, is the possible loss of information due to low resolution sampling of the low level signals. One example to illustrate this issue is shown in Table 4. An experiment for human skin stimulation is made with two different signal levels in different parts of the body. Assuming that the first signal has 1mA amplitude and the skin impedance value is 100k $\Omega$ , the maximum voltage level would be 100V. A second experiment uses 100 $\mu$ A signals and due to its uncertainty the skin impedance could be as low as 10k $\Omega$ . This would result in a maximum voltage level of only 1V, which is 100 times lower than the first signal. When using an A/D converter that operates from 0 to 3.3V, the first signal must be attenuated by a factor 60 to have peak-to-peak amplitude of 3.3V. If the conditioning block has a fixed gain, the second signal would also be attenuated by the same factor and would have only 33mV peak-to-peak amplitude. Using a 12-bits resolution ADC with 3.3V power supply, 33mV would represent only 41 of the 4095 levels. That means less than 6-bits actual resolution, what could be not enough to sample this signal with minimum quality.

**Table 4 – Two experiments showing the problems of resolution when using constant gain.**

| Parameter   | First Experiment       | Second Experiment          |
|---|------------------------|----------------------------|
| Current Amplitude                                 | $\pm 1\text{mA}$ (max) | $\pm 100\mu\text{A}$ (min) |
| Skin Impedance                                    | 100k $\Omega$          | 10k $\Omega$               |
| Max. Skin Voltage Level                           | $\pm 100\text{V}$      | $\pm 1\text{V}$            |
| Output voltage after constant attenuation = 1/60  | 3.3Vpp                 | 33mVpp                     |
| Number of LSBs for a 12 bit ADC (real resolution) | 4095 LSBs (12 bits)    | 41 LSBs (~5bits)           |

This problem can be solved by applying amplification with gain as a function of the signal amplitude. Since the gain must be known and controlled for correctly estimating the real measured value, the most common solutions are the use of variable or programmable gain amplifiers. It means that the signal passes through an amplification block, whose gain can be chosen according to the expected signal amplitude. In this solution, the signal is amplified or attenuated to a certain level, so that its amplitude is lower than the ADC supply voltage but high enough to be sampled with minimum quality.

One possible solution to this dependence is to estimate the maximum signal range (most probable maximum and minimum amplitude levels) and the minimum desired resolution to perform a sample with minimum quality. Based on these parameters, the whole range could be divided in several levels and, for each one, use an adequate gain. The following topics address the most common method for obtaining variable gain amplification.

#### 2.4.2 Programmable Gain Amplifier (PGA)

The programmable gain amplifiers or PGAs are a one-chip amplifier whose gain can be controlled from an external device, such as a microcontroller, often through digital serial protocols like I<sup>2</sup>C and SPI or through a simple parallel interface. There are several models available and most of them can vary the gain from less than 1V/V to over 100V/V in linear or logarithmic scale.

Nevertheless the gain is in most cases more than  $1V/V$ , what makes strong signal attenuation not possible. This requires a previous attenuation of the signal, with a high-impedance resistive voltage divider or fixed gain amplifier, for after amplification to an adequate level. The advantage of this solution is that it is very simple and occupies very little PC board space.



## **CHAPTER 3**

### **THE STIMULATION SYSTEM DESIGN**

#### **3.1 INTRODUCTION**

This chapter presents the design and implementation steps of this project, starting with the tools and methods used for the design, followed by the analysis of the system requirements and the definition of the system architecture. Afterwards each block of the entire system is described in details, including some problems and solutions found during the development. The integration of all modules in a final solution and the validation are further described in Chapter 4.

#### **3.2 TOOLS AND METHODS**

This topic describes the tools and methods used during the system design and can be divided into hardware and firmware development.

##### **3.2.1 Hardware development**

The hardware development process can be described in five major steps: circuit topology definition, schematics design, simulation of the proposed circuit, design of a printed circuit board (PCB) layout, implementation of a prototype and tests. However, the process is not linear and feedbacks from the simulation and tests steps were needed to improve the final circuit.

The diagram shown in Figure 8 describes the hardware development process.

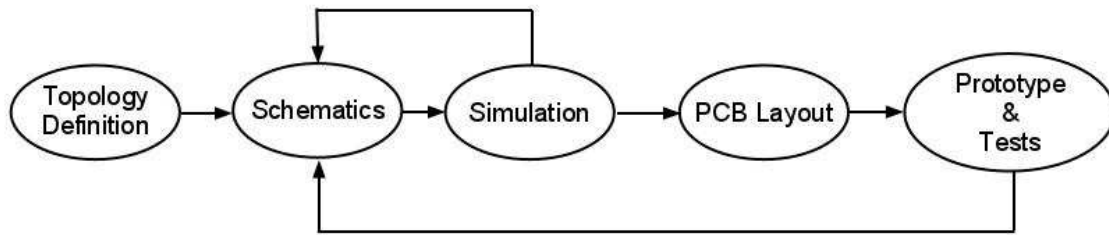


**Figure 8 – Hardware development process**

The first step of the hardware design was the topology definition for each block of the system based on the project requirements and restrictions. Afterwards the schematics were designed, validated and improved with the simulation tools.

For simulating the proposed circuits, the software *LTspice IV* was applied. This software is a high performance Spice III circuit simulator for analog and mixed signal with over 200 op amp models as well as resistors, transistors and MOSFET models. Moreover it is free, fast and easy to use.

After the simulation, the schematics were designed, the components were defined and the design of a printed circuit board (PCB) was made. Using the software *Altium Design 2003* all the schematics were designed into a PCB layout and a prototype was developed. After welding the components on the PCB several tests could be carried out verifying the practical behavior of the system. In addition, improvements were made during the tests until a good operation of the entire system was achieved.

### 3.2.2 Firmware development

Since the firmware is sometimes pre-requisite for the hardware tests and validation, the firmware development was carried out in parallel with the hardware one. Moreover some parts of the firmware are highly hardware-dependent and therefore can be only truly validated together. The process of the firmware development can also be described in five major steps: definition of the

requirements, design, code implementation, integration with the hardware and validation.

These steps are based on the V-model development process and are not linear just like the hardware development process. Feedbacks from the integration and validation phases were needed to improve the final code. Figure 9 shows a block diagram that illustrates the relation between the firmware development steps.

The first step of the firmware design was the requirements definition. This definition was made based on the system requirements and defines the basic functionality and use cases of the system. Afterwards, based on the requirements of the first step, the detailed design of the firmware was made using some UML diagrams, such as state charts sequence diagrams.

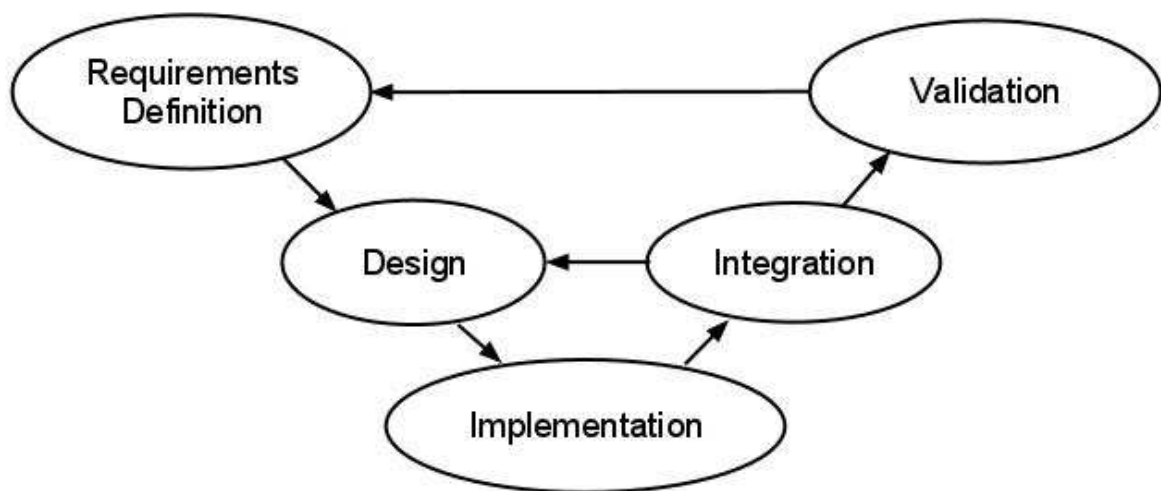


**Figure 9 – Firmware development process based on the V-model process.**

The following step was the code implementation. It consists not only in writing the firmware but also in emulating and debugging the code to find basic errors and in verifying its correct operation. For this purpose it was used the integrated development environment (IDE) *IAR Embedded Workbench for ARM 5.50 Kickstart* from *IAR Systems*. This software provides not only the source code editor but also the compiler, linker and debugger for several ARM microprocessors.

After the code implementation it was possible to integrate the firmware with the hardware and verify the correct operation of both parts. At this point, modifications of the hardware as well as firmware errors were used as feedback for

new designs, as shown in the process model.

After integrating the firmware and hardware the validation step was started. This process verified if the system met all the requirements defined in the first step. During the validation phase new requirements as well as changes on the old requirements were needed and the results from this step were used as feedback for a new development cycle until the desired operation was finally achieved.

### 3.3 SYSTEM REQUIREMENTS

This topic presents the system requirements regarding the speed, precision, and output range. The definition of these constraints were based on the objective of the project and on the theory reviewed in the theoretical foundations. This step was really important not only for the correct definition of the system architecture and components to be used but also to the definition of the requirements for the firmware implementation.

The first parameter to be defined was the maximum output current level. Based on the stimulation theory and the typical excitation pulse shown in Figure 3, a maximum absolute value of 3mA could be defined. Considering the positive and negative peaks, the maximum output current range is 6mA. Furthermore it was necessary to define the precision of the system output, which corresponds to the minimal current variation at a time. Assuming a typical stimulation signal, the minimal resolution wherewith the signals can be generated with reasonable quality is about 10 $\mu$ A. These values were important for designing the current source and signal conditioning circuits as well as for choosing an adequate digital to analog converter in the hardware design.

Another important requirement was the signal generation and sampling rate. The definition of a typical rate for the signal generation was also based on the typical stimulation pulse proposed in (SEIF, 2001). Considering the previous maximum range and resolution, a typical rate of 50 kHz was defined, corresponding to a delay of 20 $\mu$ s between samples. These values were also relevant for choosing the DAC/ADC and must be considered when choosing the microcontroller speed and some peripherals. Moreover, all the requirements had a direct influence on the

firmware development process.

As a result of this analysis, Table 5 was made listing the most important requirements of the system.

**Table 5 – Summary of the most relevant requirements of the stimulation system**

| Requirement               | Value                   | Description   |
|---------------------------|-------------------------|---|
| Signal Generation Rate    | 50kHz (typ.)            | Update rate for the DAC input in order to generate typical stimulation pulses with quality and precision. |
| Signal Sampling Rate      | 100kHz (typ.)           | Sampling rate for each ADC channel.   |
| Output Current Level      | $\pm 3\text{mA}$ (max.) | Maximum absolute value of the output current.   |
| Output Current Resolution | 10 $\mu\text{A}$        | Minimal variation of the output current at a time.  |

### 3.4 SYSTEM ARCHITECTURE

This topic describes in details the block diagram shown in Figure 1 from Chapter 1. It defines hence the system architecture, giving also a general idea of its operation.

The first block is a general microcontroller platform, based on an ARM Cortex-M3 microcontroller, which generates and acquires signals from an analog signal board and communicates through USB with a PC. The analog signal board consists of a 12-bit D/A circuit that converts the signal given from the microcontroller to an analog voltage signal, connecting it to the current source input. Moreover, the current source converts the given voltage signal into current in order to stimulate the human skin through a pair of electrodes. Another part of the analog board is the signal conditioning circuits. These blocks are responsible for conditioning the skin voltage and current signals, which are obtained from the current source during the stimulation. Each block has a preamplifier, a programmable gain amplifier, low-pass filter and a circuit for offset compensation. After the conditioning block these signals are then adequate to be acquired from the microcontroller's A/D channels. Moreover there is a circuit based on the AD5933 integrated circuit to measure unknown impedances. In addition to these blocks a switching mode power supply was developed to generate the required negative voltage levels from the USB supply.

The detailed block overview of the entire system is shown in Figure 10.

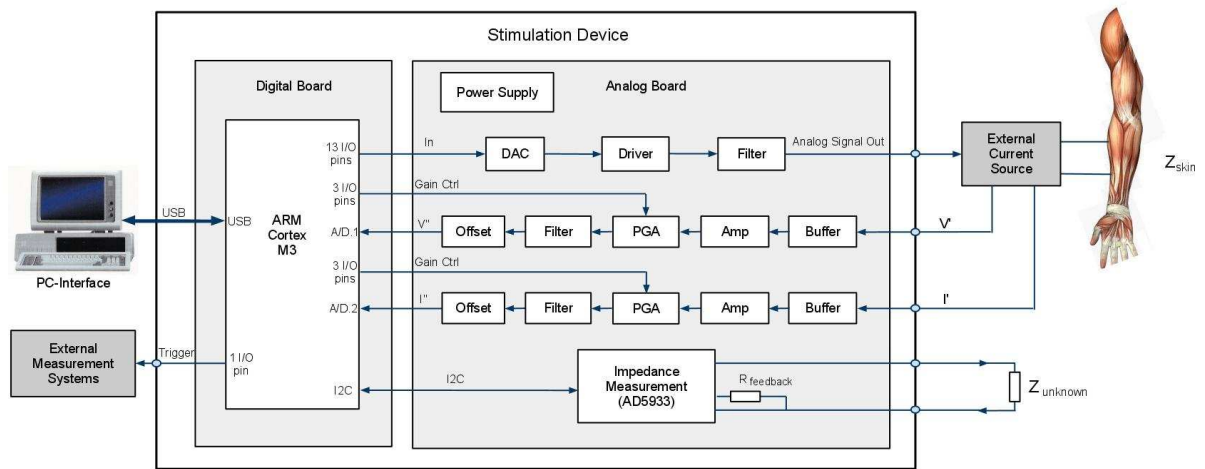


**Figure 10 – Block overview of the stimulation system architecture**

### 3.5 THE MICROCONTROLLER BOARD

This topic presents an overview of the microcontroller as well as a description of the digital board used in this project. This board was based on the ATMEL SAM3U4E Cortex-M3 microcontroller and was designed to offer the core functions of this microcontroller as a general purpose platform for the Institute for Biomedical Engineering at the Hochschule Mannheim. It contains, in addition to the microcontroller, some basic peripherals for programming the firmware and also communicating with external devices, such as USB connection, IO pins and JTAG interface for online debug.

#### 3.5.1 Microcontroller Overview

Atmel's SAM3U4E is a member of the SAM3U family of Flash microcontrollers based on the high performance 32-bit ARM Cortex M3 RISC processor. It operates at a maximum speed of 96 MHz and features 256 Kbytes of Flash and 52 Kbytes of SRAM. The peripheral set includes a High Speed USB device port with embedded

transceiver, an external Bus interface with NAND Flash controller, 4x USARTs, 2x TWIs (compatible with I<sup>2</sup>C interface), 5x SPIs, as well as 4x PWM timers, 3x general purpose 16-bit timers, an RTC, a 12-bit and a 10-bit ADC. The SAM3U4E architecture is specifically designed to sustain high speed data transfers. It includes a multi-layer bus matrix as well as multiple SRAM banks, PDC and DMA that enable to run tasks in parallel and maximize data throughput. A block diagram of the microcontroller's internal architecture is shown in Figure 12 and a picture of the chip is shown in Figure 11.

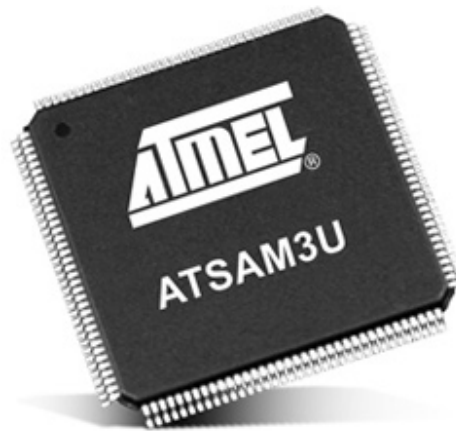


Figure 11 – Picture of the microcontroller

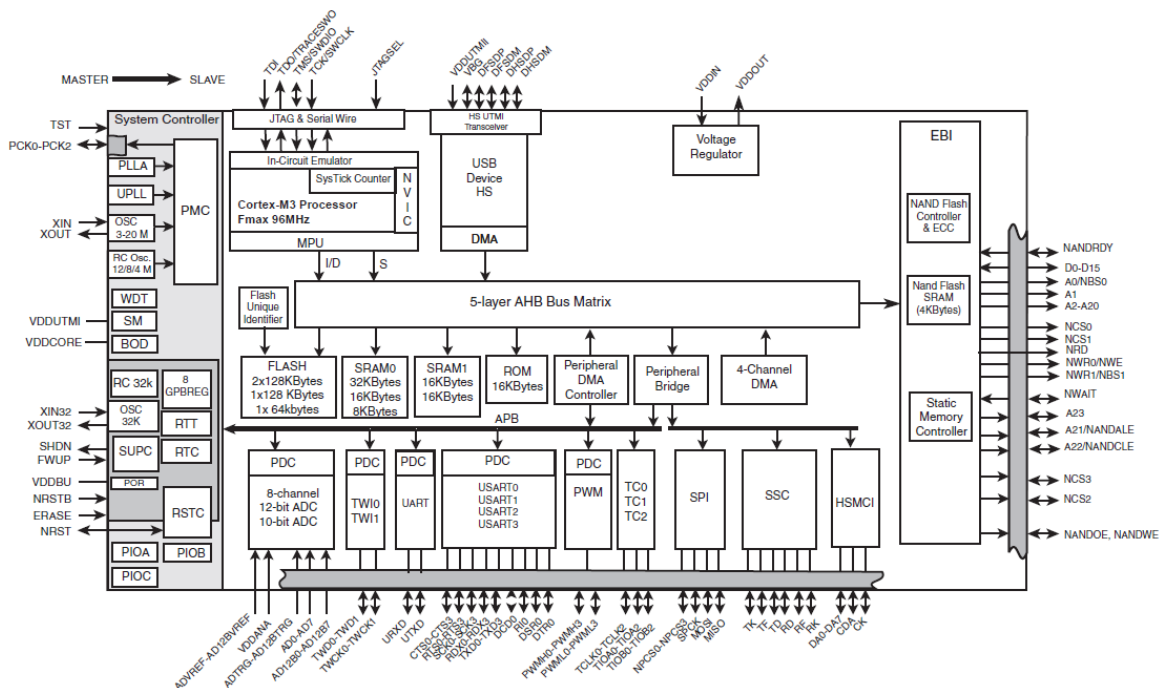


Figure 12 – Block diagram of the SAM3U4E

Font: DATASHEET Atmel AT91 ARM Cortex-M3

### 3.5.2 Digital Board Description

The digital board is responsible for controlling the signal generation and signal acquisition through the analog board. Moreover it communicates with the host computer through a high-speed USB interface. The circuit contains not only the SAM3U4E microcontroller but also some peripherals that make it work, such as voltage regulator, crystal oscillator, JTAG interface for debugging, USB connector and reset button.

Furthermore a dedicated 30-pin connector was placed for the connection between the digital and the analog board. This connector was designed to attend all the requirements of the project and consist of: 5V power supply, ground, 2 ADC channels, I<sup>2</sup>C data and clock pins and 22 IO pins, which are used for: DAC control (13 pins), PGA gain control (2x3 pins), external trigger (1), and general purpose IO (2). Table 6 summarizes the relation between the connector and the microcontroller pins.

The 5V power supply can be chosen from three different sources with a jumper: from USB, external power supply or from/to the analog board through the dedicated connector. It is important to say that only one source can be used at a time. This voltage is connected to a LM1117 voltage regulator, whose output supplies 3.3V to all the CMOS digital circuit.



**Table 6 – Pin map of the digital – analog board connector.**

| Connector Pin | Microcontroller Pin | Function in the Analog Board        |
|---------------|---------------------|-------------------------------------|
| 1             | -                   | 5V                                  |
| 2             | PA20                | DAC: DB0                            |
| 3             | PA21                | DAC: DB1                            |
| 4             | PA22                | DAC: DB2                            |
| 5             | PA23                | DAC: DB3                            |
| 6             | PA24                | DAC: DB4                            |
| 7             | PA25                | DAC: DB5                            |
| 8             | PA26                | DAC: DB6                            |
| 9             | PA27                | DAC: DB7                            |
| 10            | PA28                | DAC: DB8                            |
| 11            | PA29                | DAC: DB9                            |
| 12            | PA30                | DAC: DB10                           |
| 13            | PA31                | DAC: DB11                           |
| 14            | PA19                | DAC: CLK                            |
| 15            | GND                 | GND                                 |
| 16            | GND                 | GND                                 |
| 17            | PA11                | Function selection IO               |
| 18            | PA12                | IO for Debug                        |
| 19            | PA7                 | Trigger                             |
| 20            | PA30                | AD channel 1 (skin current signal)  |
| 21            | PA22                | AD channel 0 (skin voltage signal)  |
| 22            | PA9                 | I <sup>2</sup> C Data (for AD5933)  |
| 23            | PA10                | I <sup>2</sup> C Clock (for AD5933) |
| 24            | PA6                 | PGA2: G2                            |
| 25            | PA5                 | PGA2: G1                            |
| 26            | PA4                 | PGA2: G0                            |
| 27            | PA3                 | PGA1: G2                            |
| 28            | PA2                 | PGA1: G1                            |
| 29            | PA1                 | PGA1: G0                            |
| 30            | -                   | 5V                                  |

### 3.5.3 Schematics

The schematics of the microcontroller were divided in three blocks. The first block shown in Figure 13 corresponds to the core pins of this element such as ground and power supplies pins with decoupling capacitors and 12MHz crystal clock circuit. In addition to these pins, there are a LM1117 3.3V voltage regulator, a reset button, a JTAG connector and their components.

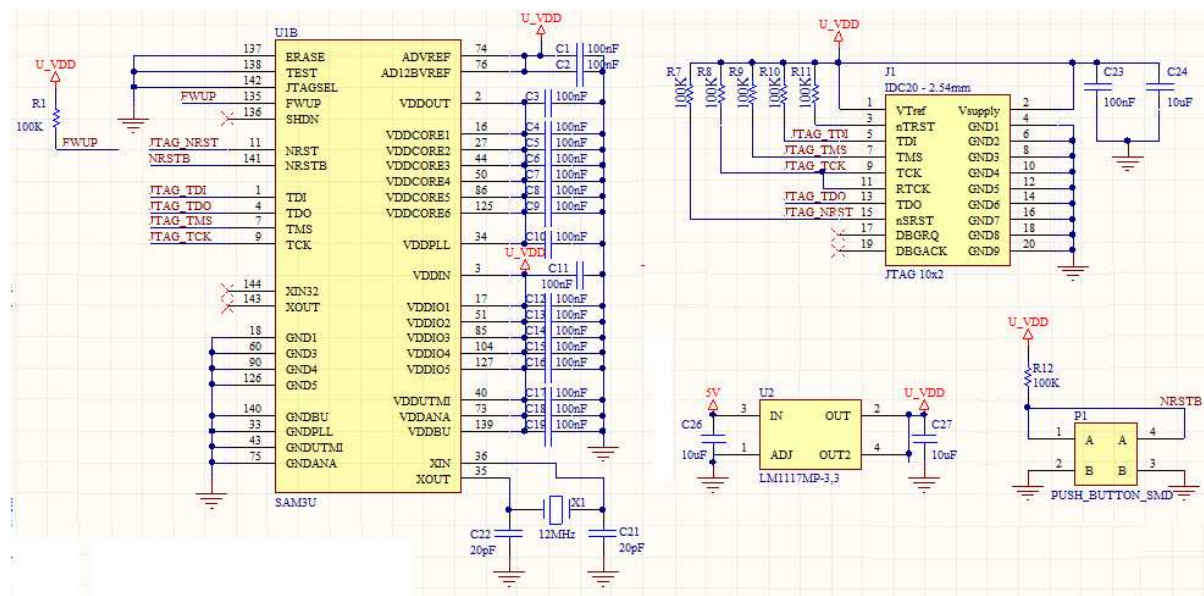


Figure 13 – Core pins, JTAG and power supply of the microcontroller.

The second block contains the communication peripheral and analog to digital converter pins. Some peripherals such as SPI and UART are not used. The most relevant part of this block is the USB circuit and the connector. Moreover two channels of the ADC are connected to the analog/digital board connector. The schematics of this block are shown in Figure 14.

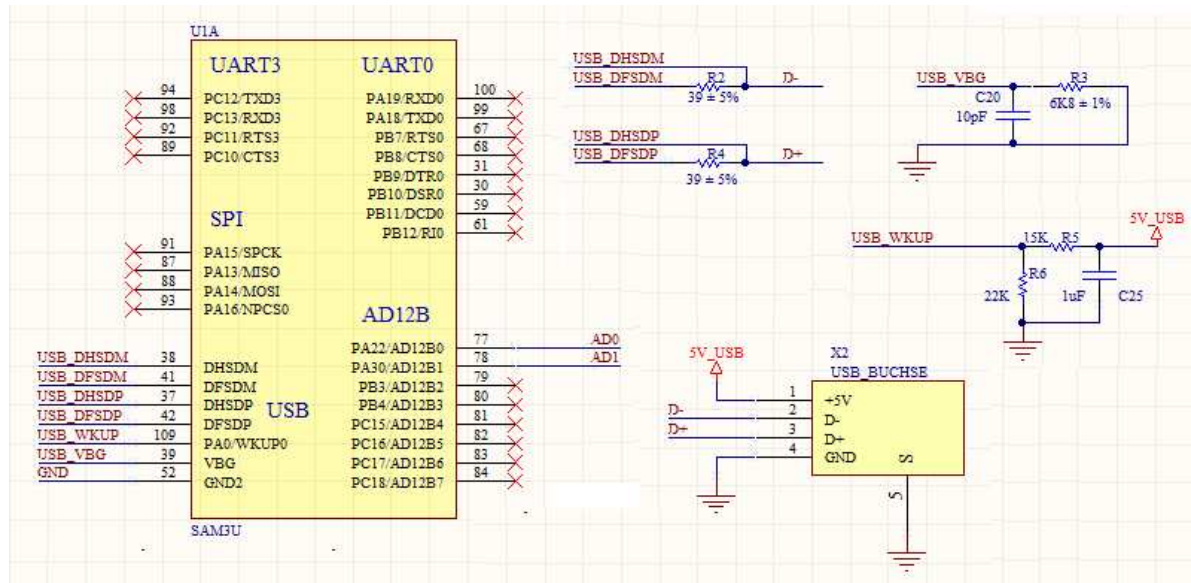


Figure 14 – USB and ADC pins

The third block consists of the IO pins and TWI bus used to control the analog board. They are connected to the analog/digital board connector as described in this chapter before. In addition there are connectors for ground, external power supply and for choosing the power supply source.

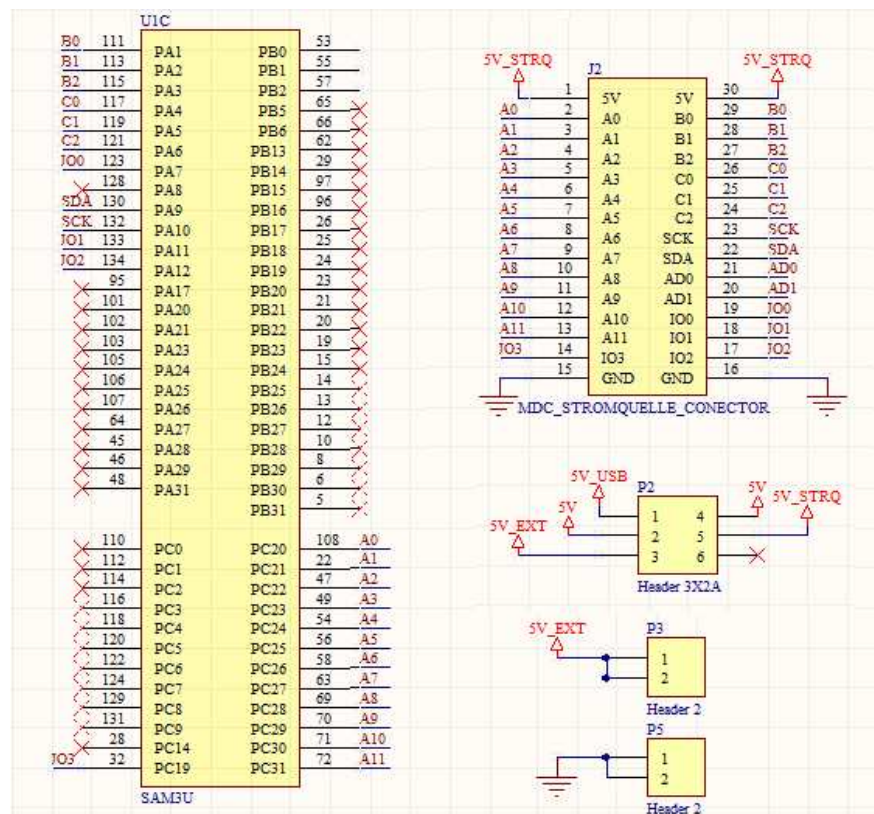


Figure 15 – Pins and connector to the analog board as well as power supply connectors.

### 3.5.4 Digital Board Layout

Once finished the design of the schematics a PCB layout for the digital board could be drawn using the software Altium Design 2003.

The most critical part was the microcontroller area which contains dedicated ground plane on the top and bottom layers below it.

The final layout was approximately 76cm<sup>2</sup> (90mm x 85mm). Figure 16 and 17 show the top and the bottom layers layout respectively.

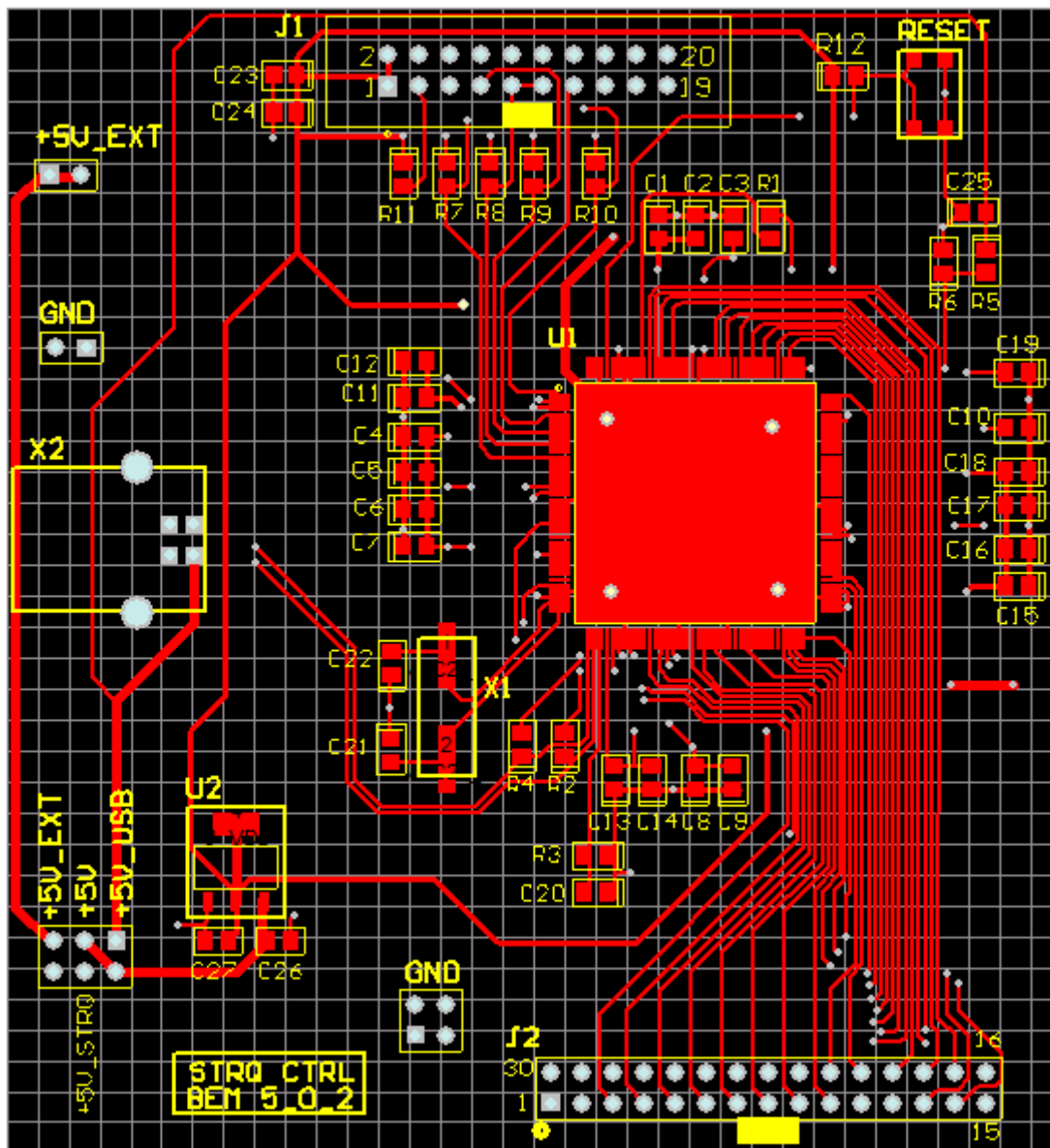


Figure 16 – Top layer of the digital board layout

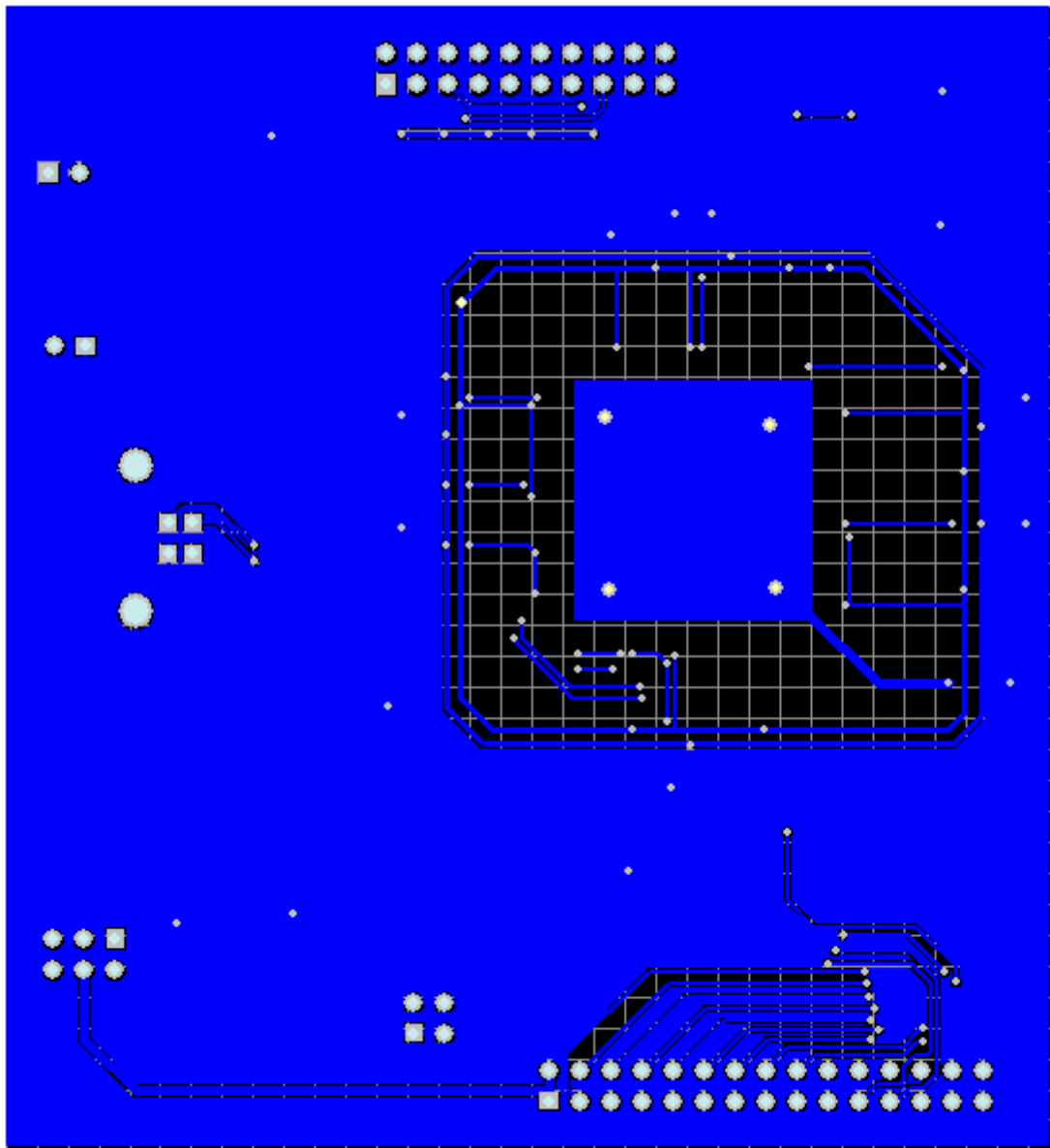


Figure 17 – Bottom layer of the digital board layout.

### 3.6 THE ANALOGUE BOARD

This topic presents the design of the analogue board, which is the main component of the entire system. It consists mainly of the DAC circuit and drivers, signal measurement circuit for the skin current and voltage signals, impedance measurement block and a switching mode power supply. The design process and the schematics of each block are presented in details in the next topics.

#### 3.6.1 The D/A Converter

One important step for generating signals from a microcontroller is the choice of an adequate digital-to-analog converter (DAC). This step was done after analyzing the project requirements and the typical features of the D/A converters.

There are basically four parameters that should be considered when choosing a digital-to-analog converter:

##### 3.6.1.1 Output mode

This parameter defines the output properties of the DAC. The analog output can be a voltage or current signal and it can operate in single or differential mode. Moreover the power supply is also important to define the full scale output value.

Concerning the power supply, the converters can also be classified in single or dual power supply. Single supply converters can't generate signals with negative values. Therefore they need a special circuit for controlling the offset when both positive and negative output values are required. Furthermore, differential current output converters may have higher noise immunity but are also more complex and expensive to produce.

### 3.6.1.2 Resolution

The resolution of a DAC can be defined as the output level rise created by increasing the least significant bit (LSB) of the input by one step. This amplitude value is a function of the number of input bits and the reference value. Increasing the number of bits results in a finer resolution.

$$Resolution = \frac{V_{ref}}{2^{nbits}}$$

Most DACs operates in the 10-18 bit range. To define the number of bits of the DAC, it is first necessary to define the desired resolution of the system. Considering a maximum absolute output value of 3mA (6mA range) and a resolution of 10μA, the minimum number of bits for this system would be:

$$10\mu A = \frac{6mA}{2^{nbits}}$$

$$nbits \geq \log_2 \left( \frac{6mA}{10\mu A} \right) = 9.22$$

### 3.6.1.3 Speed

The speed is usually specified as the conversion rate or sampling rate at which the input register is cycled through in the DAC. High speed DACs are defined as operating at update rates greater than 1 mega sample per second (Msps). The conversion of the digital input signal is limited not only by the clock speed of the input signal but also by the settling time of the DAC.

### 3.6.1.4 Settling time

Ideally a DAC would instantaneously change its output value when the digital input changes. However, in a real DAC it takes time for the DAC to reach the actual expected output value, as shown in Figure 18.

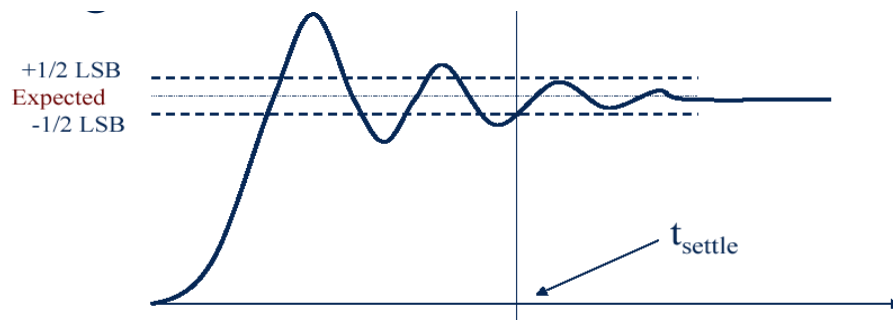


**Figure 18 – Settling time of a digital-to-analog converter.**

Based on the speed and settling time of the DAC it is possible to define how fast a digital-to-analog conversion can be performed and therefore the maximum frequency components that can be generated.

### 3.6.1.5 The LTC1666

Considering the system requirements and the analysis of most important DAC parameters the LTC1666 from Linear Technologies was chosen. It is a 12-bit, 50Msps differential current output DAC implemented on a high performance BiCMOS process with laser trimmed, thin-film resistors. The high speed and low settling time (20ns) guarantees a good performance for several signal shapes, with high frequency components without distortion. The internal circuit of the LTC1666 is represented in Figure 19.



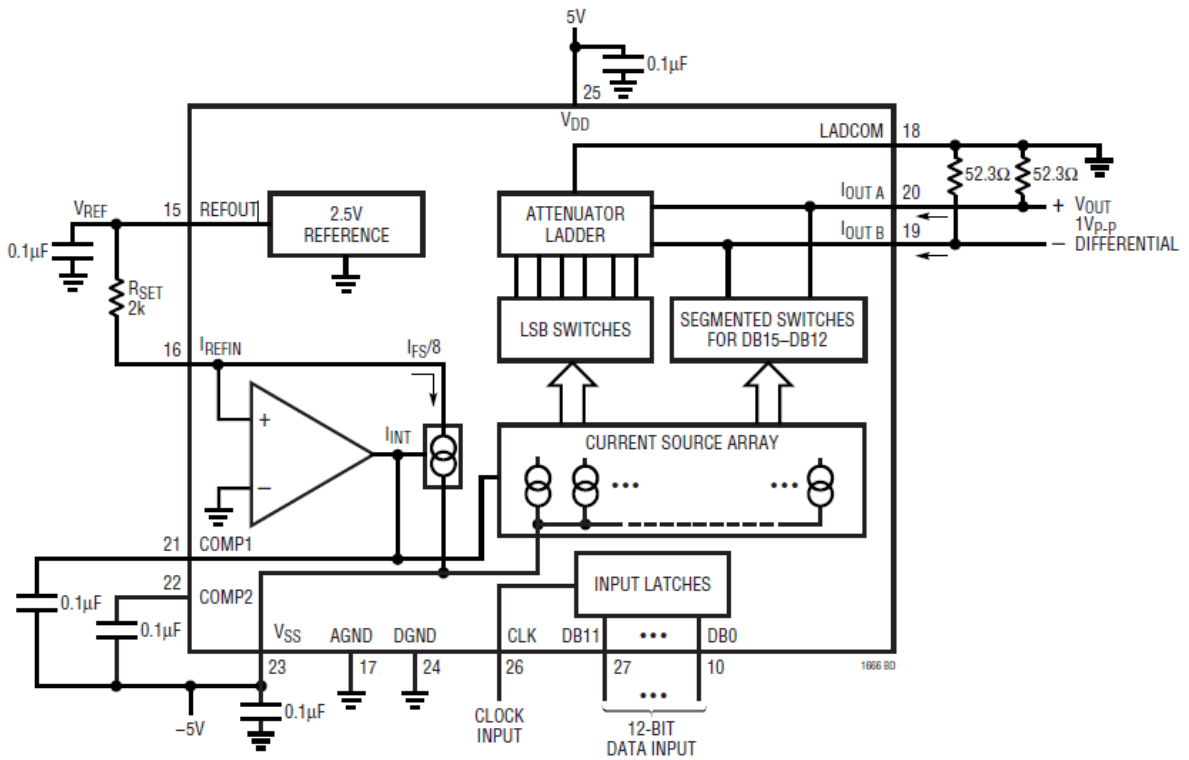


**Figure 19 – Block diagram of the LTC1666 internal circuit**

Font: DATASHEET Linear Technologies LTC1666

Operating from dual  $\pm 5V$  supplies, the LTC1666 can be configured to provide full-scale output currents ( $I_{outFS}$ ) up to 10mA, what leads to a resolution of less than  $2\mu A$ . The differential current outputs of the DACs allow single-ended or true differential operation.

The LTC1666 uses straight binary digital coding. The complementary current outputs ( $I_{outA}$  and  $I_{outB}$ ) sink current from 0 to 10mA (nominal  $I_{outFS}$ ).  $I_{outA}$  swings from 0mA when all bits are low, to 10mA when all bits are high.  $I_{outB}$  is complementary to  $I_{outA}$  and both output currents are given by the following formulas:

$$I_{outA} = I_{outFS} \cdot \left( \frac{DAC_{code}}{4095} \right)$$

$$I_{outB} = I_{outFS} \cdot \left( \frac{4095 - DAC_{code}}{4095} \right)$$

$$I_{diff} = I_{outA} - I_{outB} = I_{outFS} \cdot \left( \frac{2 \cdot DAC_{code} - 4095}{4095} \right)$$

The graphic shown in Figure 20 represents the equation for the differential output current as a function from the input DAC code. This equation is really important for designing and programming the signal generation firmware.

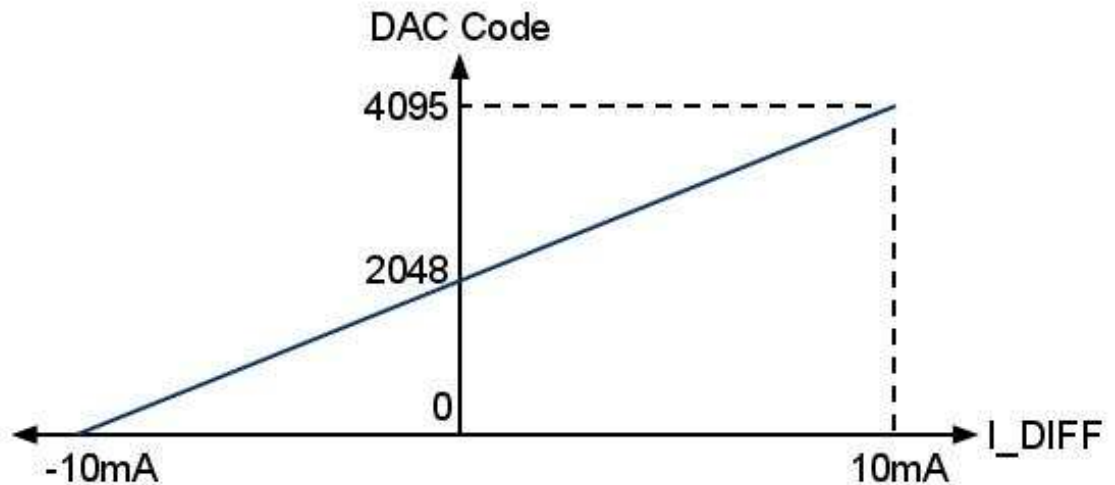


Figure 20 – Differential output current of the LTC1666 as a function of the DAC code.

#### 3.6.1.6 Circuit design

The circuit design was based on the arbitrary waveform generator circuit proposed on the LTC1666 datasheet from Linear Technologies. It was chosen for a dual power supply so that both positive and negative amplitude signals could be generated without needing any offset compensation.

The connection to the microcontroller was made through 13 IO lines, twelve for the data input and one clock signal.

In order to produce a differential output voltage without degrading the converter's linearity, the outputs can be connected to the summing junction of a high speed operational amplifier as shown in Figure 21.

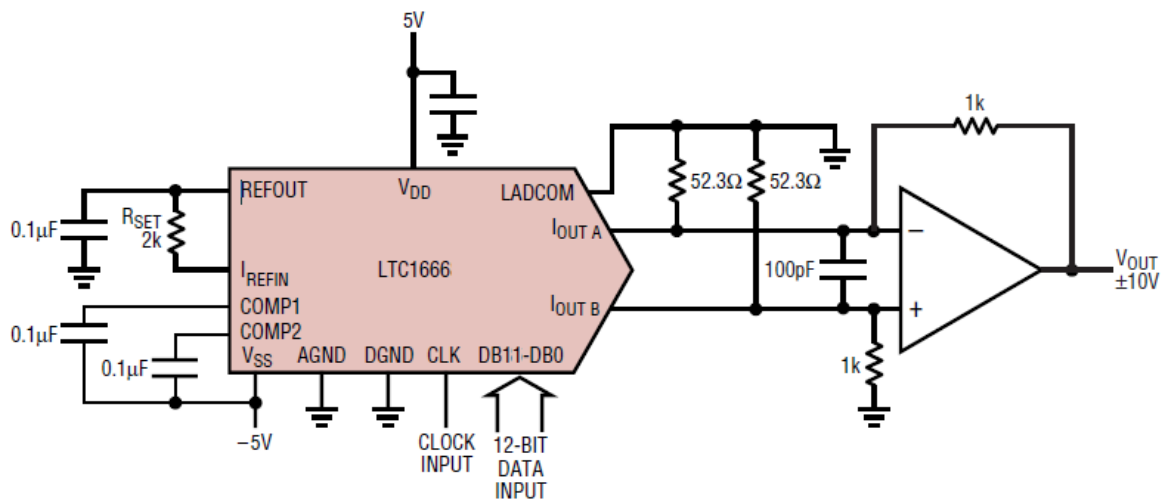


**Figure 21 – Example circuit for an arbitrary waveform generator with  $\pm 10V$  output**

Font: DATASHEET Linear Technologies LTC1666

The chosen operational amplifier was the LT1124, which is a dual high performance op amp that offers higher gain, slew rate and bandwidth than the industry standard OP-27 and competing OP-270/OP-470 op amps. It has a typical low voltage noise of  $2.7\text{nV}/\sqrt{\text{Hz}}$  and maximum of  $4.2\text{nV}/\sqrt{\text{Hz}}$ . The Gain Bandwidth Product is 12.5MHz and the maximum offset voltage is  $100\mu\text{V}$ .

The op amp is used in a differential to single-ended configuration, transforming the differential current output in a voltage signal. When setting the feedback resistors  $1\text{k}\Omega$ , as shown in Figure 21, the output swings  $\pm 10V$  around ground for 10mA input. The 100pF capacitor was used between the inputs to add a single real pole of filtering, helping also to reduce distortion by limiting the high frequency signal amplitude.

Due to the power supply limitation of  $\pm 5V$ , the maximum  $\pm 3\text{mA}$  skin current level and considering a unitary gain of the current source ( $1\text{ mA/V}$ ), the output should swing  $\pm 3V$  for full scale value ( $\pm 10\text{mA}$  from the DAC output).

At the output of the DAC circuit, a second-order low pass filter was used to reduce the high-frequency noise and the intrinsic distortions of the digital to analog conversion. The applied 2<sup>nd</sup>-order low pass filter was an active Bessel filter. The cutoff frequency was set to 10kHz but can be adjusted when higher frequencies are required. In this topology, for stability purposes, the gain  $A_i$  should be close to 1.268 for a quality factor  $Q=0.707$ .

Figure 22 shows the *LTspice* schematic used in the simulation step.

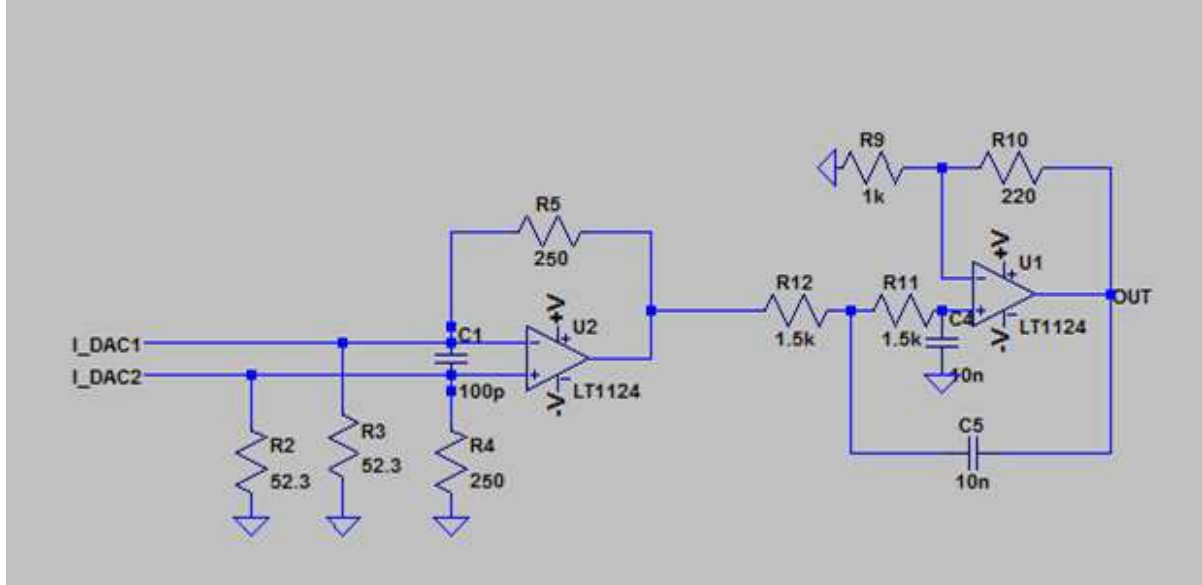


Figure 22 – Differential current to voltage amplifier with 2<sup>nd</sup> order low pass filter.

The dimensioning of the circuit can be made as follows:

$$f_{3dB} = \frac{1}{2\pi R_{11} C_4} = 10kHz$$

$$A_i = 1 + \frac{R_{10}}{R_9} = 1.268$$

Assuming  $C_4 = C_5 = 10nF$  and  $R_9 = 1k\Omega$ , the other components should be  $R_{11} = R_{12} = 1.5k\Omega$  and  $R_{10} = 268\Omega$ . In practice the feedback resistor was set  $R_{10} = 220\Omega$ .

Because of the filter, the gain of the first stage was adjusted to keep the desired gain of  $\pm 3V$  for  $\pm 10mA$  DAC output:

$$A = A_1 \times A_{Filter} = 0.3V/mA$$

$$A_{Filter} = \left(1 + \frac{R_{10}}{R_9}\right) = 1.22$$

The first stage gain can be calculated as follows when  $R_4 = R_5$ :

$$A_1 = R_5 V/A$$

As result:

$$R_4 = R_5 = \frac{A}{A_{Filter}} = \frac{0.3V/mA}{1.22} \sim 247\Omega$$

Figure 23 shows a simulation of the circuit for a sinusoidal input current of 1mA peak-to-peak. The represented signal shows the output after the filter proving the total gain of 0.3V/mA.

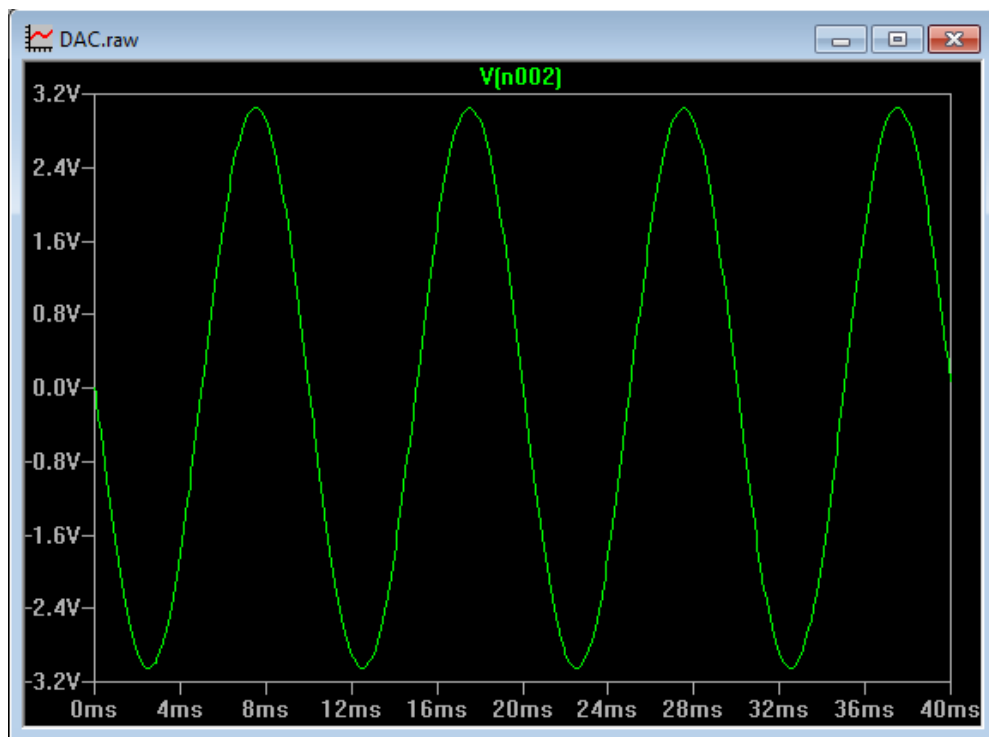


**Figure 23 – Output voltage for a DAC sinusoidal differential output current of 1mA peak-to-peak.**

Figure 24 shows the frequency response of the designed low pass filter. It is important to see that, without filter, higher frequencies such as 1MHz or greater were less attenuated than the base band signal, what could lead to a noisier circuit.

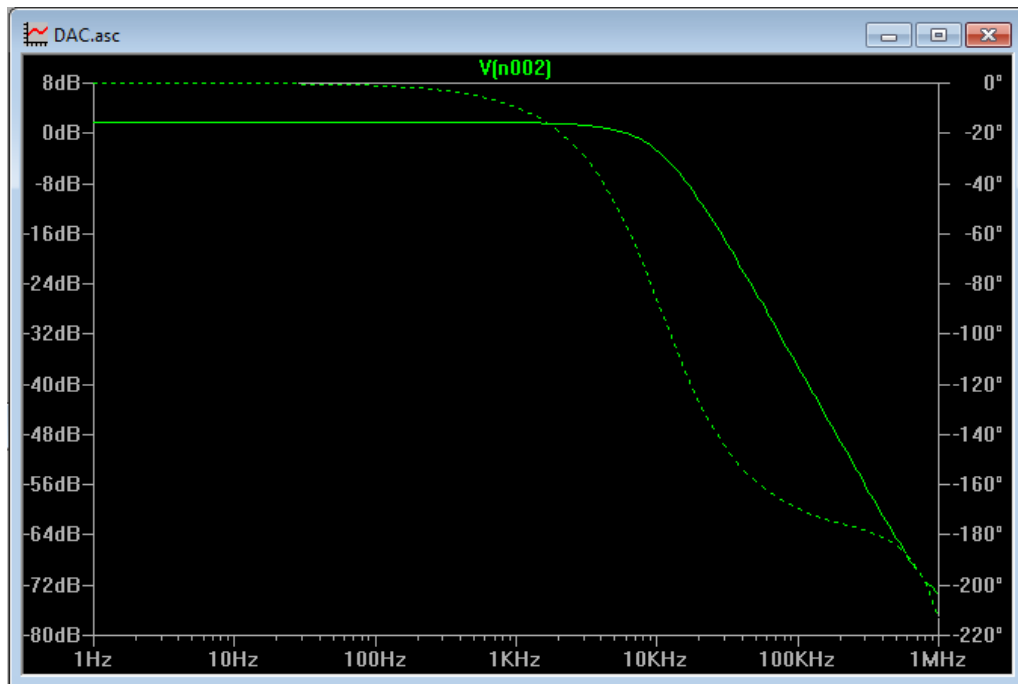


Figure 24 – Frequency response of the low-pass filter.

### 3.6.1.7 Schematics

Figure 25 shows the schematic of the DAC circuit and the differential current to voltage amplifier. It was design based on example circuit of the LTC1666 datasheet shown in Figure 21.

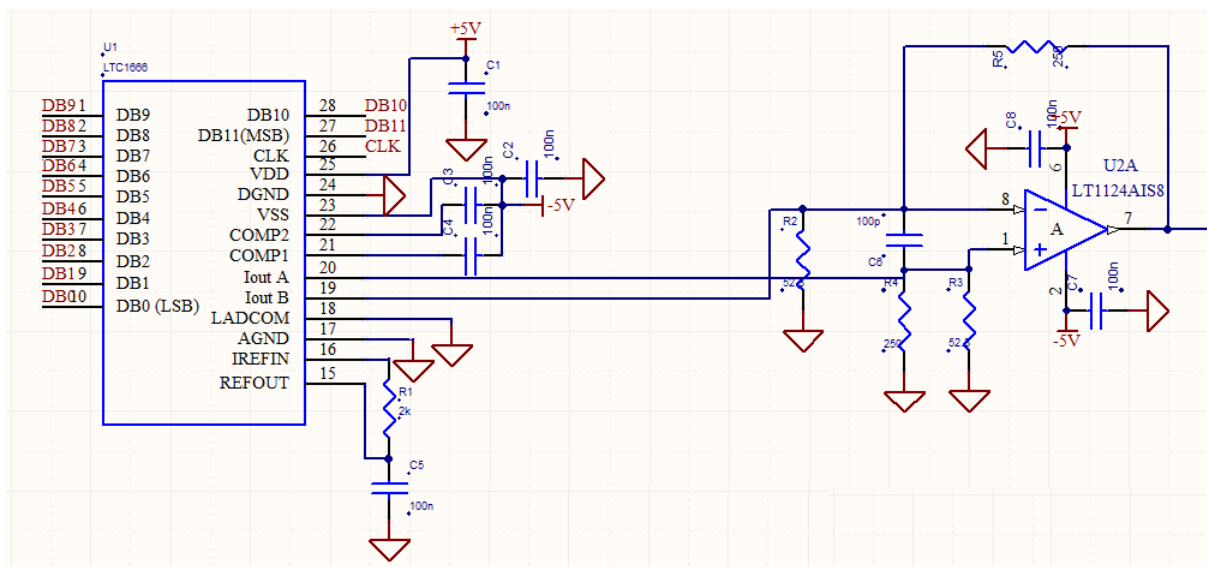
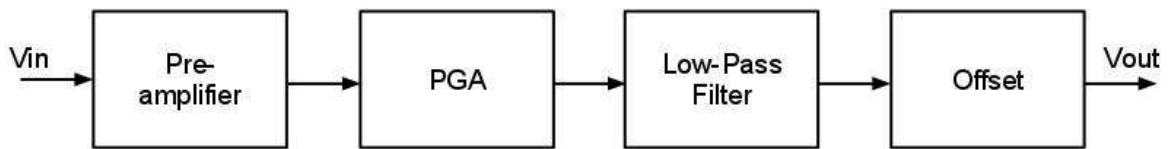


Figure 25 – DAC Schematic and current to voltage converter



Each signal is then processed by a signal conditioning circuit and connected to the AD channels of the microcontroller. There are two conditioning circuits, one for each signal and each of them consists of a pre-amplifier, a programmable gain amplifier (PGA), a low-pass filter and a circuit for offset compensation. Figure 27 shows a basic block diagram that illustrates one of the circuits.



**Figure 27 – Block diagram of the signal conditioning circuit.**

Since the absolute skin voltage level can be as large as 100V, the signal must be first attenuated before being processed and then sampled from the microcontroller. Therefore a high-impedance voltage divider in parallel with the skin should be used to reduce the voltage signal to an adequate level for further processing. Moreover the impedance needs to be higher than the load impedance not to interfere with the current signal. Assuming that the minimum gain of the conditioning circuit is unitary and that the maximum peak-to-peak output value is 3.3V, so that it can still be acquired from the microcontroller's AD channel, the minimum attenuation (maximal gain  $A_{max}$ ) of the voltage divider can be calculated as follows:

$$A_{max} = \frac{V_{out\ max}}{V_{skin\ max}} = \frac{3.3V}{200V} = \frac{1}{60}$$

Furthermore, assuming a maximum impedance value of 100k $\Omega$ , the voltage divider impedance should be at least 10 times higher (>1M $\Omega$ ) so that when in parallel, it doesn't sink much of the load current. Considering these parameters, the voltage divider shown in Figure 28 could be calculated as follows:

$$\frac{R_2}{R_1 + R_2} = \frac{V_{sample}}{V_{load}} \leq \frac{1}{60}$$



$$R_1 + R_2 > 1M\Omega$$

Assuming a high resistance  $R_1 = 3.9M\Omega$ , to meet the second condition,  $R_1$  could be set to  $65k\Omega$ , resulting in an attenuation of:

$$\frac{65k}{65k + 3.9M} = \frac{1}{61}$$

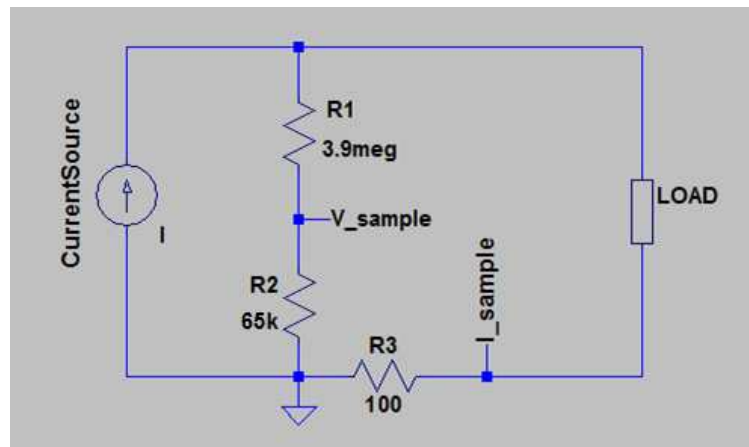


**Figure 28 – High-impedance voltage divider and shunt resistor for sampling the skin (Load) stimulation signals (voltage and current).**

For measuring the skin current signal a shunt resistor can be set in series between the skin and the ground. The shunt resistor must have a low impedance value not to interfere with the load. For these reason, it is recommended to keep it at least 10 times lower than the minimum load impedance. Assuming the minimum load  $10k\Omega$  and the maximum absolute current amplitude of  $3mA$ , the maximum shunt resistor  $R_3$  can be calculated according to the following equations. In this case the minimum gain of the conditioning circuit is also considered unitary and the maximum peak-to-peak output voltage  $V_{out\ max}$  is  $3.3V$ .

$$R_3 \leq 1k\Omega$$

$$\frac{V_{out\ max}}{V_{shunt\ max}} = \frac{3.3V}{R_3 \cdot 6mA} \geq 1$$

$$R_3 \leq \frac{3.3V}{6mA} = 550\Omega$$

In practice it is better to use  $R_3 = 100\Omega$  in case more current is needed.

The following topics present separately the design of each block of the signal measurement circuit.

### 3.6.2.2 Pre-Amplifier

The first signal conditioning step is the pre-amplifier. It consists of a high-impedance voltage follower, which transmits the signal from the voltage divider or shunt resistor to an inverter amplifier without sinking current from the load. The basic schematic is shown in Figure 29. The inverter amplifier was then necessary to compensate the gain of the low-pass filter later applied in this block. Moreover the inversion compensates the  $180^\circ$  phase shift caused by the afterwards applied PGA. A capacitance of 470pF was set in parallel to the feedback resistor in order to avoid high frequency noise before the PGA. The total gain of the amplifier for lower frequencies could be calculated as a regular inverter amplifier:

$$A = -\frac{R_5}{R_6} = -\frac{820}{1k} = 0.82$$

$$f_{3dB} = \frac{1}{2\pi R_5 C_2} = 400kHz$$

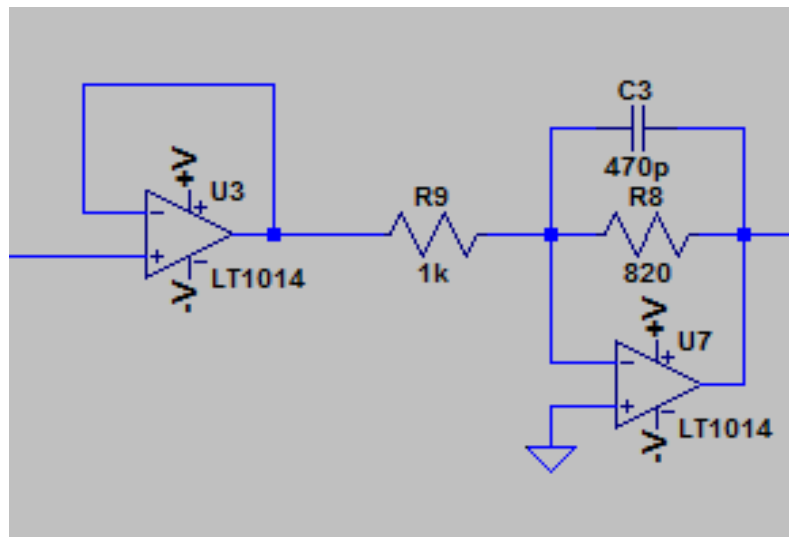


Figure 29 – High input-impedance voltage follower and pre-amplifier.

The pre-amplifier output was then connected to the PAG's input for further amplification. The feedback resistor of  $820\Omega$  was designed to compensate the gain of the further filtering steps, which are better described in the following section.

### 3.6.2.3 PGA

As discussed in the theoretical foundations, a solution for the problem of conditioning large voltage range signal is to use a programmable gain amplifier. In this project, the large range is given from the stimulation parameters and could be calculated as a function from the highest and lowest signals to be conditioned.

Concerning the skin voltage level, the highest level could be given by the voltage divider when the skin voltage reaches the high-voltage supply of the external source (for example  $\pm 100\text{V}$ ). On the other hand, the lowest value could be given as a function of the lowest current level ( $\pm 50\mu\text{A}$ ) and lowest load impedance ( $10\text{k}\Omega$ ). Considering the attenuation factor 61 in the divider, as described before, the highest voltage to be conditioned was then  $\pm 1.65\text{V}$  and the lowest  $\pm 16.5\text{mV}$ , which is 100 times lower.

For the skin current signal, these parameters could be easily defined with the shunt resistor ( $100\Omega$ ). The maximum signal was given by the maximal current ( $\pm 3\text{mA}$ ) through the shunt as  $\pm 300\text{mV}$  and the lowest could be estimated with the lowest current level ( $\pm 50\mu\text{A}$ ) as  $\pm 5\text{mV}$ , which is 60 times lower.

Without the PGA, the gain would have to be set constant to 1 not to saturate the  $3.3\text{V}$  of the AD converter for the higher signals, what would lead to a loss of precision when sampling the lower signals. As can be seen in Table 7, the signal's amplitude is inversely proportional to the current level, for a constant load. Therefore the control of the PGA gain could be set as a function of the skin current level to be generated and, consequently, could be programmed from the microcontroller itself.

**Table 7 – Maximal gain for each measuring circuit considering a constant 50k $\Omega$  load and maximum final amplitude of 3.3Vpp.**

| Skin Current Amplitude | Shunt Signal (100 $\Omega$ ) | Maximal Gain | Skin Voltage Amplitude | Voltage Divider (1/61) | Maximal Gain |
|------------------------|------------------------------|--------------|------------------------|------------------------|--------------|
| 50 $\mu$ A             | 5mV                          | 330          | 5V                     | 82mV                   | 20           |
| 500 $\mu$ A            | 50mV                         | 33           | 25V                    | 410mV                  | 4            |
| 1mA                    | 100mV                        | 16.5         | 50V                    | 820mV                  | 2            |
| 2mA                    | 200mV                        | 8.25         | 100V                   | 1.64V                  | 1            |

The chosen PGA was the Linear Technology LTC6910-2, a low noise digitally programmable gain amplifier that is easy to use and occupies very little PC board space. The inverting gain is adjustable using a 3-bit digital input to select gains of: 0, 1, 2, 4, 8, 16, 32 and 64V/V. When operated with unity gain, it can process rail-to-rail input signals, operating from single or split supplies from 2.7V to 10.5V. The 11MHz gain bandwidth product allow up to 200kHz for the maximum gain.

Figure 30 shows the schematic used in the simulation and the internal block diagram of the LTC6910-2.

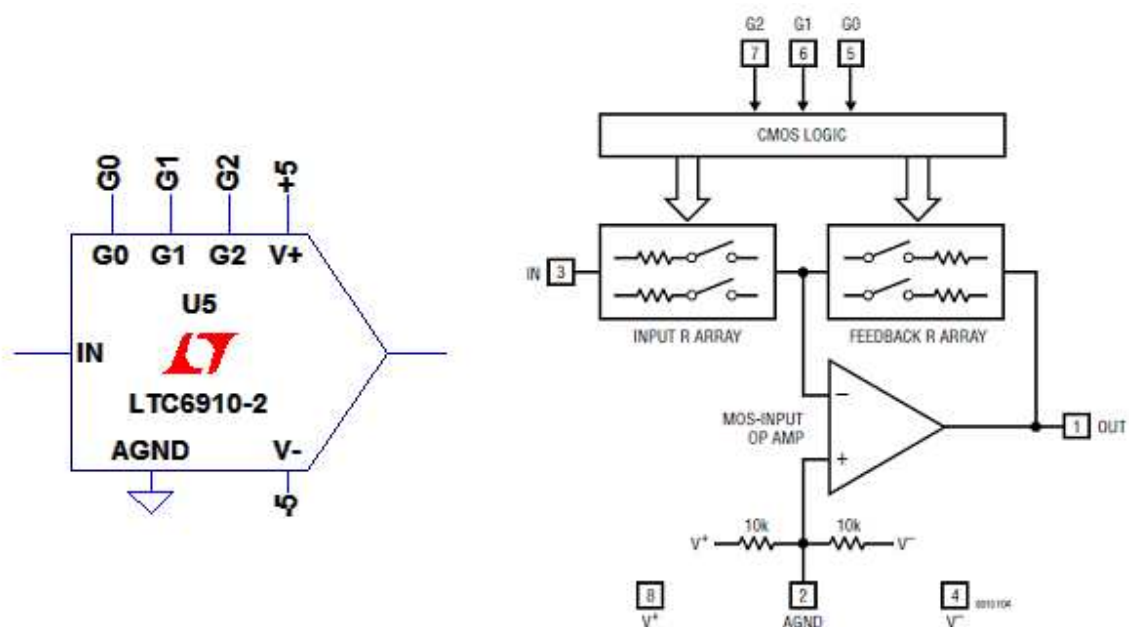


**Figure 30 – PGA simulation schematic and internal block diagram.**

Font: DATASHEET Linear Technologies LTC6910

One problem of this integrated circuit is the high input offset voltage of 1.5mV for unitary gain. When amplifying small signals using large gain, this offset can be as high as 100mV. Although it can be later digitally compensated in the data processing step and doesn't affect much the objectives of this project, this is a disadvantage of the circuit, and an analog solution could be implemented in the future as an improvement of this circuit.

Table 8 shows the programmable gain settings of the PGA and the input impedance. The gain configuration is given by a three bits parallel bus (G0, G1, G2). Each binary code corresponds to a different nominal voltage gain level and hence to different nominal linear input range. Moreover, the table gives the nominal input impedance for each gain setting, which varies from 1.25k $\Omega$  to 10k $\Omega$ . This impedance can be considered very low comparing to the skin impedance. Therefore the PGA circuit was applied after the high-impedance pre-amplifier and not before it.

**Table 8 – Gain settings and properties of the LTC6910-2 PGA.**

| G2 | G1 | G0 | Nominal Voltage Gain |      | Nominal Input Impedance (k $\Omega$ ) |
|----|----|----|----------------------|------|---------------------------------------|
|    |    |    | Volts/Volts          | (dB) |                                       |
| 0  | 0  | 0  | 0                    | -120 | (Open)                                |
| 0  | 0  | 1  | -1                   | 0    | 10                                    |
| 0  | 1  | 0  | -2                   | 6    | 5                                     |
| 0  | 1  | 1  | -4                   | 12   | 2.5                                   |
| 1  | 0  | 0  | -8                   | 18.1 | 1.25                                  |
| 1  | 0  | 1  | -16                  | 24.1 | 1.25                                  |
| 1  | 1  | 0  | -32                  | 30.1 | 1.25                                  |
| 1  | 1  | 1  | -64                  | 36.1 | 1.25                                  |

Font: DATASHEET Linear Technologies LTC6910

### 3.6.2.4 Low-Pass Filter

After the amplification of the pre-amplifier and PGA, a low-pass filter was designed to filter the high frequency noise of the signals. The chosen circuit was a 2<sup>nd</sup>-order active Bessel filter as shown in Figure 31. The cutoff frequency was set to 16 kHz. In this topology, for stability purposes, the gain  $A_i$  should be close to 1.268

for a quality factor  $Q=0.707$ .

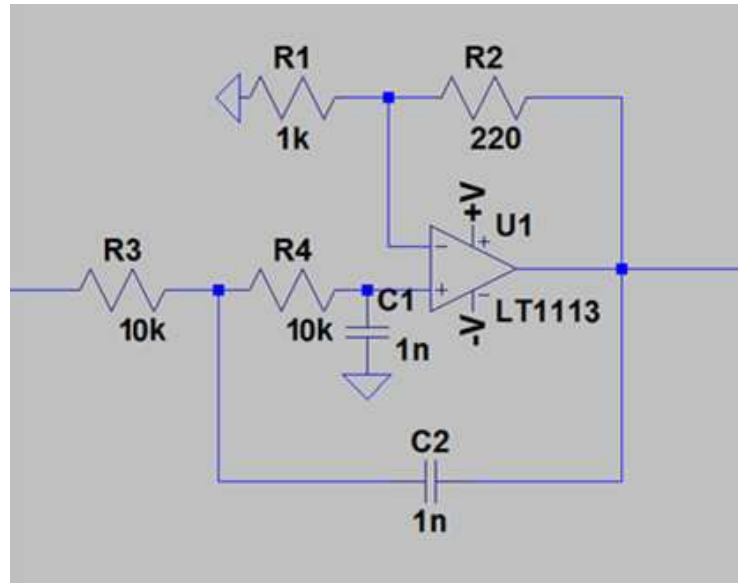


**Figure 31 – Low-pass Bessel filter.**

The dimensioning of the circuit could be made as follows:

$$f_{3dB} = \frac{1}{2\pi R_3 C_1} = 16kHz$$

$$A_i = 1 + \frac{R_2}{R_1} = 1.268$$

Assuming  $C_1 = C_2 = 1nF$  and  $R_1 = 1k\Omega$ , the other components should be  $R_3 = R_4 = 10k\Omega$  and  $R_2 = 268\Omega$ . In practice the feedback resistor was set  $R_2 = 220\Omega$ .

The chosen  $f_{3dB} = 16kHz$  was calculated so that the total cutoff frequency of the signal conditioning block was 10 kHz when added up to the pre-amplifier filter and the op amps finite gain-bandwidth product.

The filter gain of 1.22V/V has defined the pre amplifier gain of 0.82V/V as already shown in this chapter.

$$A_{Filter} = \left(1 + \frac{R_2}{R_1}\right) = 1.22 = \frac{1}{0.82}$$

Figure 32 shows the frequency response before and after the filter.

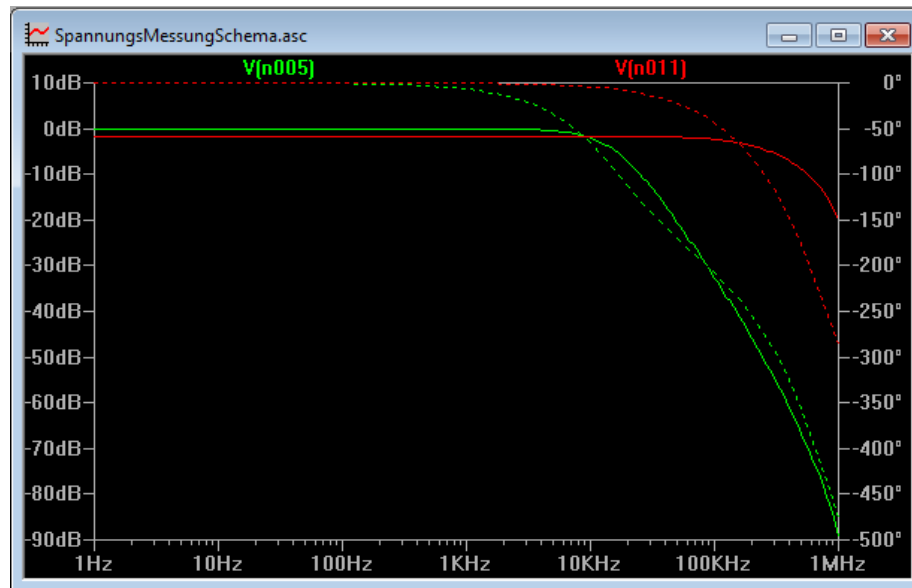


Figure 32 – Frequency response before (red) after (green) the low-pass filter.

### 3.6.2.5 Offset compensation

After the amplifier and filter the signal has adequate peak-to-peak amplitude not to saturate the AD converter of the microcontroller (3.3V). However it is still a bipolar signal with theoretically zero mean value. Given that the microcontroller can only sample signals from 0V to 3.3V it was necessary to add an offset voltage of 1.65V to the signal before connecting it to an AD channel. For this purpose an adder circuit was developed as shown in Figure 33. The feedback resistors were set 10kΩ so that the total non inverting gain was 2. In addition the signal from the filter was connected to the non-inverting input of the op amp through a 10kΩ resistor. The offset level was then obtained from the 5V supply and a voltage divider, whose total impedance should be also 10kΩ.

$$V_{offset} = 5V \cdot \left( \frac{R_{13}}{R_{12} + R_{13}} \right) = 1.65V$$

$$V_{out} = \left[ V_{in} \cdot \left( \frac{R_{12} // R_{13}}{R_{16} + R_{12} // R_{13}} \right) + V_{offset} \cdot \left( \frac{R_{16}}{R_{16} + R_{12} // R_{13}} \right) \right] \cdot \left( 1 + \frac{R_{11}}{R_{10}} \right)$$

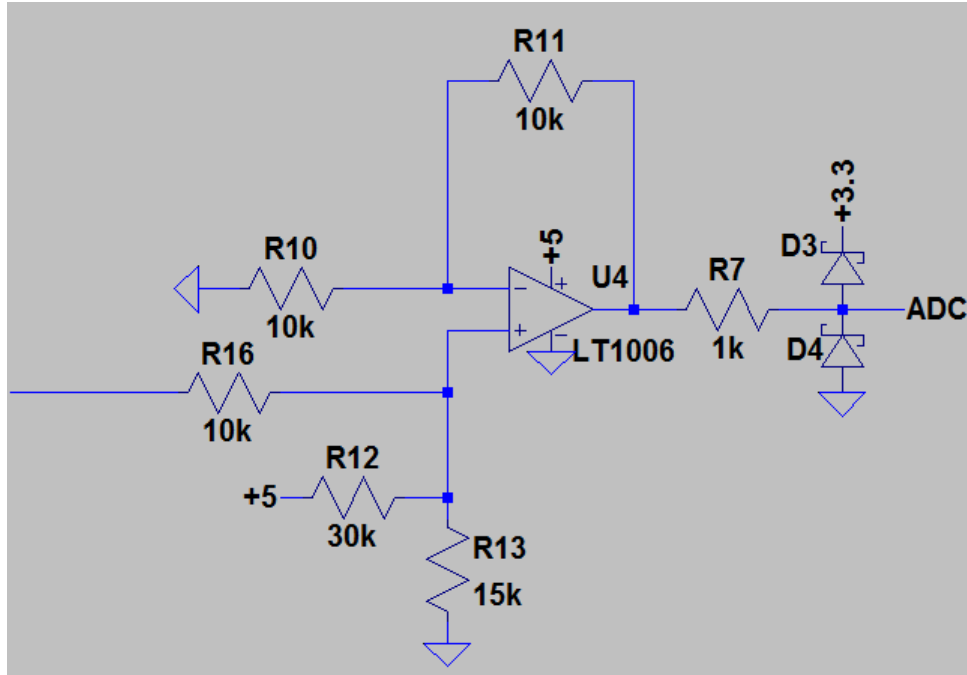


**Figure 33 – Adder for offset compensation.**

For  $R_{10} = R_{11} = R_{16} = R_{12} // R_{13} = 10k\Omega$ , the output voltage could be simplified to:

$$V_{out} = \left[ \frac{V_{in}}{2} + \frac{V_{offset}}{2} \right] \cdot (2) = V_{in} + V_{offset}$$

After this compensation the signal's amplitude should be between 0V and 3.3V and could be connected to the ADC. Nevertheless as a protection for the further circuit, two Schottky diodes with very low forward-voltage drop were applied and connected to ground and 3.3V. This guarantees that the output voltage keeps between 0V and 3.3V even if it tries to rise outside these limits, as shown in Figure 34. The red signal shows a sinus with 5Vpp, which is higher than the maximal range of 3.3V allowed at the microcontroller's input pins. Furthermore the green and blue signals are the output of the offset compensation circuit with and without the protection Schottky diodes. It is clear to see that with the protection the maximum amplitude is a few mV higher than 3.3V (approximately 3.45V), because of the diode voltage drop, what is still tolerated by the microcontroller. With no protection diodes, the voltage reaches almost 4V and could possibly damage the microcontroller. Since the 3.3V source is not ideal (output from a voltage regulator), a 1k $\Omega$  resistor was needed between the op amp output and the diodes in order to hold the voltage



difference that exceeds 3.3V. Without a resistor, the source output would increase instead of sinking the current and keeping 3.3V at the output.

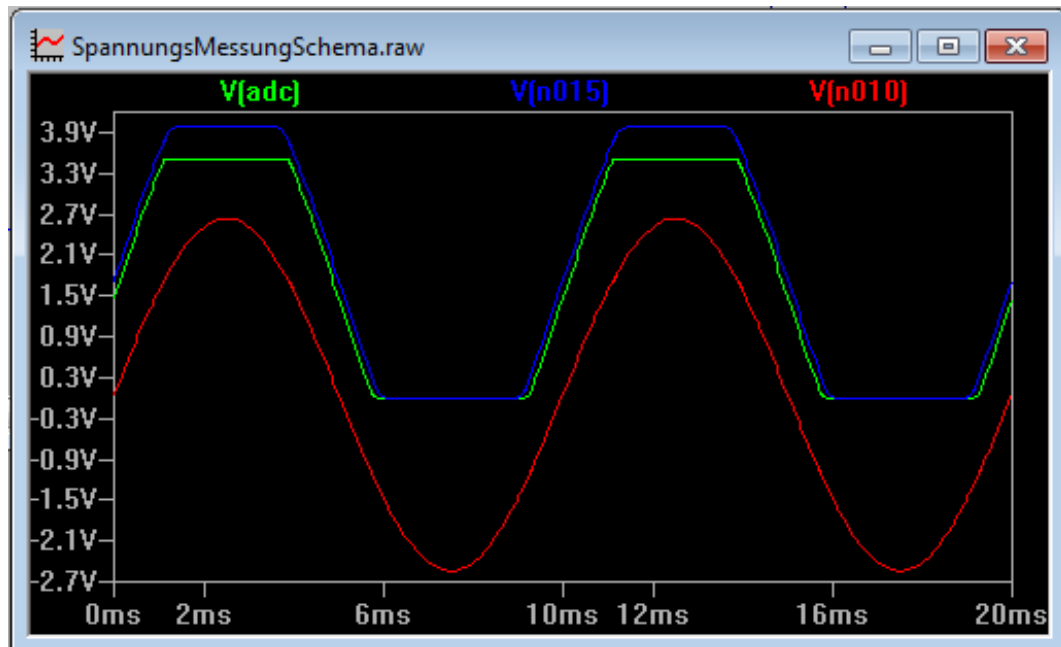


Figure 34 – Effect of the protection Schottky diodes.

Figure 35 shows the frequency response of the entire signal conditioning circuit (pre-amplifier, PGA, low-pass filter, offset compensation). As expected the circuit works as a very sharp low-pass filter with the cutoff frequency in 10kHz, what guarantees a low influence of the high-frequency noise.

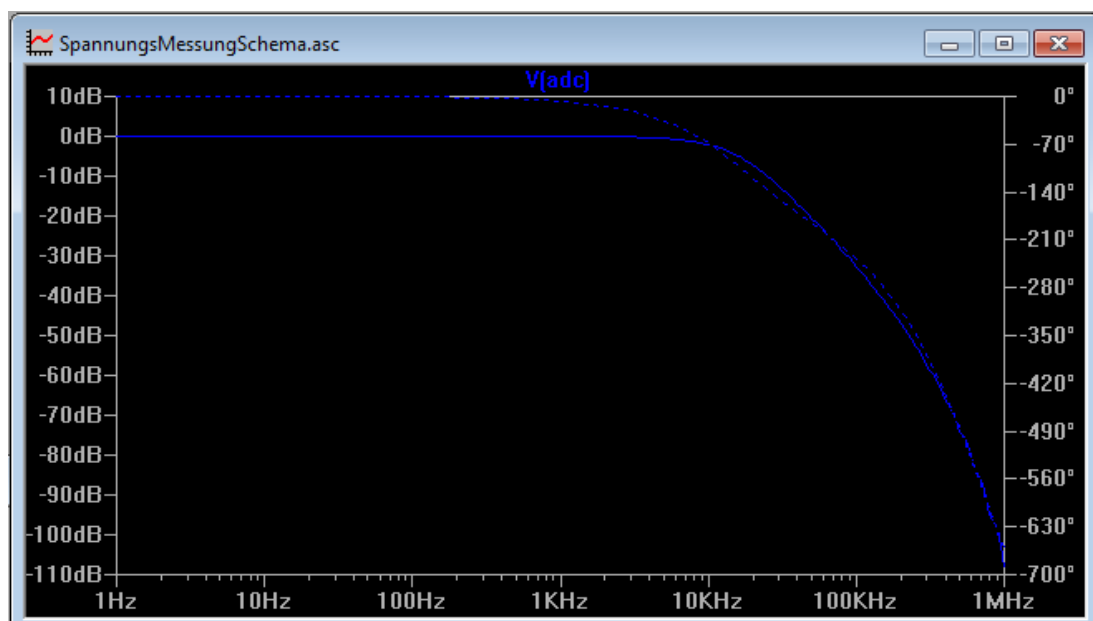


Figure 35 – Frequency response of the entire signal conditioning circuit

### 3.6.2.6 Schematics

The schematics of the signal measuring circuits for the skin voltage and current signals are equivalent. For this reason it is shown only one of them in this section, which corresponds to the skin voltage measuring circuit. Figure 36 shows the high impedance buffer and pre-amplifier schematic. The input is through a BNC connector.

The LT1014DS operational amplifier consists of four amplifiers on a chip. The other two are used for the same purpose in the skin current signal measuring circuit.

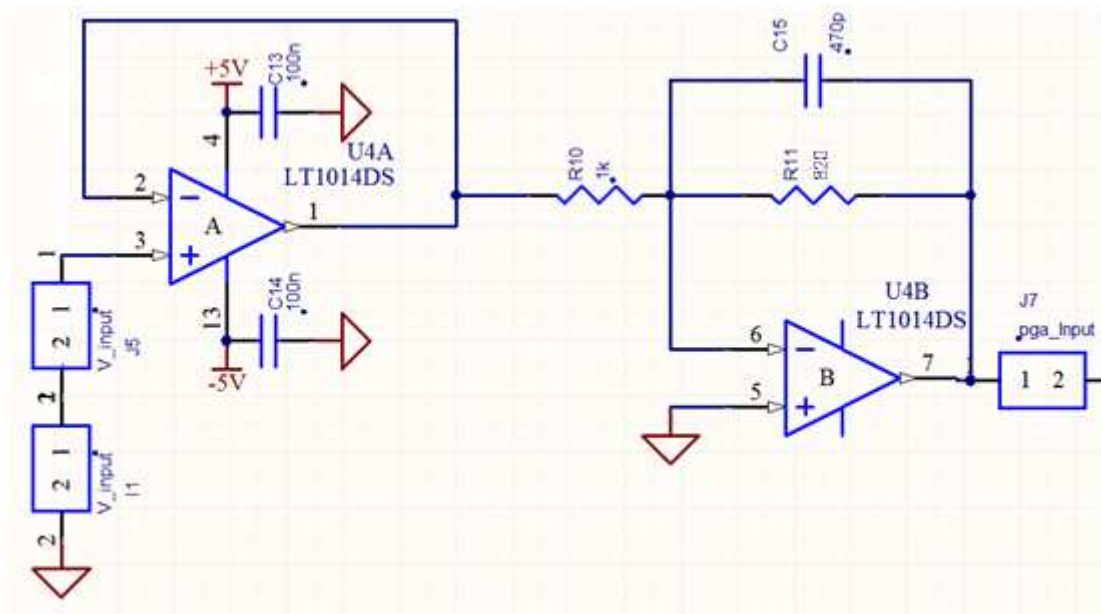
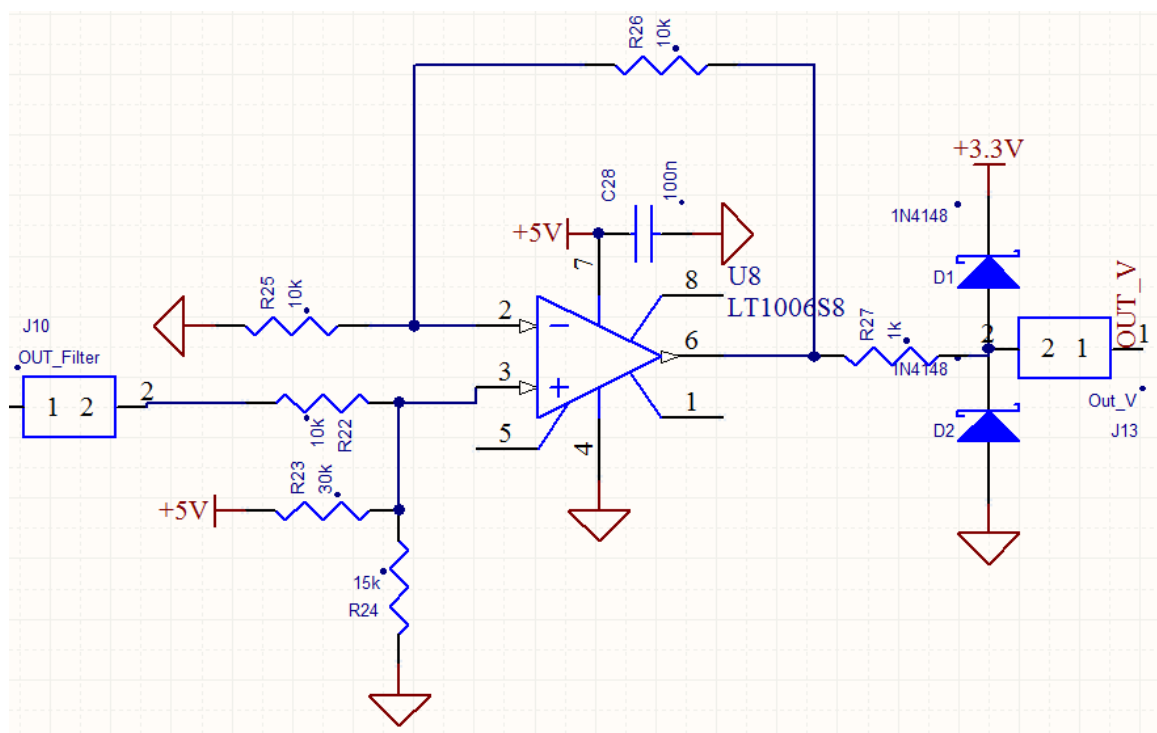


Figure 36 – Buffer and pre amplifier

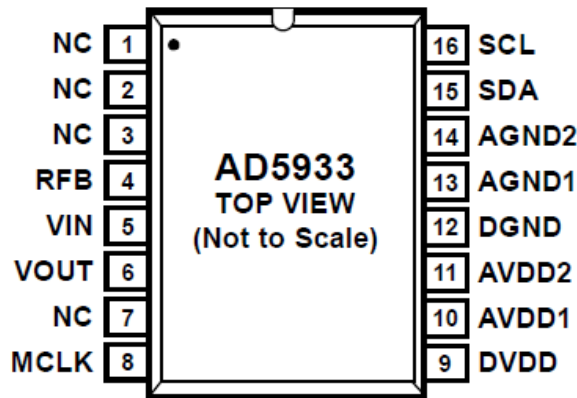
Figure 37 shows the PGA and low pass filter schematics. The LT1013S8 is a two operational amplifier on a chip CI and its second part is also the filter used in the skin current signal measuring circuit.

Figure 38 shows last part of these schematics (offset and protection diodes). The output is connected to the analog/digital connector and leads to the microcontroller ADC channel.



**Figure 38 – Offset compensation and Schottky diodes for protection**





**Figure 40 – Pin configuration of the AD5933**

Font: DATASHEET Analog Devices AD5933

The circuit design for the AD5933 is not so complicated. According to the datasheet it is recommended to tie all supply connections (Pins 9, 10 and 11) and run from a single supply between 2.7 and 5.5V. It is also recommended to connect all ground signals together (Pins 12, 13, 14).

The connection to the microcontroller is done through the I<sup>2</sup>C pins (SCL and SDA). They are open drain and require 10kΩ pull-up resistors to VDD. The MCLK pin can be left not connected since the integrated circuit has an internal oscillator of 16MHz.

The load should be connected between VOUT and VIN. VOUT is the output for the constant voltage excitation signal that makes a current flow through the load. VIN represents a virtual ground voltage of  $VDD/2$ , making the current a direct function of the load impedance. Then current flows back into the integrated circuit through the external feedback resistor that should be placed between VIN and RFB and defines the gain of the transimpedance amplifier on the receiver stage.

The choice of the feedback resistor should be made considering the output voltage amplitude and minimal impedance value in order not to saturate the receiver amplifier. Considering a maximal output of 3.3V (VDD) and a minimal load of 10kΩ the maximal current would be 330μA. As a consequence the external feedback resistor should be less than 10kΩ so that the maximal voltage is 3.3V and doesn't saturate the amplifier. For this reason a 1kΩ feedback resistor was used.

Table 9 shows a description of each pin of the AD5933.

**Table 9 – Description of the AD5933's pins.**

| Pin No. | Mnemonic | Description   |
|---------|----------|---|
| 1,2,3,7 | NC       | No connect  |
| 4       | RFB      | External Feedback Resistor. Used to set the gain of the current-to-voltage amplifier on the receive side. |
| 5       | VIN      | Input to Receive Transimpedance Amplifier. Presents a virtual earth voltage of VDD/2.                     |
| 6       | VOUT     | Excitation Voltage Signal Output.   |
| 8       | MCLK     | The master clock for the system if supplied by the user.  |
| 9       | DVDD     | Digital Supply Voltage.   |
| 10      | AVDD1    | Analog Supply Voltage 1.  |
| 11      | AVDD2    | Analog Supply Voltage 2.  |
| 12      | DGND     | Digital Ground.   |
| 13      | AGND1    | Analog Ground 1.  |
| 14      | AGND2    | Analog Ground 2.  |
| 15      | SDA      | I <sup>2</sup> C Data Input. Open-drain pins requiring 10 k $\Omega$ pull-up resistors to VDD.            |
| 16      | SCL      | I <sup>2</sup> C Clock Input. Open-drain pins requiring 10 k $\Omega$ pull-up resistors to VDD.           |

### 3.6.3.2 Schematics

Figure 41 shows the schematic of the AD5933 circuit used to measure the skin impedance. The Out\_Z connector is where the impedance should be connected and the resistor R34 controls the gain of the internal transimpedance amplifier. Moreover there are the clock and data bus of the I<sup>2</sup>C interface with pull-up resistor, ground and power supply pins.

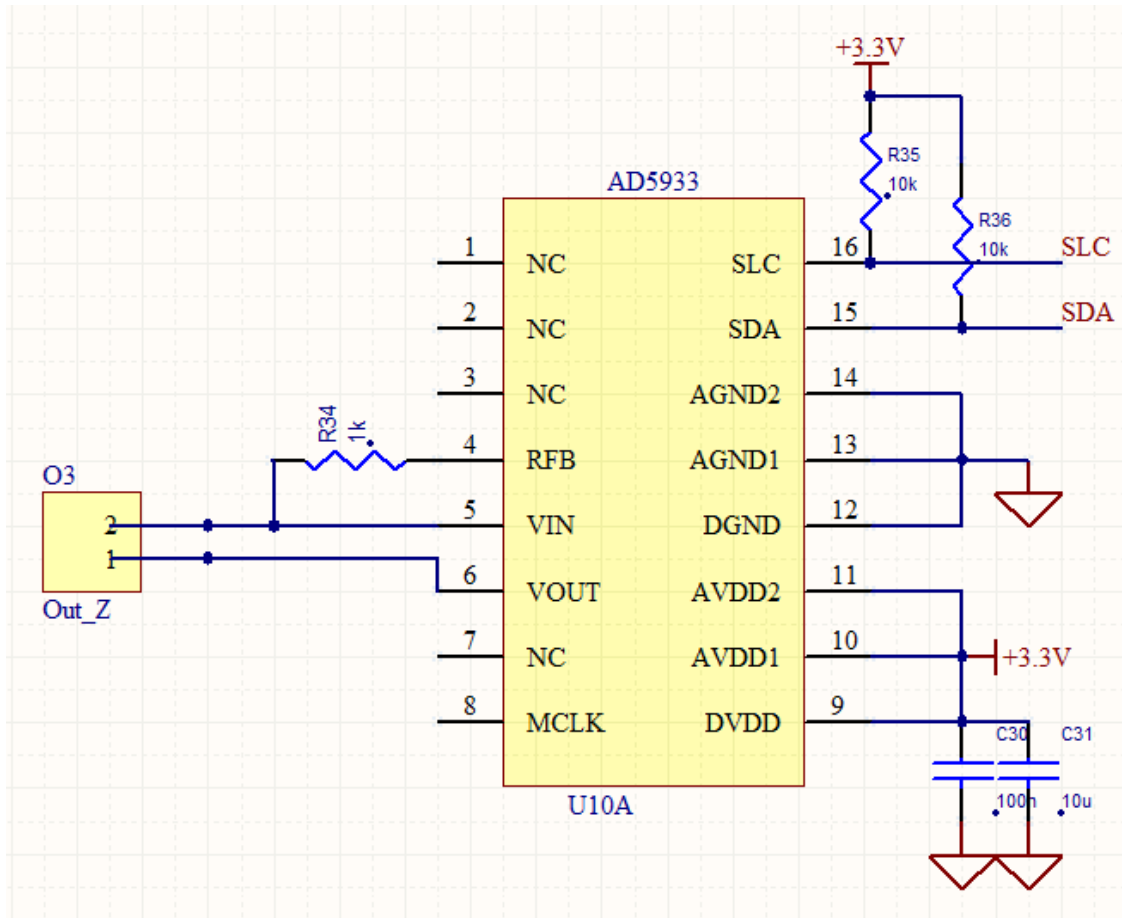


Figure 41 – Schematic of the AD5933

### 3.6.4 The Power Supply

The analog board components previously described need not only +5V but also -5V and 3.3V to work properly. However as the main power supply was chosen to be +5V so that it could be supplied from the USB port, two additional circuits were necessary to generate the desired voltage levels. The first one was a simple linear voltage regulator based on the LM1117 to generate +3.3V. The other circuit was a switching mode power supply (SMPS) based on the DC/DC converter LT1931 from Linear Technology, which generates the negative voltage level of -5V from the +5V with good efficiency.

### 3.6.4.1 Circuit Design

The +3.3V voltage regulator needs no special design. As recommended on the datasheet, it is only necessary to use one capacitor at the input and one at the output of the integrated circuit for decoupling and filtering. The switching mode power supply is more complex. In addition to the DC/DC converter LT1931 it is necessary to use some inductors, capacitors and resistors to achieve the desired operation.

The LT1931 a high power inverting SOT-23 current mode DC/DC converter, which includes a 1A integrated switch allowing high current outputs to be generated in a small footprint. The LT1931 switches at 1.2MHz, enabling the use of tiny, low cost capacitors and inductors. Fixed frequency switching ensures a clean output free from low frequency noise typically present with charge pump solutions. As recommended in the datasheet, two ferrite inductors of 10 $\mu$ H were used as well as a schottky Diode MBR.

### 3.6.4.2 Schematics

Figure 42 shows the 3.3V linear voltage regulator schematic based on the LM1117.

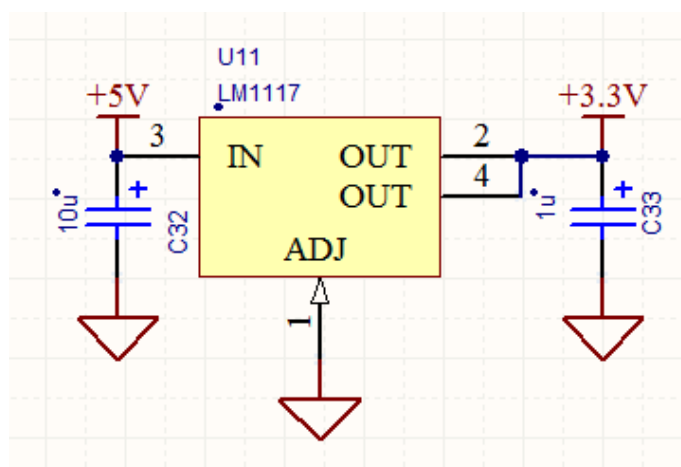


Figure 42 – 3.3V Linear Voltage Regulator



Figure 43 shows the schematics of the switching mode power supply based on the LT1931. The topology was based on the datasheet of the DC/DC converter.

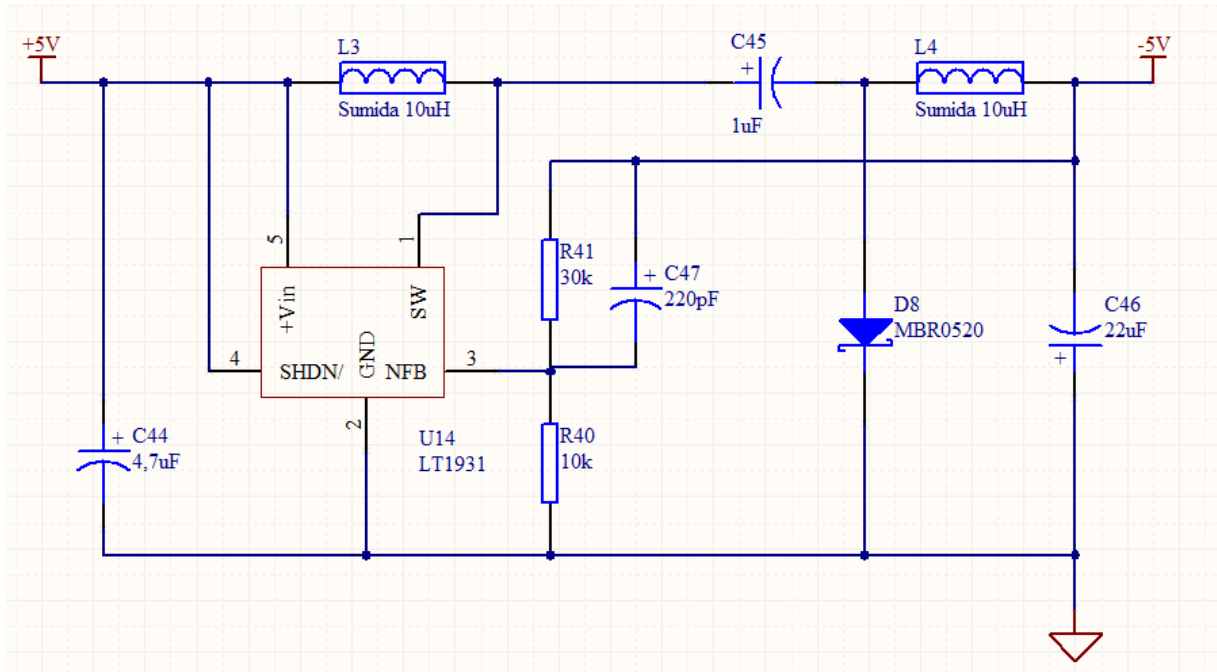


Figure 43 – Switching mode power supply to generate -5V from +5V

### 3.6.5 Layout of the Analog Board

Once finished the design and simulation process of the circuits, all the previously described schematics were put together and a PCB layout for the analog board could be drawn using the software Altium Design 2003.

It was chosen to use a simple two layers layout with all the components placed on the top layer. Moreover it was preferred to use surface mount devices (SMD) elements in order to make it easier to route and to save board space.

A special attention was given to the switched mode power supply. The correctly placement of the components and position of the signal planes is essential for a low noise operation and a high-performance of the DC/DC converter LT1931. In addition, it was used a ground plane in both top and bottom layers to reduce ground impedance and reduce noise effects.

The final layout was approximately 90cm<sup>2</sup> (108mm x 83mm). Figure 44 and 45 show the top and bottom layers of the layout respectively.

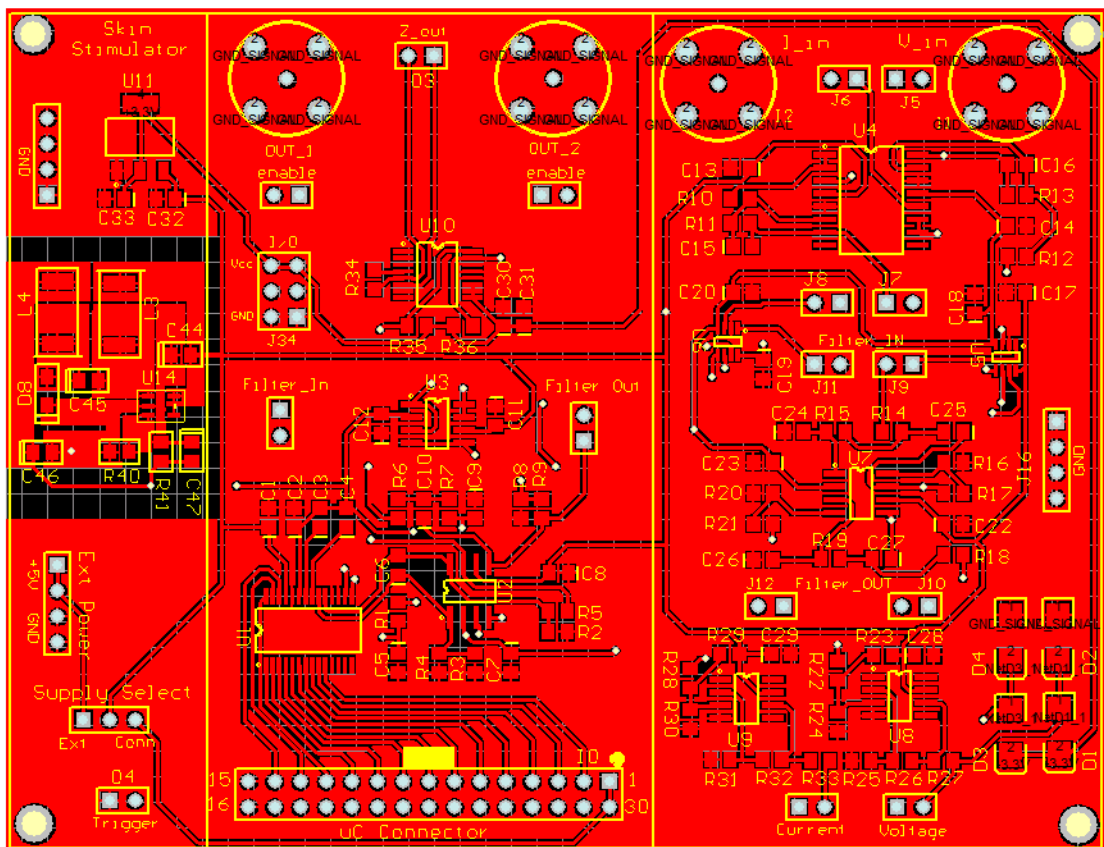


Figure 44 – Top layer and top overlay of the analog board.

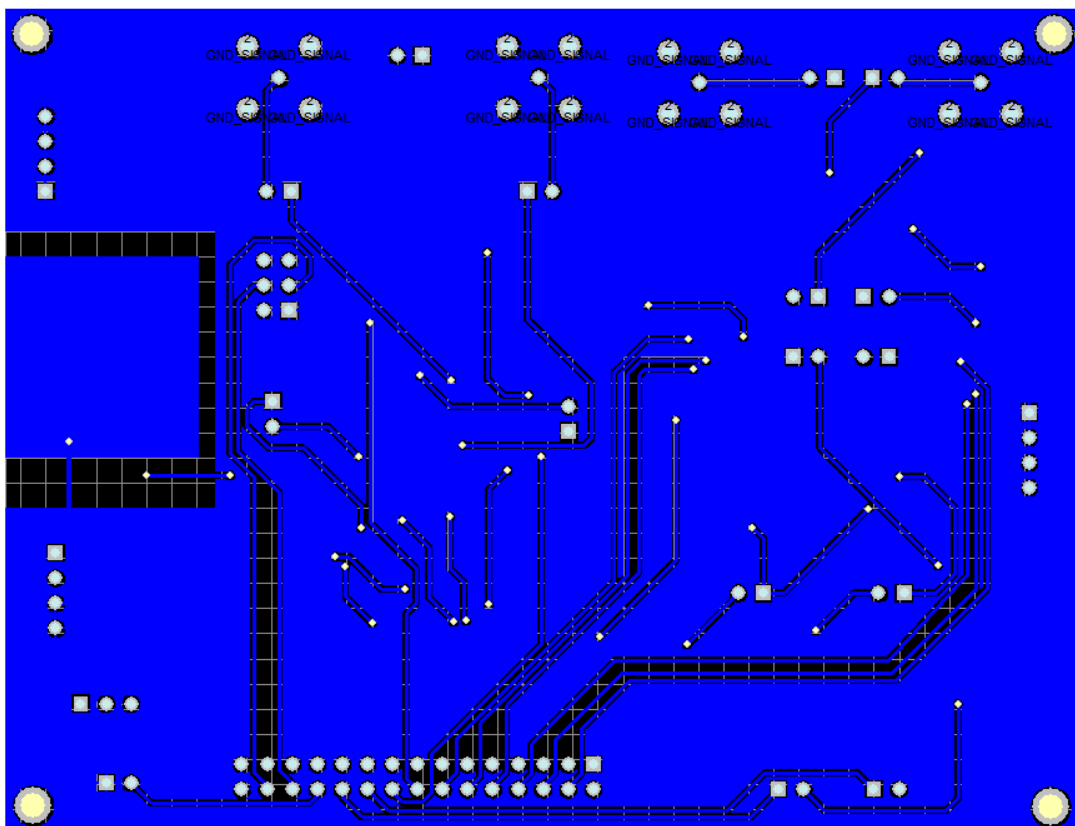


Figure 45 – Bottom layer of the analog board.

### 3.7 FIRMWARE OF THE STIMULATION SYSTEM

This topic presents the design of the firmware implemented for the ATMEL's microcontroller SAM3UE4 used in this project. As already explained, the firmware design was based on the V-model for software development and can be divided into five steps: requirements definition, design, code implementation, integration with the hardware and validation. The first three steps are described in this chapter and the integration, tests and system validation are shown in Chapter 4.

#### 3.7.1 Requirements Definition

The main purpose of the firmware is to control the microcontroller in order to perform all tasks that are necessary to achieve the objectives of the project. These tasks can be firstly seen as requirements of the firmware and are basically:

- Measuring the skin impedance value;
- Loading data from the host computer;
- Generating analog signals through the analog board based on the received data;
- Acquiring the skin voltage and current signals from the analog board;
- Transmitting the acquired data back to the host;
- Controlling the peripherals that are needed to perform these tasks.

All these requirements are represented in the UML use case diagram shown in Figure 46, and are further detailed in this topic.

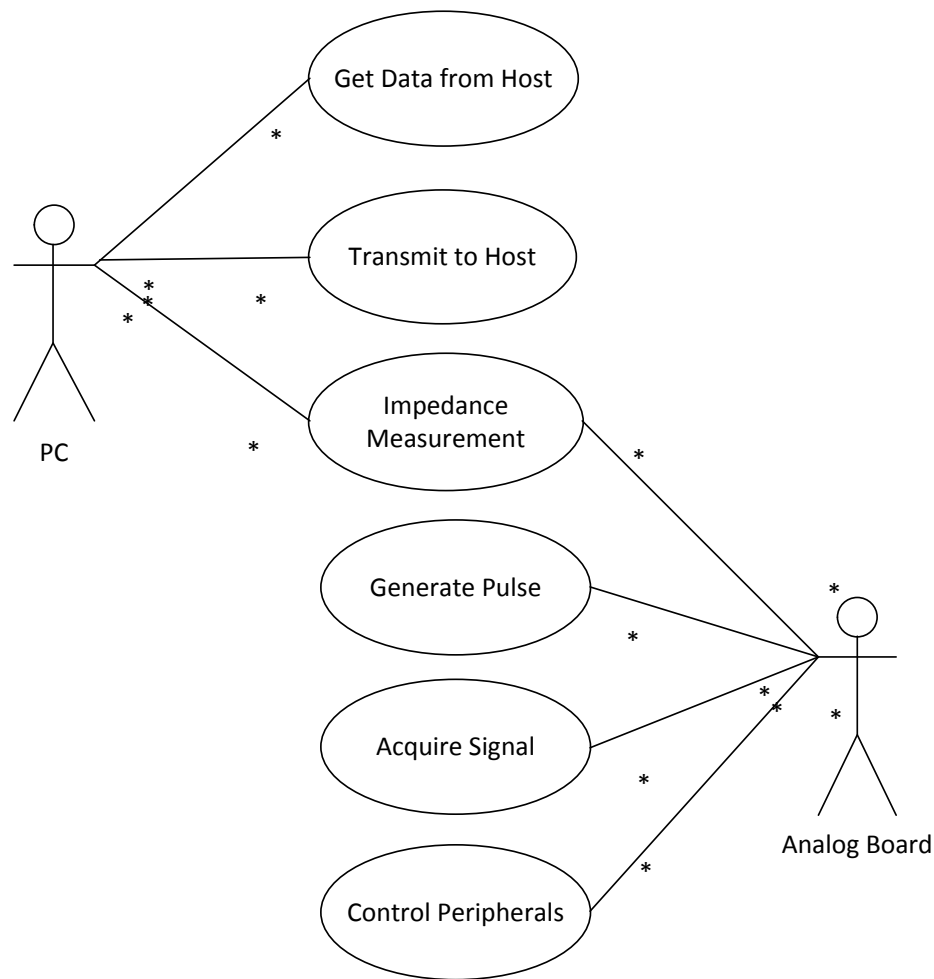


**Figure 46 – Use case diagram of the firmware**

Having defined the requirements and mapped them on a use case diagram, it was possible to design in details the tasks of each case as presented in the next topic.

### 3.7.2 Firmware Design

The firmware design is here described based on some basic UML diagrams such as state chart and sequence diagram. Figure 47 shows the state chart that represents the general functionality of the firmware. It describes the main function of the program and runs continuously until an interrupt occurs. The interrupt state chart is further described in this topic.

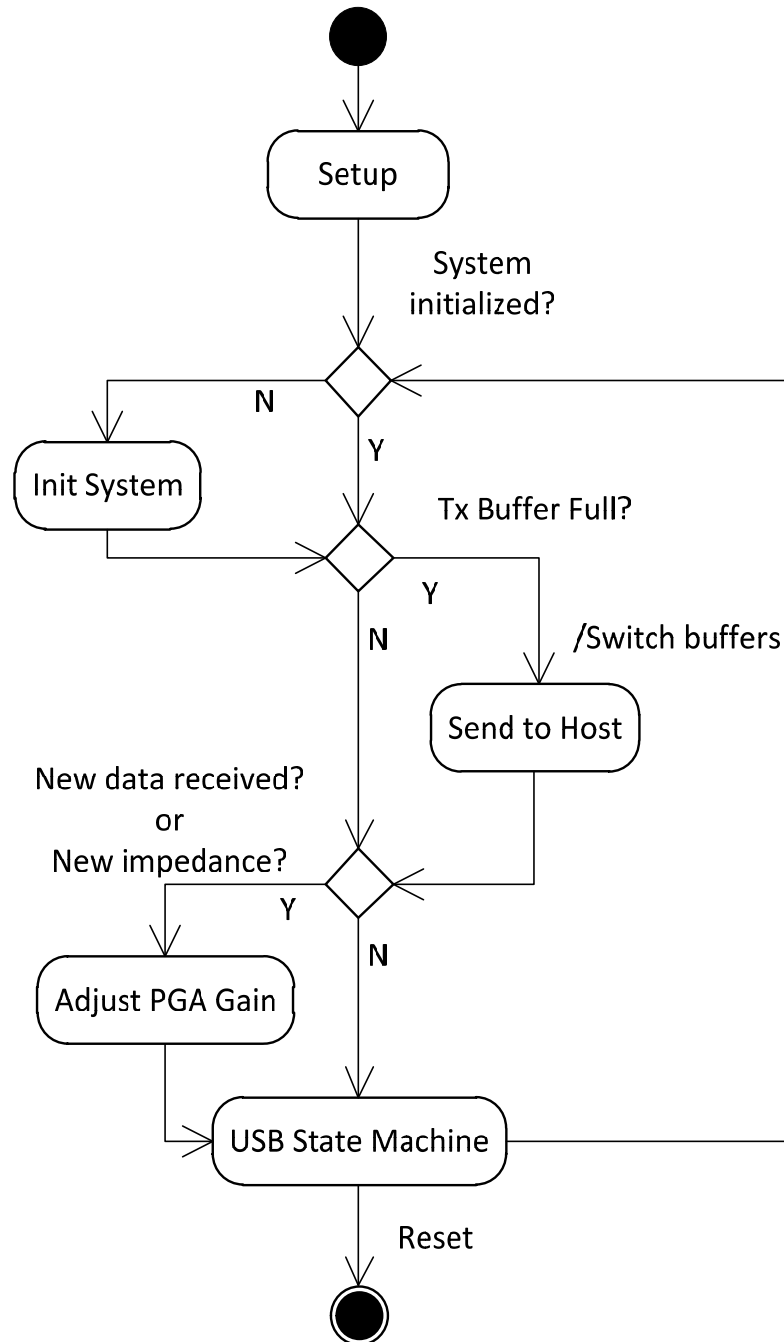


**Figure 47 – General state chart of the firmware**

The first state is called “Setup” and represents the initial configuration of the system, such as device drivers, communication interfaces, IO ports and some basic peripheral configurations. After the setup, the system verifies the connection to the host, checking if the USB connection is established and if the serial driver is ready.

After the setup the system checks if it has already been initialized and case not, it performs an initialization. It consists in measuring the skin impedance, receiving data from the host and configuring the PGA gains. This state is controlled by the

remote user interface and is further described as the “init System” state.

After being initialized the system keeps checking if the transmit buffer is full. When the buffer which contains the actual data read from the ADC channels is full, the controller sends it to the host. Afterwards, the system checks if new data was received and adjust the PGA gains if necessary. At last, the USB state machine is performed and the loop is restarted.

The next topics describe in details the most important states of the diagram above.

### 3.7.2.1 Setup State

The “Setup” state makes some basic configurations of the system and can be divided into five different tasks: USB, IOs, Timers, ADC and TWI configurations, as shown in Figure 48.

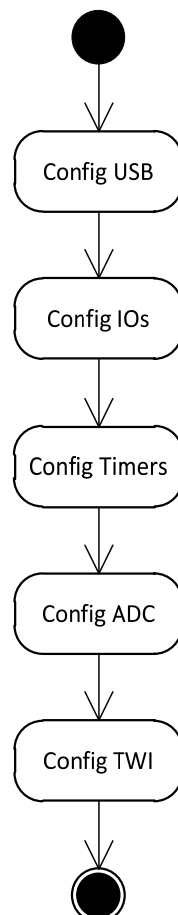


**Figure 48 – Sate flow of the Setup state.**

At first it is made the configuration of the USB communication interface beginning with the initialization of an USB device driver instance. After that, the connection is performed and the microcontroller waits for the host connection. The driver used for this communication was a CDC serial driver that emulates a serial port with the USB interface. It makes it easier to implement a host application and device driver.

After the correct establishment of the USB connection, the firmware performs the IO pins configuration. Each pin can be configured as a general purpose IO or connected to a special peripheral of the microcontroller. In the first case, it is necessary to configure if the pin is input or output among other features. Table 10 shows the list of IO interfaces and their chosen configurations.

**Table 10 – IO Configuration Table**

| Microcontroller Pin | Function  | Configuration |
|---------------------|---|---------------|
| PA1, PA2, PA3       | PGA1 gain control                                 | IO output     |
| PA4, PA5, PA6       | PGA2 gain control                                 | IO output     |
| PA7                 | Trigger   | IO output     |
| PA9                 | I <sup>2</sup> C Data (for AD5933)                | TWD0          |
| PA10                | I <sup>2</sup> C Clock (for AD5933)               | TWCK0         |
| PA11                | Function selection (stimulation or Z measurement) | IO input      |
| PA12                | IO for Debug                                      | IO output     |
| PA22                | AD channel 0                                      | AD12B0        |
| PA30                | AD channel 1                                      | AD12B1        |
| PC19                | DAC clock   | IO output     |
| PC20 to PC31        | DAC pins (signal out)                             | IO output     |

Having the IOs configured, the next task was to configure the timers. Two timers were used to control the generation of the stimulation pulse and the data acquisition's sample rate. Both of them were configured to count until the value stored in the respectively Counter Value register and then caused an interrupt every time it reached this limit. The interrupt handle routines are further described in the next states.

Another initialization is the configuration of the AD converter. First the AD clock

must be configured, for example to 12MHz, as well as the sample-and-hold time and mode register with default values. At last the channels AD0 and AD1 are enabled and the ADC is ready to be used.

The last initialization consists in configuring the TWI interface for the AD5933 and in initializing a driver for this interface. The most important feature to be configured is the clock frequency. According to the AD5933 datasheet, the I<sup>2</sup>C clock should be no more than 400KHz. The chosen value was set to 100KHz.

### 3.7.2.2 System Initialization State

The “Init System” is performed after the setup state at the first time the system is turned on. It consists in waiting the commands from the user interface in order to perform the following tasks: measurement of the skin impedance, receiving the stimulation signal from the host and configuring the PGA’s initial state. This state is described as a diagram in Figure 49.

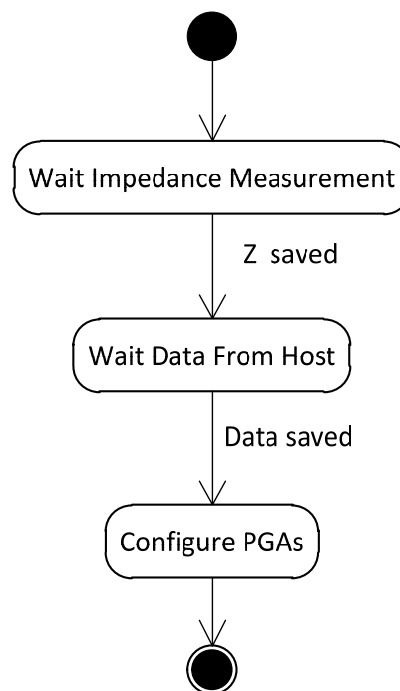


**Figure 49 – State chart of the system initialization**

At first the system waits for a command from the host to perform the skin



impedance measurements and transmits the results to the host. This is done until the host sends a command to save the last read impedance value. After that, the program waits to receive the signal generation data from the host. Afterwards the PGA's gains are configured based on the saved impedance value and the received data. These gains are then sent back to the host computer.

### 3.7.2.3 Impedance Measurement State

After initializing and configuring the hardware, the firmware starts the impedance measurement state. The basic task of this state is to configure the AD5933 properly, control the impedance measurement flow and calculate the impedance value with the data received from the integrated circuit. The communication with the IC was made thorough the serial I<sup>2</sup>C protocol. Actually the Atmel Two-wire Interface (TWI) was used. It interconnects components on a unique two-wire bus, made up of one clock line and one data line with speeds of up to 400 Kbits per second, based on a byte-oriented transfer format. It can be used with any I<sup>2</sup>C compatible device and configured as master or slave. Figure 50 shows the state chart of this state.

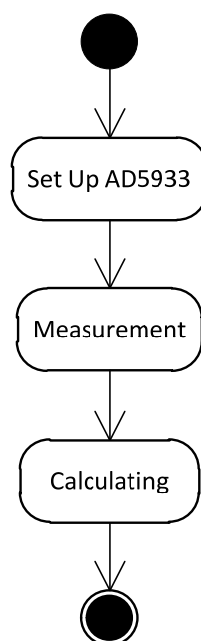


**Figure 50 – State chart of the impedance measurement state**

After the configurations, the microcontroller is ready to communicate with the AD5933. The next task is then setting up the registers of the IC so that it works properly as desired. The registers to be configured are shown in Table 11.

**Table 11 – Registers to be configured in the initialization state**

| Register             | Function  |
|----------------------|---|
| Control Register     | Output voltage range (2Vpp, 1Vpp, 400mVpp, 200mVpp) Internal PGA gain (x1 or x5) Operation Mode       |
| Start Frequency      | Start frequency of the excitation signal (1KHz – 100kHz)  |
| Increment Frequency  | Frequency increment between consecutive frequency points along the sweep                              |
| Number of Increments | Number of frequency points in the frequency sweep (0 - 511)   |
| Settling Time Cycles | Number of output excitation cycles through the impedance before a conversion is performed (0 – 2044). |

The registers were configured to work with an excitation voltage of 2Vpp, unitary PGA gain and 255 cycles for settling time. The start frequency and increments are configured through the user interface. After these settings, the IC is ready to start measuring the unknown impedance value.

Therefore the next state consists in controlling the measurement flow until valid values for the real and imaginary impedance are available in the AD5933 registers. This is done using the bits 12 to 15 of the control register, as shown in Table 12.

**Table 12 – Control Register Map (D15 to D12) of the AD5933**

| D15 | D14 | D13 | D12 | Function                        |
|-----|-----|-----|-----|---------------------------------|
| 0   | 0   | 0   | 0   | No operation                    |
| 0   | 0   | 0   | 1   | Initialize with start frequency |
| 0   | 0   | 1   | 0   | Start frequency sweep           |
| 0   | 0   | 1   | 1   | Increment frequency             |
| 0   | 1   | 0   | 0   | Repeat frequency                |
| 1   | 0   | 0   | 0   | No operation                    |
| 1   | 0   | 0   | 1   | Measure temperature             |
| 1   | 0   | 1   | 0   | Power-down mode                 |
| 1   | 0   | 1   | 1   | Standby mode                    |

At first the device must be placed into standby mode. Afterwards it can be initialized with the start frequency and the excitation signal is turned on. After a sufficient amount of settling time has elapsed, the firmware starts the frequency sweep command and the AD5933 starts measuring the impedance value. It is necessary to poll the status register in order to identify if valid data is available to be read. When the corresponding flag is set, the firmware can read the values from real and imaginary registers. If the sweep is not over a command to increment the frequency or to repeat it must be performed and new values can be read. After the sweep is complete, the AD5933 must be programmed back to Power-Down Mode. The flow diagram of this state is better described in Figure 51.

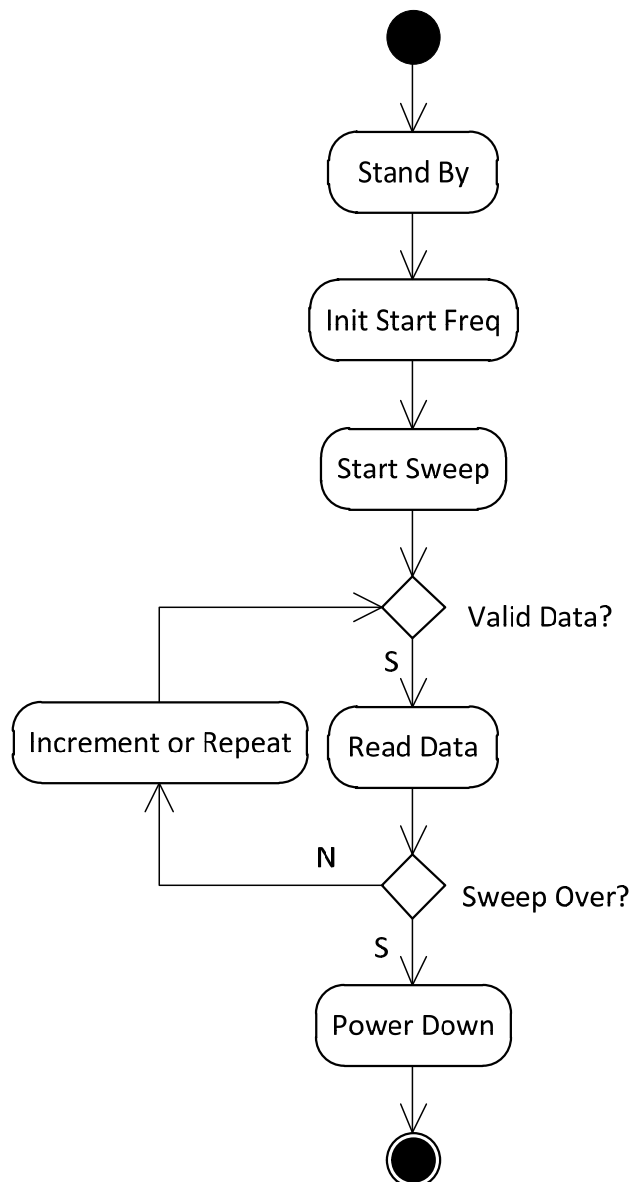


**Figure 51 – Flow chart of the impedance measurement**

Once the measurement is done and the real (R) and imaginary (I) values are available, the magnitude can be easily calculated as follows:

$$Magnitude = \sqrt{R^2 + I^2}$$

To convert this number into impedance, it must be multiplied by a scaling factor called the gain factor. The gain factor is calculated during the calibration of the system with a known impedance connected between the VOUT and VIN pins.

$$GainFactor = \frac{1}{\frac{Known\_Impedance}{Magnitude}}$$

Once the gain factor has been calculated, it can be used in the calculation of any unknown impedance between the VOUT and VIN pins.

$$Unknown\_Impedance = \frac{1}{GainFactor \times Magnitude}$$

#### 3.7.2.4 Get Data From Host State

The purpose of this state is to receive two data buffer representing, for each sample of a whole period, the amplitude in  $\mu A$  and time in  $\mu s$  that the sample value should be hold. This data must be stored and then used to generate the stimulation pulse. Figure 52 shows how the received data buffers should be used.

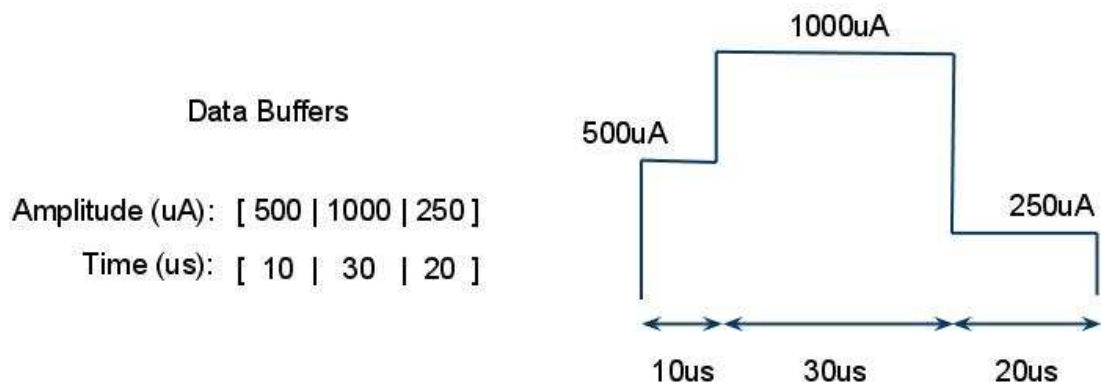


Figure 52 – Example of received buffers and how they are used to generate a pulse

After saving the buffers it is necessary to convert the amplitude values from amperes to a 12-bit code that the DAC can understand. Considering a unitary gain of the current source (1 mA/V), assuming the maximal current of  $\pm 3\text{mA}$  as defined on the requirements and the 12-bit DAC resolution, the relation between the output current and the input code of the DAC, can be defined as shown in the graphic of Figure 53.

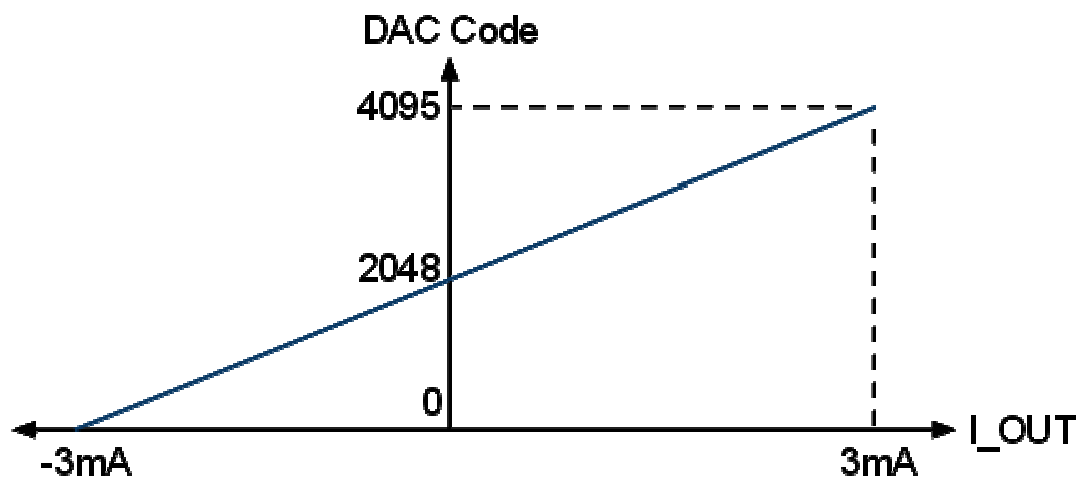


Figure 53 – Input DAC code and output current.

This conversion must be done for each value of the amplitude buffer, as follows:

For example, if the amplitude value stored in the buffer is 0, the DAC code is 2048, which corresponds to 0mA at the DAC output and 0V at the current source input leading to 0mA skin current. Furthermore, if the buffer amplitude is 3000 $\mu$ A (3mA), the DAC code is 4095, which corresponds to 10mA at the DAC differential output, 3V at the current source input and therefore to 3mA in the skin.

### 3.7.2.5 Configure PGAs State

The next state after receiving the data is to configure some peripherals that depend on these data such as the programmable gain amplifiers (PGAs) applied to conditioning the skin voltage and current signals. The gain of each PGA can be defined based on the highest absolute skin current value to be generated and the average skin impedance value as already discussed on section 3.9.1.2. As a consequence, the first step of this task is to find the highest absolute current value in the received buffer and calculate the highest voltage value (with the measured skin impedance). With these two parameters, the voltage divisor factor and shunt resistor the gain of each PGA can be configured according to the following equations and summarized in Table 13.

$$\text{Skin Voltage Signal} = \frac{I_{max} \times Z_{skin}}{V_{divisor\_factor}}$$

$$\text{Skin Current Signal} = I_{max} \times R_{shunt}$$

**Table 13 – Relationship between the absolute skin maximal voltage and current levels and the PGA's gains.**

| Maximal Skin Voltage/Current Signal | PGA Gain |
|-------------------------------------|----------|
| $V > 1.65V$                         | 0        |
| $825mV < V \leq 1.65V$              | 1        |
| $412mV < V \leq 825mV$              | 2        |
| $206mV < V \leq 412mV$              | 4        |
| $103mV < V \leq 206mV$              | 8        |
| $52mV < V \leq 103mV$               | 16       |
| $26mV < V \leq 52mV$                | 32       |
| $V \leq 26mV$                       | 64       |

In this case  $V_{divisor\_factor}$  must be at least 60, considering the highest voltage of 100V and the shunt no more than 500 $\Omega$  for 3mA maximal absolute current amplitude. In case one of these values are changed, for example by programming the external current source gain to be more than 1mA/V, increasing the maximum output current, the shunt resistor should be also adjusted for properly calculating the PGAs' gains.

The gain is then configured by setting the 3-bit code of each PGA corresponding to the gain through the respective IO lines. These gains are also used when acquiring the current and voltage samples in order to convert them to the original value, as shown in the next sections. After configuring the gain it is sent back to the host computer.

#### 3.7.2.6 Send to Host State

The main task within this state is monitoring the transmit buffer size, which holds the skin voltage and current samples as well as controlling the double buffering task. When the buffer size reaches its capacity, the firmware switches the flag assigning that the second buffer should be used and starts the transmission of the full buffer to the host through the USB interface.

At this point it is important to consider the amount of data to be sent and the speed of the data transfer. As already shown in this chapter, the buffer contains multiple samples of four bytes: two bytes for the skin voltage sample and two for the skin current samples. Considering the minimum sample period of 10 $\mu$ s as specified in the system requirements the amount of data generated per second is 250 kB. For this reason it is necessary to have a data transfer rate higher than 2 Mbps, which can be achieved with the microcontroller's high speed USB interface.

#### 3.7.2.7 Interrupts

During the main loop execution, the system can be interrupted to perform some

relevant tasks. There are mainly three different interrupt sources: two timers and the USB received callback. Figure 54 represents the interrupt handling routines.

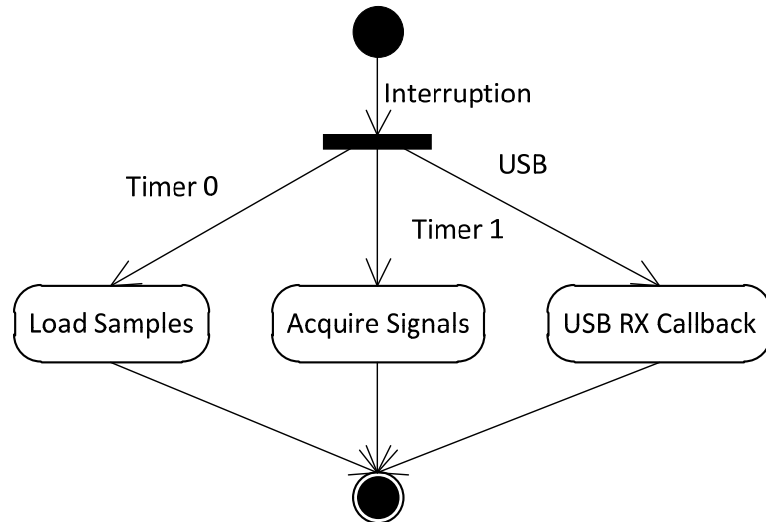


**Figure 54 – State chart of the interrupt sources**

Timer 1 interruption handling routine is responsible for generating the stimulation signal and is here called “load sample” state. The Timer 2 synchronizes the “acquire signals state” and the USB interruption is performed when any data is received on the USB buffer. In the following topics the interrupt states are better described.

#### 3.7.2.8 Load Samples (Timer 0 interrupt)

This state makes use of Timer 0 to synchronize the signal generation. It consists in continuously loading each amplitude value from the amplitude buffers to the DAC input and holding it for the specified time read from the time buffer. When the timer reaches its limit, an interruption occurs and the next sample is loaded. This is done for every sample within a period and then restarted indefinitely until the timer is stopped. Furthermore a trigger pulse is generated every time a new period begins. This is useful for external measurements devices to get synchronized. The next diagram represents the task flow of this state.



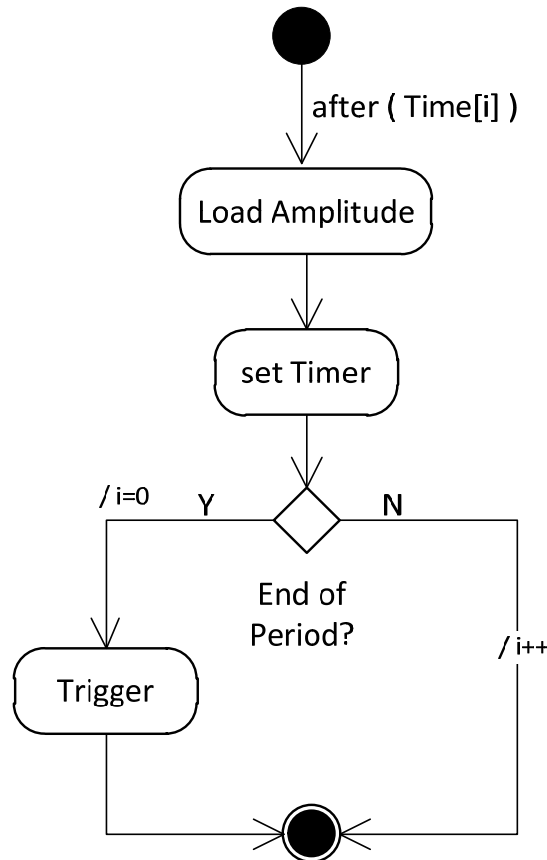


**Figure 55 – State chart representing the signal generation task**

### 3.7.2.9 Acquire Signals (Timer 1 interrupt)

In this state the skin voltage and current signals are sampled from the analog board and saved in a buffer for further transmission to the host. Similar to the “load sample”, this state makes use of the Timer 1 for synchronizing the sampling rate. After a pre-defined period is elapsed, a timer interrupt is generated and the main task is executed.

The first step is to start an AD conversion and read the two channels corresponding to the voltage and current signals respectively. Afterwards each 12-bit value that ranges from 0 to 4095 (0V to 3.3V) is converted to a corresponding 16-bit value in dozens of millivolts (10 x mV) or microamperes ( $\mu\text{A}$ ). This is done based on the parameters of the analog board such as voltage divider, shunt resistor and PGAs gain as better shown in the following equations.

For the voltage signal, which is sampled after passing through a voltage divider

attenuation of  $V_{div}$ , a PGA with gain  $G_{pga1}$  and an offset shift of 1.65V, the conversion is:

$$V_{skin} = \left[ ADC_{code1} \cdot \left( \frac{3300mV}{4095} \right) - 1650mV \right] \cdot V_{div} \cdot \frac{1}{G_{pga1}} \text{ mV}$$

Because of the system's parameters and implementation this value is given in mV and should be further divided by factor 10 before saved in order to guarantee a maximum size of 16-bits. For this reason, the transmitted value that corresponds to the skin voltage level is given in dozens of millivolts.

Regarding the skin current signal, the conversion is quite different since the signal is sampled from a shunt resistor of  $R_{shunt}$  ohms and not a voltage divider. Besides that, the equation is similar to the voltage signal, as follows:

$$I_{skin} = \left[ ADC_{code2} \cdot \left( \frac{3300mV}{4095} \right) - 1650mV \right] \cdot \frac{1}{R_{shunt}} \cdot \frac{1}{G_{pga2}} \text{ mA}$$

In this case it is important to multiply the value by a factor 1000 in order to obtain the value in  $\mu A$ .

At last, these values are separated in two bytes each (high and low part) and stored in a buffer. First comes the low part then the high part of the voltage signal and after that the low and high parts of the current signal, as shown in Figure 56. For this task two buffers are used to avoid delays or losses of data. While one buffer is full and waits to be transmitted, a second buffer is used to store the sampled values. This method is well known as double buffering.

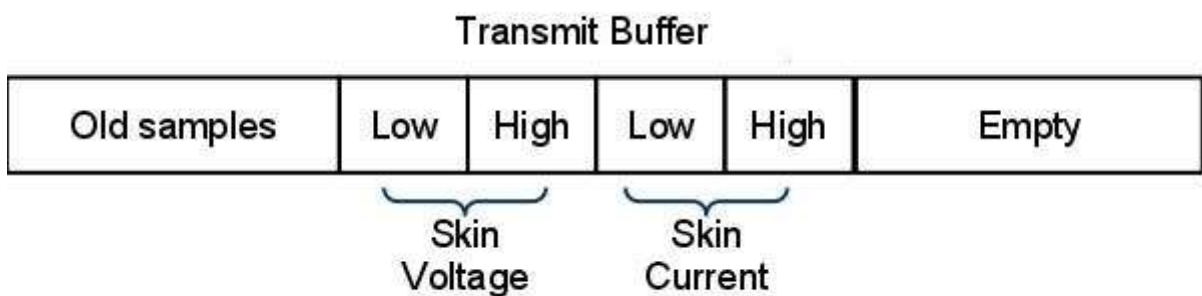


**Figure 56 – Representation of the transmit buffer: in every cycle four bytes are saved in the buffer until it is full.**

A basic state chart of the signal acquisition state is represented in Figure 57.

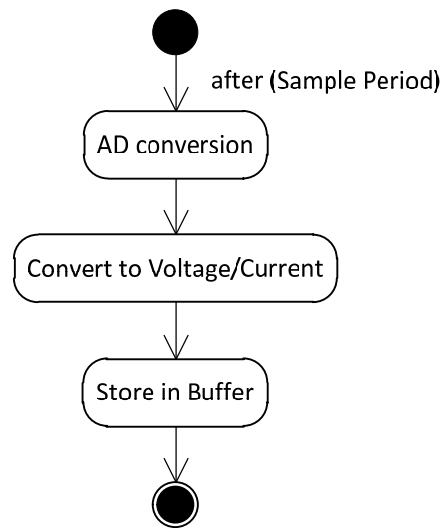


**Figure 57 – State chart of the signal acquisition**

#### 3.7.2.10 USB Received Data Callback (USB interrupt)

The last interrupt source is the USB received data. The main purpose is to check the headers of the received buffer and identify which task should be performed: start or stop stimulation, measure impedance, save impedance value and get data from host, as described in Figure 58.

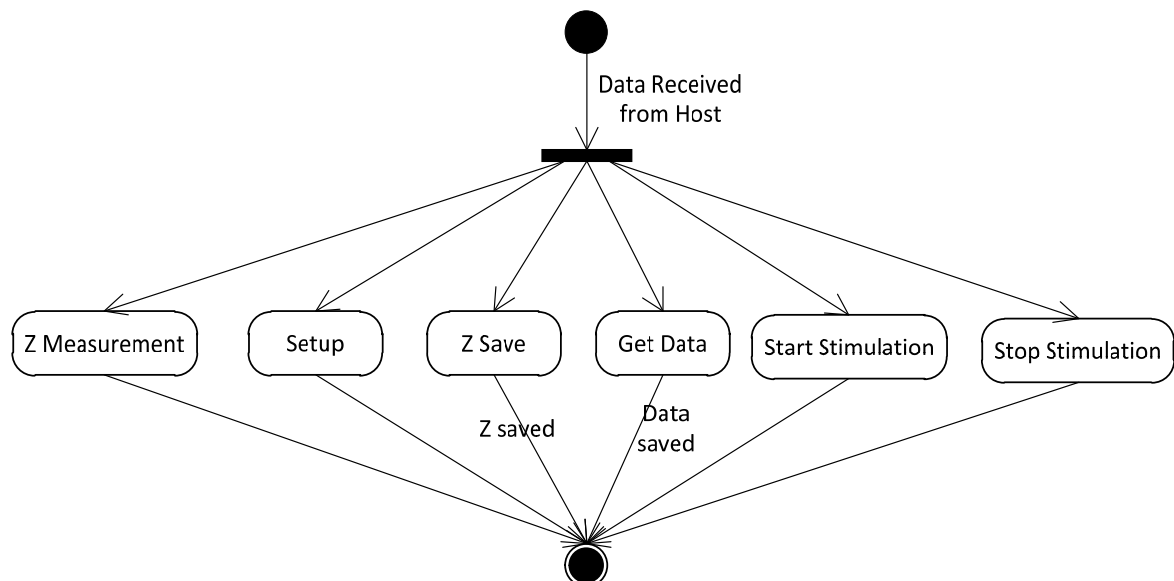


**Figure 58 – USB Received Data interrupt handler state diagram**

If the system receives a start or stop command from the host, both timers 0 and 1 are started or stopped respectively. The impedance measurement command performs an impedance measurement task and sends the results back to the host.

A setup command configures some hardware parameters such as voltage divisor and current shunt resistor values used for data acquisition. Moreover the sampling period of the ADC channels are also configured. These values are already initialized with the default values and are only changed if the user decides to change it, being not mandatory.

The get data command means that a new stimulation signal was sent from the host, and the “get data from host state” is performed as already described. In this case, after receiving the data a flag is set to assert to the main loop that new data was received. Similar occurs when a save impedance value command is received. After saving the last impedance value read as the skin impedance value, a flag is also set. These flags are used to identify if the PGA gains need to be adjusted, as described on the first state chart of the system.

It is important here to say that for safety reasons the electrodes should be disconnected from the impedance measurement connector before the stimulation begins. That is necessary because the high voltages produced during the stimulation could damage the AD5933 integrated circuit. To avoid that, a safety key was connected to an IO pin of the microcontroller and its status is always verified before the stimulation or an impedance measurement begins. If the safety pin is set, the impedance measurement can be performed. If the user attempts to start the stimulation without switching the key, the microcontroller will not allow it and will send a warning back to the host. The idea is to help the user to remember to disconnect the electrodes from the impedance measurement input before the stimulation begins, hence protecting the system.

#### 3.7.2.11 Communication Protocol

This topic describes the communication protocol implemented in order to exchange data between the microcontroller and the user interface in the host. This was done based on headers and command bytes to validate and identify the

received data.

Every buffer to be transmitted receives first a header byte that is used to identify it as the beginning of a new buffer. There are two different headers. One identifying the buffer with the skin voltage and current signals sampled during the stimulation (H\_SIGNAL\_HEADER) and another header for all the other data (H\_DATA\_HEADER).

As already described in the previous topics, after the signal header, the signal buffer contains samples of the skin voltage and current level. Figure 59 shows the signal buffer with header. Each data field corresponds to two bytes (High and Low) of the 16-bits skin voltage and current samples.

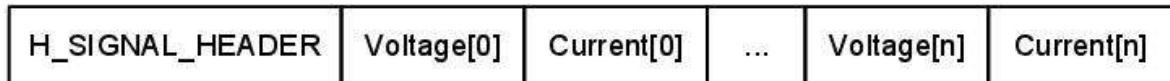


**Figure 59 – Signal buffer with the samples of the skin signals**

On the other hand, the data buffers have a command byte in addition to the header byte, which identifies the content of the buffer and which task should be executed, as shown in Table 14.

For data buffers, the data field is not mandatory. Some of them consist only of the header and command bytes, such as: stop/start stimulation, save impedance, safety pin set/not set. This is enough to indicate tasks to be executed which do not require any parameter.

The get impedance, get data from host, setup, PGA gain, impedance and impedance vector commands are followed by a data field. The structures of these buffers are shown in Figure 60.

The “get impedance” data field contains the parameters for configuring the AD5933 properly before the impedance measurement. They are the initial frequency, the increment frequency and number of increments to be used. Each field corresponds to two bytes (High and Low) of a 16-bit value.

In the “get data from host” data field, the first field is the number of samples that are being sent from the host (one period of the stimulation pulse). After that, there are the amplitude of the signal and the time this amplitude is going to be hold on the output, as already described in the previous topics. Each field also consists of two

bytes (High and Low).

**Table 14 – Headers and commands of the communication protocol**

| Header Bytes    |       |  |
|-----------------|-------|--|
| Name            | Value | Function                                     |
| H_DATA_HEADER   | 0xAA  | Identifies the beginning of a data buffer.   |
| H_SIGNAL_HEADER | 0xBB  | Identifies the beginning of a signal buffer. |

| Commands from the host to the microcontroller |       |   |
|---|-------|---|
| Name  | Value | Function  |
| C_SETUP                                       | 0x31  | Setup new data acquisition parameters.  |
| C_STOP_STIMULATION                            | 0x33  | Stop the timers that control the stimulation.   |
| C_START_STIMULATION                           | 0x35  | Start the timers that control the stimulation.  |
| C_DATA_FROM_HOST                              | 0x37  | Identifies the buffer with the stimulation signal to be generated received from the host. |
| C_GET_IMPEDANCE                               | 0x39  | Starts an impedance measurement.  |
| C_SAVE_IMPEDANCE                              | 0x3B  | Saves the last measured impedance value.  |

| Commands from the microcontroller to the host |       |  |
|---|-------|--|
| Name  | Value | Function   |
| C_SAFETY_PIN_SET                              | 0x3D  | Informs the host that the safety pin is not set.                                   |
| C_SAFETY_PIN_NOT_SET                          | 0x3F  | Informs the host that the safety pin is set.                                       |
| C_IMPEDANCE                                   | 0x41  | Identifies the buffer with the result of a single point impedance measurement.     |
| C_IMPEDANCE_VECTOR                            | 0x43  | Identifies the buffer with the results of a frequency sweep impedance measurement. |
| C_PGA_GAIN                                    | 0x45  | Send the gain of the PGAs to the host  |

The “impedance” and “impedance vector” data buffers are similar. The first field is a two byte value (High and Low) indicating the number bytes being sent. After that each field is a 24-bit (3 bytes) value that corresponds to each frequency point of the measurement. In the case of a single frequency point measurement (C\_IMPEDANCE), there is just one value. If it is a sweep frequency measurement (C\_IMPEDANCE\_VECTOR) there are as many values as specified by the user in the number of increments field of the get impedance buffer.

The “setup” buffer contains two bytes for each parameter to be configured. The voltage divisor in V/V (min. 60) and shunt resistor in ohms (max. 550 V/A) correspond to the hardware used to sample the skin voltage and current. The last two

two-byte fields correspond to the sampling period of the ADC channels in  $\mu\text{s}$  (typical 20  $\mu\text{s}$ ) and the impedance ratio between the measured value with the AD5933 and the real value.

The “pga gain” buffer contains two bytes representing the PGA1 and PGA2 gain respectively.

| HEADER        | COMMAND              | DATA              |                     |                  |                 |                |          |
|---------------|----------------------|-------------------|---------------------|------------------|-----------------|----------------|----------|
| H_DATA_HEADER | C_GET_IMPEDANCE      | Initial Frequency | Increment Frequency | Increment Number |                 |                |          |
| H_DATA_HEADER | C_DATA_FROM_HOST     | Number of Samples | Amplitude [0]       | Time [0]         | ...             | Amplitude [n]  | Time [n] |
| H_DATA_HEADER | C_IMPEDANCE_VECTOR   | Number of Points  | Impedance [f1]      | impedance [f2]   | ...             | Impedance [fn] |          |
| H_DATA_HEADER | C_IMPEDANCE          | Number of Points  | Impedance           |                  |                 |                |          |
| H_DATA_HEADER | C_SETUP              | Voltage Divisor   | Shunt Resistor      | Sampling Period  | ImpedanceFactor |                |          |
| H_DATA_HEADER | C_PGA_GAIN           | Gain PGA1         | Gain PGA2           |                  |                 |                |          |
| H_DATA_HEADER | C_STOP_STIMULATION   |                   |                     |                  |                 |                |          |
| H_DATA_HEADER | C_START_STIMULATION  |                   |                     |                  |                 |                |          |
| H_DATA_HEADER | C_SAVE_IMPEDANCE     |                   |                     |                  |                 |                |          |
| H_DATA_HEADER | C_SAFETY_PIN_NOT_SET |                   |                     |                  |                 |                |          |
| H_DATA_HEADER | C_SAFETY_PIN_SET     |                   |                     |                  |                 |                |          |

**Figure 60 – Structures of the data buffers**

### 3.7.2.12 System Sequence Diagram

Now that all the blocks of the system are designed and the communication protocol is defined, a sequence diagram is shown for better illustrating the global operation of the entire system and the interaction between all the main components (Figure 61).

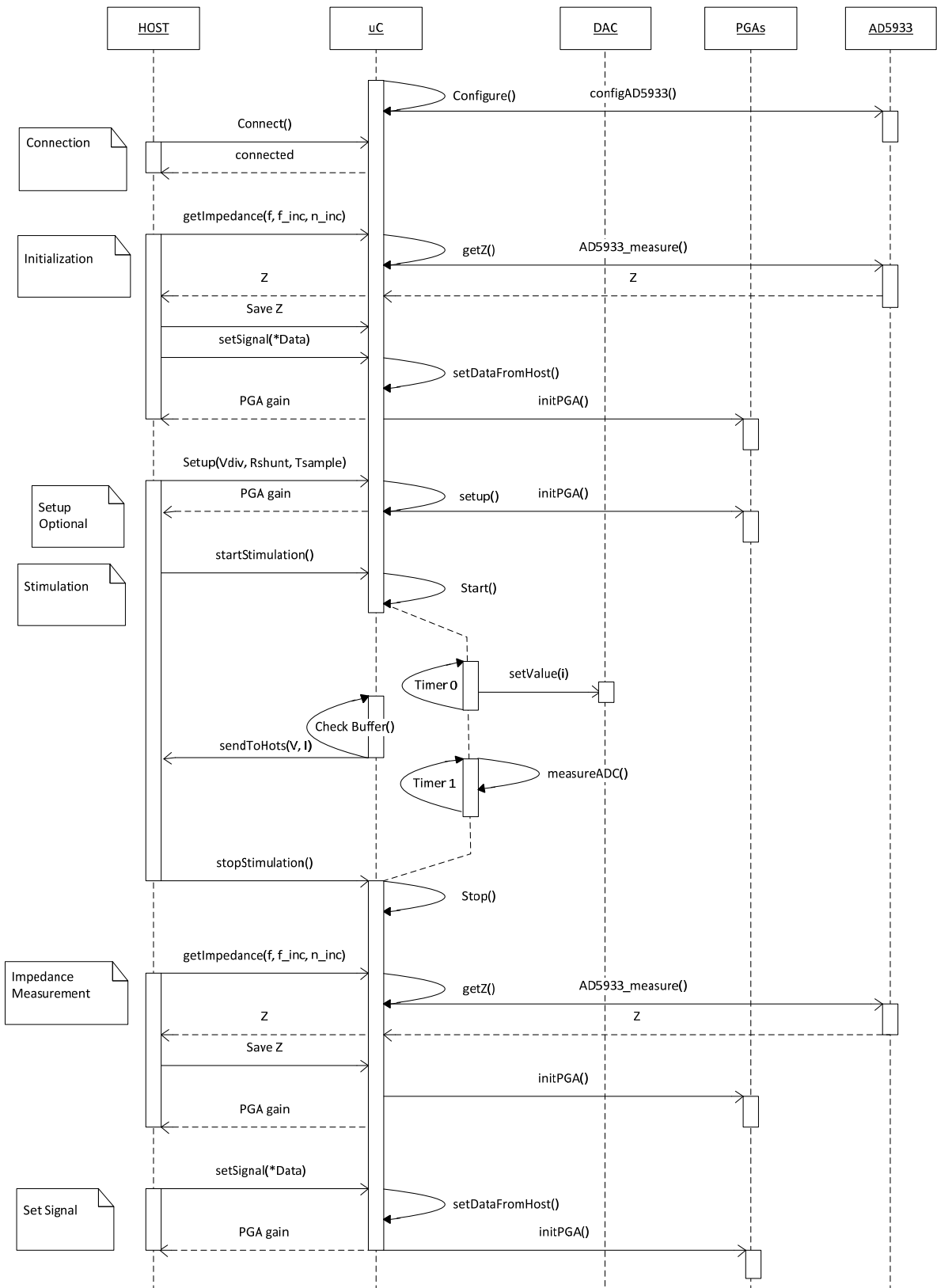


Figure 61 – Sequence diagram of the entire system



### 3.7.3 Implementation

The code was implemented in embedded C programming language, using some basic libraries for the microcontroller supplied by ATMEL. The code was then compiled with the integrated development environment from IAR Workbench for ARM and downloaded to the microcontroller's flash memory through a JTAG interface Flash loader, which was also used for debugging.

The source code was divided in six different files. The *main.c* corresponds to the main file and five other device drive files, one for each important peripheral: IOs, PGA, USB, ADC and AD5933. These files are useful to abstract the close-to-the-hardware functions to the main program. This topic describes the function and basic structure of each file.

#### 3.7.3.1 Main

The main contains the code file *main.c* and the header file *stimulation.h* and contains some basic definitions of the system such as buffer sizes, data acquisition definitions and headers of the communication protocol. Important here are the data acquisition definitions that must be adjusted according to the system architecture, such as R\_SHUNT and VOL\_DIV that represents the shunt resistor used to sample the skin current (or equivalent factor in V/A) and the voltage divider factor used to sample the skin voltage level (or equivalent factor in V/V) respectively. There is also the SAMPLE\_PERIODE, which defines in  $\mu\text{s}$  the sampling period used for reading the ADC and the IMP\_FACTOR, which defines the relationship between the real impedance and the measured with the AD5933.

```
/*----- Buffers Definitions-----*/
#define SIZE 500 // Maximum size of the receiving
#define DATABUFFERSIZE 801 // Size in bytes of the buffer to/from host

/*----- Definitions for data acquisition-----*/
#define SKIN_IMPEDANCE 10000 // Default value for skin resistance
```

```

#define IMP_FACTOR    8      // Factor for 10kHz and low frequency skin impedance
#define R_SHUNT       100    // Shunt resistor for current signal measurement
#define VOL_DIV       60     // Voltage divider factor for the skin voltage signal
#define SAMPLE_PERIODE 20    // Sample period for ADC in us
#define V_SIGNAL      ADC_CH0 // Skin voltage connected to channel 0
#define I_SIGNAL      ADC_CH1 // Skin voltage connected to channel 1
#define AD_MASK       (1<<V_SIGNAL | 1<<I_SIGNAL)
/*----- Definitions for Communication Protocol -----*/
// Headers
#define H_DATA_HEADER    0xAA // Header of data
#define H_SIGNAL_HEADER  0xBB // Header of data (signal from AD)
// Host to uC
#define C_SETUP          0x31  // Save Z
#define C_STOP_STIMULATION 0x33 // Stop sending
#define C_START_STIMULATION 0x35 // Start sending
#define C_DATA_FROM_HOST  0x37  // Data Signal
#define C_GET_IMPEDANCE    0x39  // get new Z
#define C_SAVE_IMPEDANCE   0x3B  // Save Z
//uC to Host
#define C_SAFETY_PIN_SET    0x3D  // Request data to USB
#define C_SAFETY_PIN_NOT_SET 0x3F  // Inform that safety pin is not set
#define C_IMPEDANCE         0x41  // Sending Impedance to host
#define C_IMPEDANCE_VECTOR  0x43  // Sending imp to host (sweep)
#define C_PGA_GAIN          0x45  // Sending PGA gains

```

In addition to those definitions, there are some global flags and variables such as the data buffers for storing the amplitude and time buffers received from the host as well as a flag with the number of samples in a period of the received signal. Moreover there is a buffer for receiving data from the USB interface, two transmit buffers for storing the samples data using the double buffering method and a flag to tell which buffer is being used at the time.

There are also other global variables for storing the skin impedance value, the maximum current amplitude of the stimulation pulse, the sampling period, the voltage divisor factor, the shunt resistor, the counters and flags used for controlling and monitoring the system.

```

/*-----Global Variables-----*/
// Stimulation data buffer
int amp[SIZE] ;           // Amplitude buffer
int time[SIZE] ;          //Time buffer

```

```

unsigned int periodSamples = 0;      // Size of a period

// Buffer for storing USB data.
unsigned char usbBufferRX[SIZE];      // Buffer for receiving USB data
unsigned char usbBufferTX1[DATABUFFERSIZE]; // Buffer1 for sampled data
unsigned char usbBufferTX2[DATABUFFERSIZE]; // Buffer2 for sampled data
unsigned int actualBuff = 0;          // Flag to tell which buffer is used
int impedanceValue = SKIN_IMPEDANCE; // Single point impedance (Default init)
int maxAmplitude = 0;                // Maximum current of the received signal
unsigned int sampleCounter = 0;      // Counter of samples for signal generation
unsigned int dataCounter = 1;        // Counter of the tx (header + command + data)
unsigned int dataReceived = 0;       // Flag set when data is received from host
unsigned int impSaved = 0;           // Flag 1 = Impedance Saved
unsigned int initDone = 0;           // Flag set when the initialization is done
unsigned int newSetup = 0;           // Flag set when new setup is performed

```

In the main file there are also some general purpose functions that were defined and are used during the main function or the interrupt routines, which are also here defined. Important are the timers' configuration and their interrupt handling routines, responsible for generating and sampling signals synchronously.

```

/*-----Timers interrupt and related functions -----*/
// Configure Timer Counter 0 to generate an interrupt every 'time' us.
void ConfigureTc0(int time);
// Configure Timer Counter 1 to generate an interrupt every 'time' us.
void ConfigureTc1(int time);
// Interrupt handler for TC0 interrupt - Generates the signal defined by amp(amplitude
values) and time(time between samples) vectors.
void TC0_IrqHandler(void);
// Interrupt handler for TC1 interrupt - Reads the ADC's channels to obtain the skin
voltage and current signals.
void TC1_IrqHandler(void);

// Set the value in "num" (12 bits) to the DAC pins
void setDACvalue(unsigned int num);
// Convert a digital value from ADC to skin Voltage level in 10*millivolt
short convert2Voltage( unsigned int valueToConvert );
// Convert a digital value from ADC to current level in microampere
short convert2Current( unsigned int valueToConvert );

```

Also relevant is the USB received data interrupt handling routine and their

dependent functions, which performs important tasks such as impedance measurement and saving data from the host.

```
/*-----USB interrupt and related functions-----*/
// USB received data interrupt handler routine
static void UsbDataReceived(unsigned int unused, unsigned char status, unsigned int
                           received, unsigned int remaining);
// Measure the impedance and send to host
void getImpedance(unsigned int f, unsigned int finc, unsigned int ninc);
// Saves data (amp and time vectors) from host
void setDataFromHost();
```

The last definition of the *main.c* file is the programs' main function, responsible for the configuration, initialization control and the main loop execution.

```
int main(void);      // Main function: application entry point
```

### 3.7.3.2 IOs

This file contains the definitions used to assign all the IO pins used by the system. It defines the base address, pin number, function and output/input features of each IO. Furthermore three functions were implemented to clear, set and get the status of a general purpose IO pin.

```
void clearPin(AT91S_PIO *IOaddr, unsigned int pinMask);
void setPin(AT91S_PIO *IOaddr, unsigned int pinMask);
unsigned int getPin(AT91S_PIO *IOaddr, unsigned int pinMask);
```

### 3.7.3.3 PGA

In this file two global variables that represent the gain of each PGA of the analog board are defined.

```
unsigned int gainPGA1 = 0;
unsigned int gainPGA2 = 0;
```

In addition, two functions were written to control the PGAs. The first was used to set the PGA gain, which means to receive a gain and set the corresponding IO pins that control it. The second function performs the initialization of both PGA gains based on the maximal amplitude of the stimulation current signal received from the host, on the saved measured skin impedance value and on hardware parameters of voltage divisor and shunt resistor.

```
void setPGAgain(unsigned int gain, unsigned int pga);
void initiatePGAs(unsigned int maxCurrent, unsigned int impedance, unsigned int
volDiv, unsigned int shunt );
```

### 3.7.3.4 USB

This file defines the states of the USB state machine used for monitoring the USB connection. Moreover there are the functions that control the connection as well as the data exchange.

```
#define STATE_IDLE      0    // Use for power management
#define STATE_SUSPEND   4    // The USB device is in suspend state
#define STATE_RESUME    5    // The USB device is in resume state
// State of USB, for suspend and resume
unsigned char USBState;
void ISR_Vbus(const Pin *pPin);
void VBus_Configure( void );
void LowPowerMode(void);
void NormalPowerMode(void);
void USBDCallbacks_Resume(void);
void USBDCallbacks_Suspended(void);
```

```
void USB_configure();
```

### 3.7.3.5 ADC

In this file there are some definitions useful for controlling the analog-to-digital converter. One global variable is necessary in this file. It is a vector of size NUM\_CHAN (number of the ADC channels used) representing the number of the channels being used (from 0 to 7).

Furthermore two functions are used to abstract the ADC to the main program. The first is used to configure the AD, enabling and configuring the clock, setting startup and sample-and-hold time, among others. The second function is used to get the converted data available in a specific channel.

```
#define NUM_CHAN    2    // Number of used channels
unsigned int chns[NUM_CHAN];
void configureADC12 ();    // ADC Functions
unsigned int  ADC12_GetConvertedData(AT91S_ADC12B *pAdc, unsigned int
channel);
```

### 3.7.3.6 AD5933

This file contains some functions used to abstract the AD5933 to the main program. It includes the two wire interface (TWI) driver configuration, system initialization, functions for reading from and writing to the AD5933 registers among others.

```
void AD5933_configTWI();    // Configure the TWI driver
unsigned char AD5933_readRegister(unsigned char regAddr); // Read the register
unsigned char AD5933_getStatus(); // Get the actual status from the CI
int AD5933_getRealData();    // Read the real part of the measured impedance
int AD5933_getImagData();    // Read the imaginary part of the impedance
```

```

void AD5933_init(unsigned int startFreq, unsigned int freqIncrement, unsigned int
                numIncrement);    // AD5933 Initialization
void AD5933_setMode(unsigned int mode); // Put the AD5933 in a specified mode
int AD5933_measure_sweep(unsigned char* impedance); // Performs a freq sweep

```

### 3.8 HUMAN MACHINE INTERFACE (HMI)

In order to make it easier to control the system, a human machine interface was developed. Though this software the user can configure some parameters as well as see the measurements' results. The software was programmed in C++ using the Borland Builder 5 and can be described in five different states, as shown in Figure 62. For each state a different window was created with a specific user interface. The changing states commands shown on the diagram are generated by button clicks.

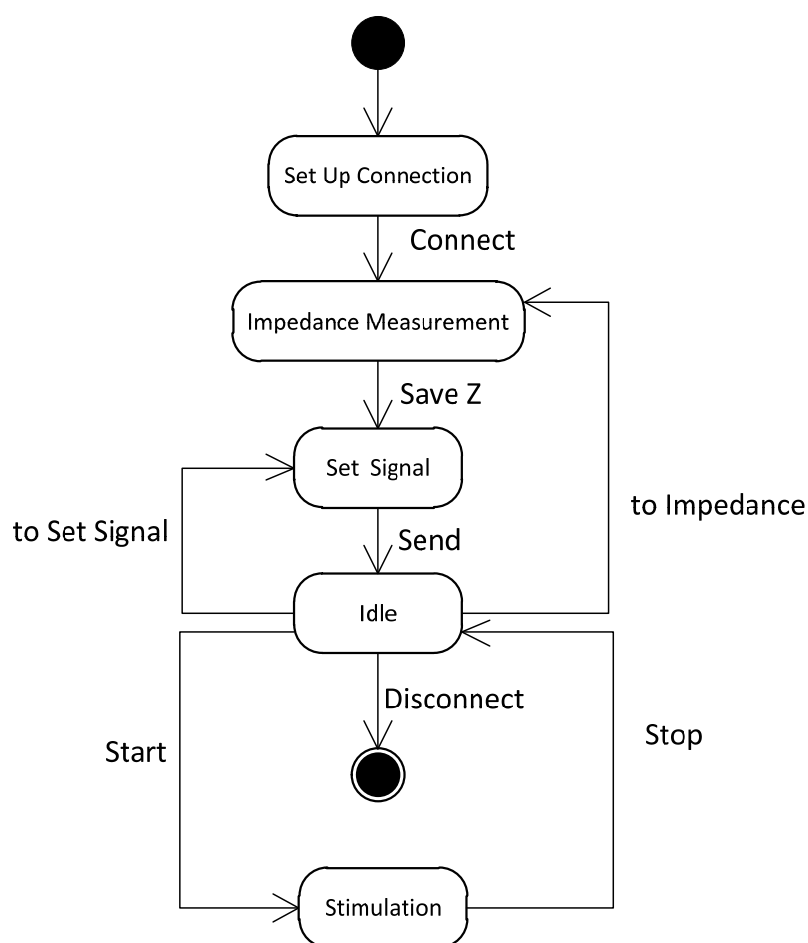


**Figure 62 – State chart of the HMI**

At first it is necessary to setup the connection between host and microcontroller. On the host side, it means initializing and connecting to the virtual serial port opened by the microcontroller and listening to it. After the connection, it is possible to perform measurements of the skin impedance. In this state the user can pass parameters to the controller and request as many measurements as desired until he/she decides to tell the microcontroller to save the last read value as the skin impedance. After this step the user should set the stimulation signal and send it to the microcontroller. The software enters now the idle state and waits for a command. Whenever the user decides to measure the impedance or set a new signal it goes back to the respective state. Moreover the user can send a start command to the controller in order to start the stimulation process. In this state the system keeps receiving the measured signals from the microcontroller and processing this data. During the stimulation a stop command can be sent to suspend the stimulation, going back to idle state. At last, if the user decides to disconnect, the connection is terminated and the software can then be restated from the beginning.

The next topics show the interface of each state and a brief description of their operation.

### 3.8.1 Setup Connection

The first window when loading the program is the main menu, as shown in Figure 63. At first only two of the buttons are enabled, forcing the user to setup the connection to host before any other process is started.

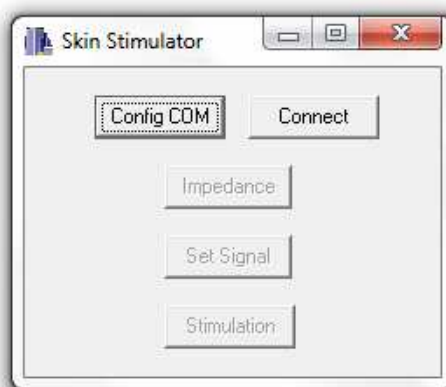


**Figure 63 – Main menu of the skin stimulator HMI**



By clicking on the “Config COM” button, the connection setup window opens and the user can configure and open the connection at the virtual port created by the driver of the microcontroller. The settings include Port name, Baud rate, number of data, stop and parity bits and flow control, as shown in Figure 64. Important here is only the port name since it is a virtual port over the USB protocol.

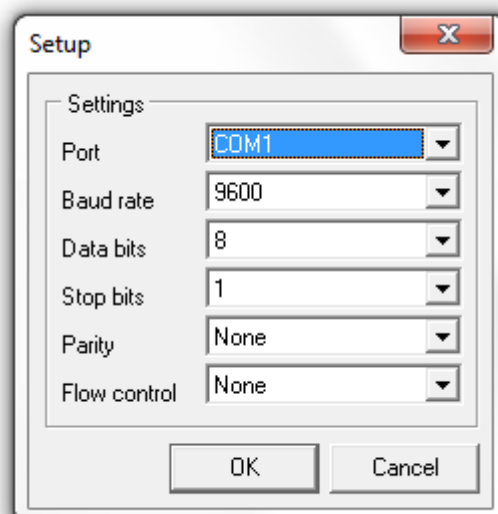


**Figure 64 – Setup connection window.**

After the setup, the button “Connect” can be clicked connecting the host to the configured port and starting listening to it. The “Impedance” button is then enabled, allowing the user to start carrying out impedance measurements. The “Connect” button turns to “Disconnect” and closes the connection to the microcontroller when clicked on. Figure 65 shows the main menu after a successful connection.

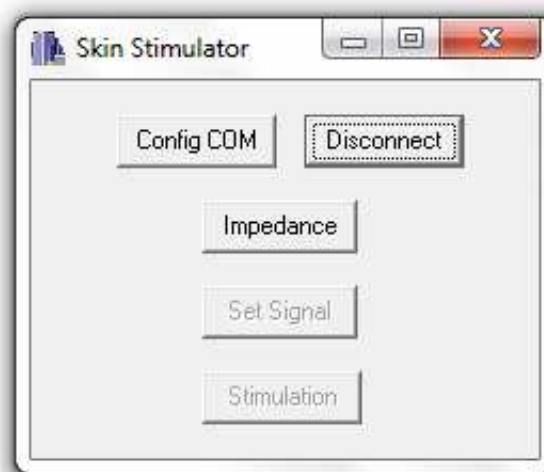


**Figure 65 – Main menu after connecting to the microcontroller.**

### 3.8.2 Impedance Measurement

When clicking on the “Impedance” button a new window is opened to control the skin impedance measurement (Figure 66). There are two possibilities for this task: single frequency or sweep frequency measurement. In the first case the user specifies the frequency in Hz of the stimulating signal. After clicking on “Get Impedance”, the software sends a C\_GET\_IMPEDANCE command to the controller as described in the previous topic (communication protocol) and waits for the response. The microcontroller in turn performs the measurement and sends the result back to the host with a C\_IMPEDANCE command header. By receiving this command the software shows the result in ohms to the user.

It is important to reinforce that, before starting the impedance measurement, the microcontroller checks the safety pin status to ensure it is set. In case it is not set, the microcontroller sends a C\_SAFETY\_PIN\_NOT\_SET command and the software alerts the user about this problem.

Figure 66 shows an example of the Impedance Measurement interface after a single 10 kHz measurement of a 10k $\Omega$  resistor.

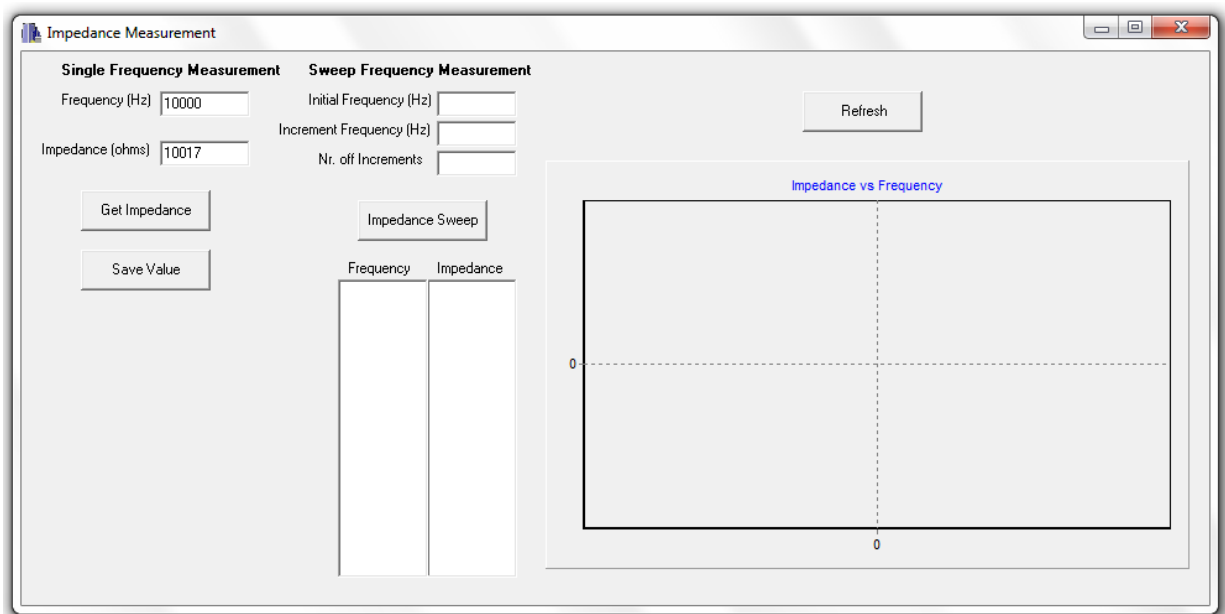


**Figure 66 – Single frequency impedance measurement.**

The second option is the frequency sweep. In this case the user needs to enter the initial frequency, the increment frequency and the number of increments of the measurement. After clicking on the “Impedance Sweep” button the system sends the data with a `C_GET_IMPEDANCE` command to the controller and waits. The microcontroller sends then the results with a `C_IMPEDANCE_VECTOR` command back to the host, which in turn fills the lists and shows the results to the user in a graphic of impedance vs. frequency.

Figure 67 shows the interface after a sweep impedance measurement with: 10kHz start frequency, 1kHz increment frequency and 10 increments for a 10k $\Omega$  resistor.

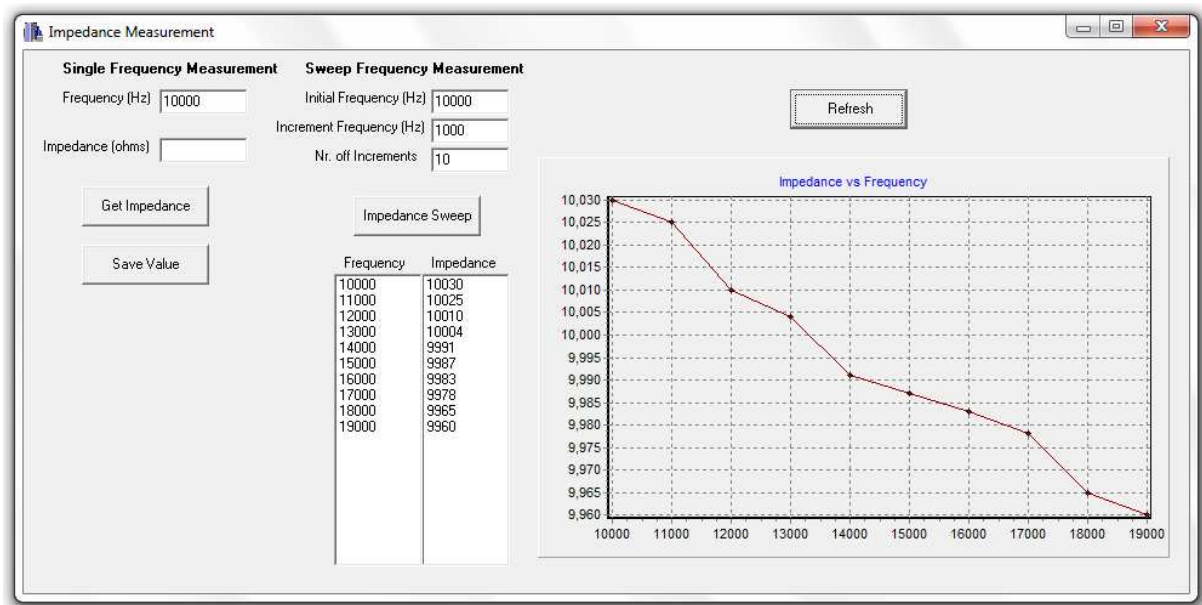


**Figure 67 – Interface after a sweep frequency measurement.**

It is important to highlight that the user can make as many measurements as one wants before one decides to save it. Hence when clicking on the “Save Value” button, the host sends a `C_SAVE_IMPEDANCE` command to the microcontroller, which in turn saves the last single frequency impedance value as the real skin impedance. This parameter is important for defining the PGA gains during the stimulation, as already explained before.

### 3.8.3 Set signal

After saving the impedance, the “Set Signal” button on the main menu is enabled. By clicking on this button, the set signal window is opened and the user can enter the data needed to generate the stimulation pulse.

As shown in Figure 68, the user has the possibility to enter point by point the amplitude of the current pulse in  $\mu\text{A}$  as well as the time this value should be hold in  $\mu\text{s}$ .

For simplifying purposes, it is also possible to load a square wave or the proposed QT-Signal pattern (similar to the signal shown in Figure 3) only by configuring some basic parameters such as frequency, peak amplitude and time parameters.

For the pulsed square wave, the time parameter  $T(\mu\text{s})$  represents the low and high time of the pulse. For the QT-signal, the parameter  $T1(\mu\text{s})$  and  $T2(\mu\text{s})$  represent the low time and the rising time respectively. The positive peak amplitude of this signal was set constant to  $100\mu\text{A}$  and the rising and falling time are  $100\mu\text{s}$ . The high time is then automatically calculated so that the positive area is the same as the negative to balance the injected charge. In these two signals the minimal hold time was set to  $25\mu\text{s}$  (40kHz).

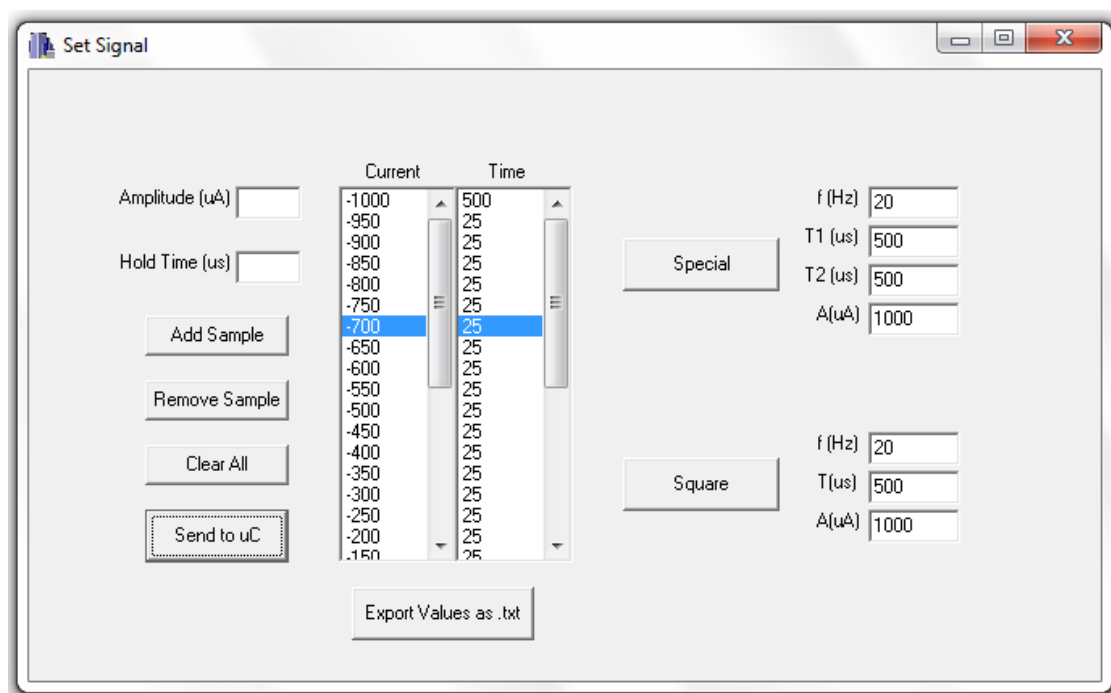


Figure 68 – Set signal window with the QT-Signal signal loaded.

After entering all the values the button “Send to uC” should be clicked on. This event makes the host to send the buffer with the signal data with the command C\_DATA\_FROM\_HOST to the microcontroller.

### 3.8.4 Idle

After sending the data, the “Stimulation” button on the main menu is enabled and the software enters the idle state. At this moment the microcontroller is initialized and ready to start the stimulation. However at any time during this state new impedance measurements can be performed or new signal shapes can be loaded to the controller. At any time the connection can be closed restarting the system from the beginning.

Figure 69 shows the main menu window during the idle state.

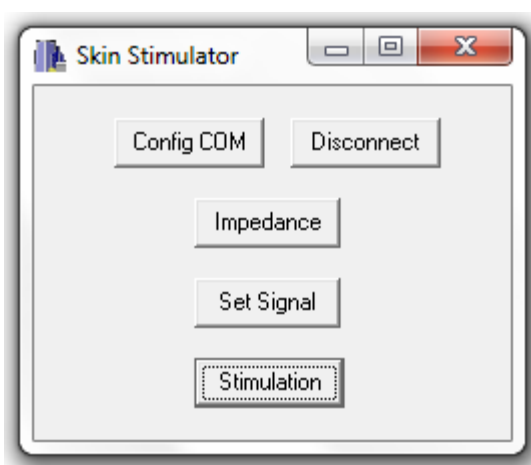


**Figure 69 – Main menu after during the idle state.**

### 3.8.5 Stimulation

By clicking on the “Stimulation” button the system opens the stimulation window. Here the user can send the C\_START or C\_STOP commands to the controller in order to start or stop the stimulation.

At this point the microcontroller checks again the status of the safety pin to see

if it is not set before starting the stimulation. In case it is set, the host receives a C\_SAFETY\_PIN\_SET command and alerts the user about the problem.

When the stimulation begins, the microcontroller starts sending the acquired signals to the host with the H\_SIGNAL\_HEADER header. During this state the host keeps reading these buffers and showing the data to the user. It also calculates the real time skin impedance with the received data.

Another option here is the setup of hardware parameters. This step is not mandatory, since they are initialized with default values if no external change is made. However the user has the possibility to set the voltage divisor factor, the shunt resistor value, the sampling period as well as a correction factor between the measured impedance (with the AD5933) and the real value obtained from the current and voltage signals.

Figures 70 and 71 show the stimulation window during a setup configuration and a stimulation process respectively. By clicking on the Start/Stop button the stimulation can be started or stopped. The maximal absolute voltage and current amplitude within each period cycle and the skin impedance value are also shown. In addition the signals are drawn on a picture box showing the measured signals similar to a digital oscilloscope.

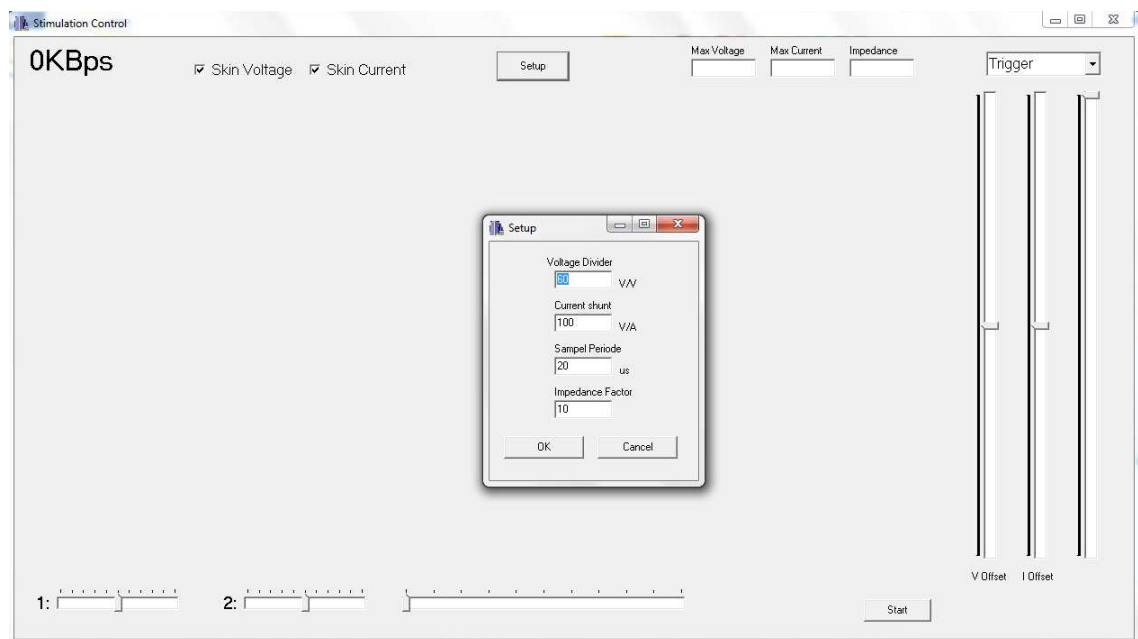


**Figure 70 – Stimulation window for stimulation control**

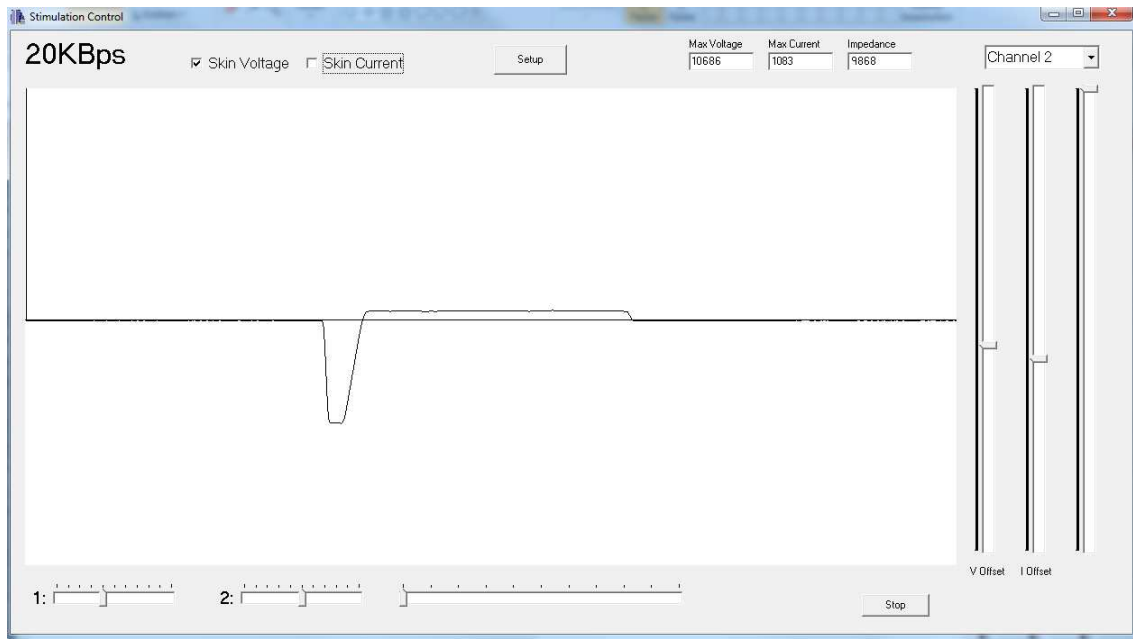


**Figure 71 – Example of the stimulation window during a stimulation process.**

## CHAPTER 4

### SYSTEM INTEGRATION AND VALIDATION

This chapter presents how the several blocks that were separately explained in Chapter 3 were integrated into a unique system. Furthermore it shows some tests that were carried out to validate the system. These tests were important to verify the functionality of the project.

#### 4.1 HARDWARE INTEGRATION

After the schematics design and the board layout the PCB was sent to manufacturing and afterwards the electronic components could be soldered on it. The following topics explain the connections and operation of the developed prototype and its interface with external systems such as PC, external current sources and measurement devices.

##### 4.1.1 The external source

The external current source used to verify the operation of the system was a Digitmer DS5 (Isolated Bipolar Constant Current Stimulator) developed for the field of clinical nerve excitability tests. It consists of a configurable voltage controlled current source used to stimulate the human skin and nerves. It was preferred to use this equipment instead of the self designed current source because of its features that guarantee patient safety. Among other features, one may list: high voltage and current blocking circuits, isolated output and energy balance control, meeting all the requirements of the Medical device Directive (MDD) by implementing the EN 60601 standard.

Figure 73 shows a picture of the Digitmer DS5 and Figure 72 shows its front panel.





Figure 72 – Front panel of the Digitimer DS5



Figure 73 – Picture of the DS5 used on the experiments

The operating principle is quite simple. The current output follows the voltage signal at the input according to the programmed gain. It was chosen for a unitary gain (1A/V), as already described in the previous chapter, although this feature can be configured for other values. The input connection was made through a coaxial cable from the analog board and the output was connected directly to the human skin using a pair of Ag/AgCl electrodes as shown in Figure 74.

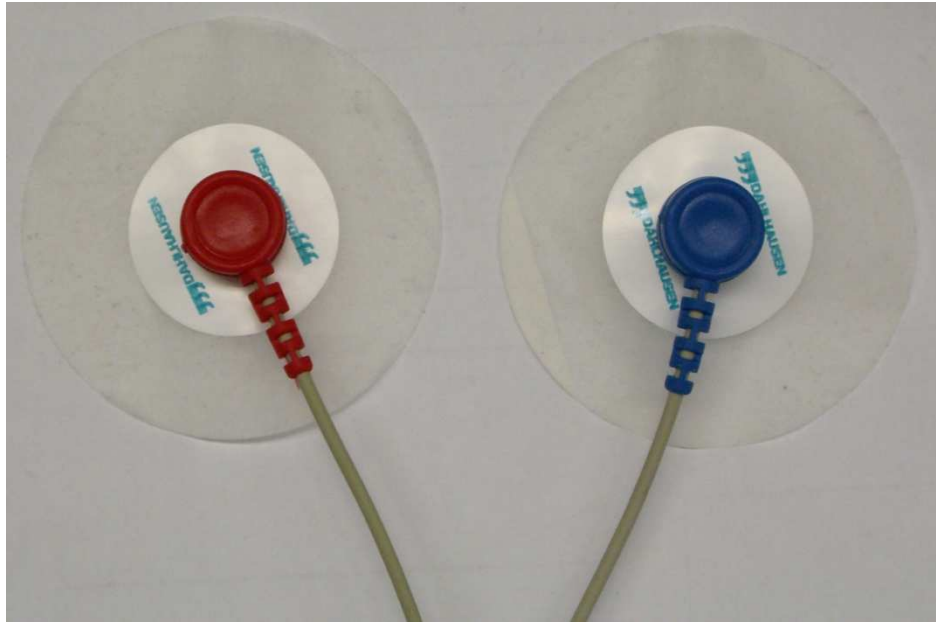


Figure 74 – Ag/AgCl electrodes used on the experiments

Another important feature of the DS5 is the availability of external connectors for measuring the output voltage and current signals generated on the load during the stimulation. These signals are available as voltage output through two BNC connectors in a gain of 50mV/V (output voltage) and 100V/A (output current) respectively, as shown in Figure 75. As already explained in the previous chapter, these signals could be obtained using a voltage divisor and shunt resistor respectively. However in the DS5 they are already available with no need of external hardware.



Figure 75 – Back view of the Digitimer DS5

### 4.1.2 Prototype

The developed prototype consists of the analog and digital boards connected with a dedicated connector. In addition it is connected to the host PC via USB, which was used not only to the data communication but also as power supply.

The analog board output was connected with a coaxial cable to the DS5 input and the two inputs for voltage and current signals were also connected to the respectively outputs of the external source.

The following figures show pictures of the boards and their connections. Figure 76 shows a picture of the digital board, Figure 77 shows the analog board and Figure 78 shows the prototype with the connection between digital and analog board, USB connection and coaxial cable for the external current source.

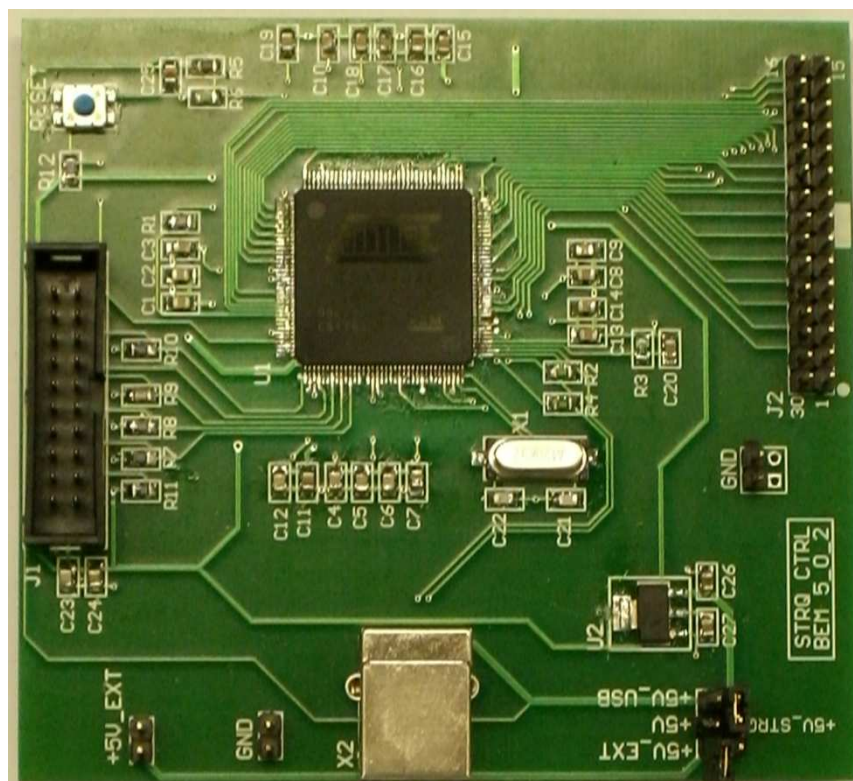


Figure 76 – Digital board



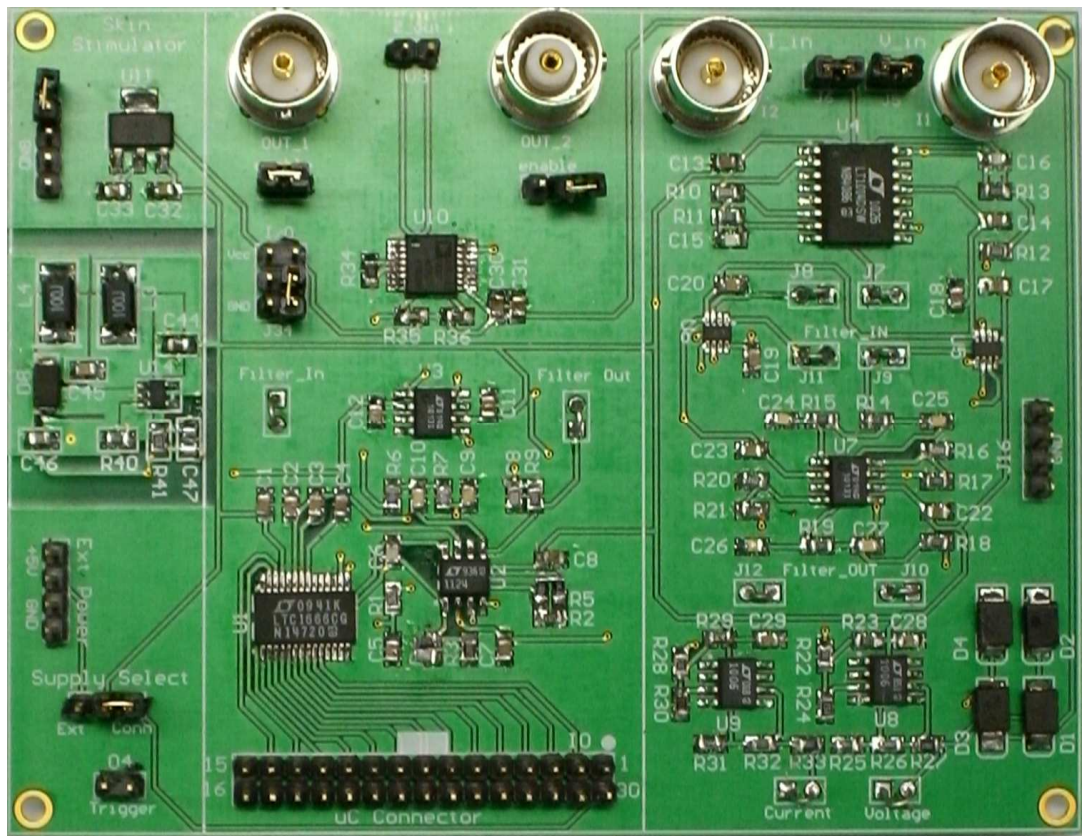


Figure 77 – Analog board

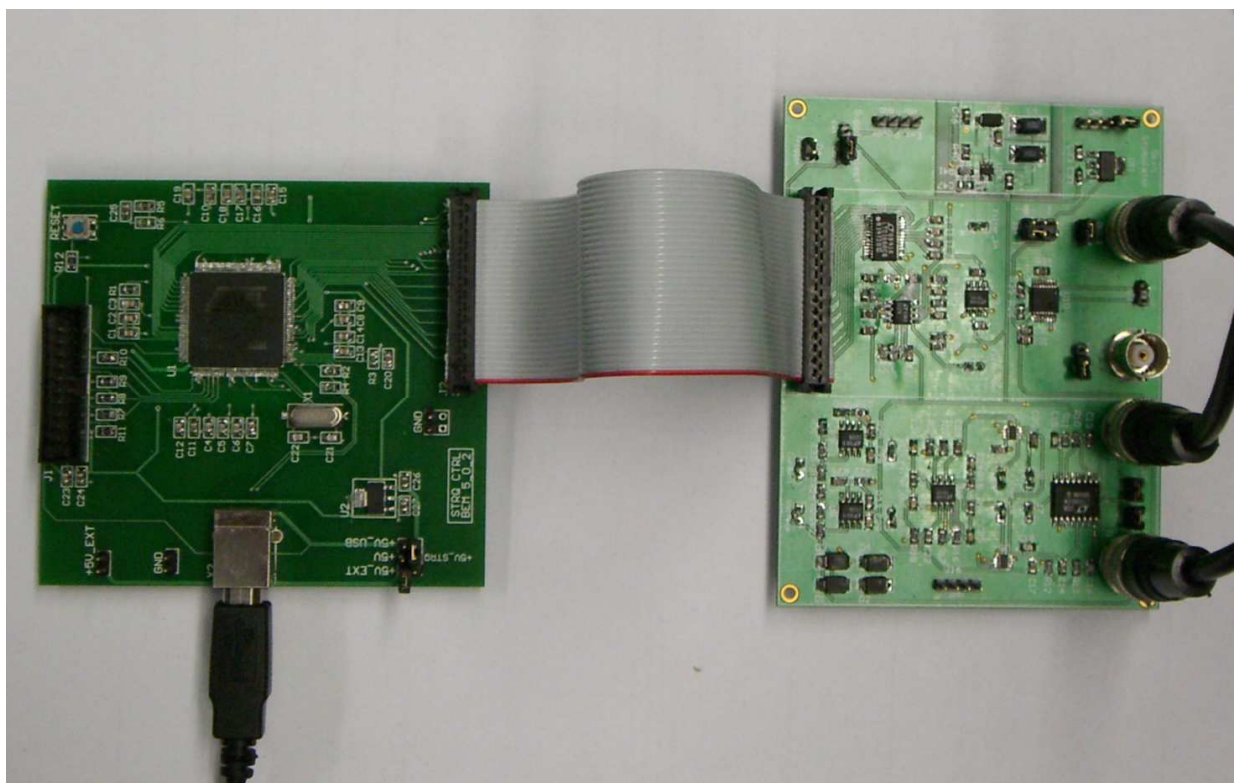


Figure 78 – Digital board, analog board and connections

The 50mV/V gain for the output voltage available on the DS5 corresponds to a factor 20 of attenuation, which is lower as the factor 60 needed to properly conditioning the signal in the analog board and sampling with the microcontroller's ADC. Therefore a change in the hardware of the analog board's voltage measurement circuit was needed. The gain of the pre-amplifier was changed from 1 to 1/3 by changing the feedback resistor of 820 $\Omega$  to 270 $\Omega$ . This modification leads to factor 60 skin voltage signal attenuation, as desired in the design.

Regarding the current signal measurement, the 100VA gain of the DS5 corresponds exactly to a 100 $\Omega$  shunt resistor as proposed in the hardware design and hence no hardware change was needed.

## 4.2 SYSTEM VALIDATION

The system validation was done by testing the entire integrated system as a final solution and comparing the results and performance with those expected on the requirements definition step.

### 4.2.1 Impedance Measurement

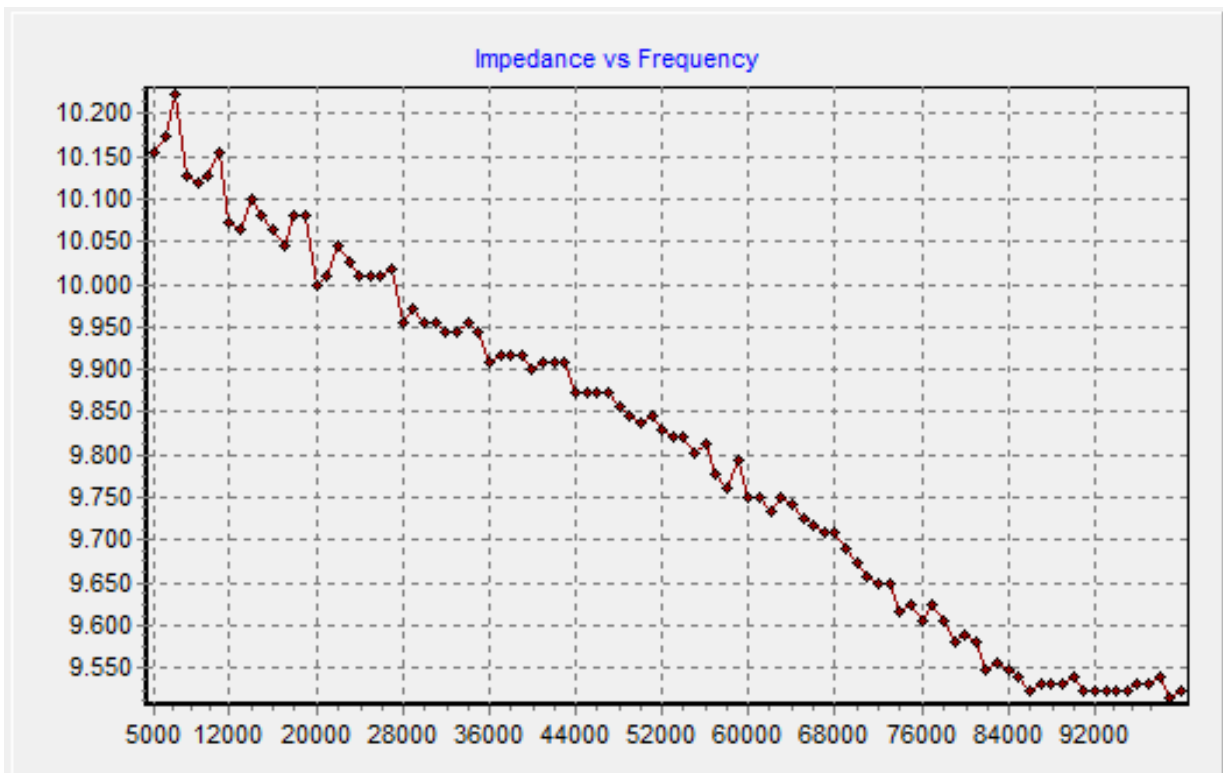
In order to validate the impedance measurement two tests were carried out. At first three different probe resistors (10k $\Omega$ , 50k $\Omega$  and 100k $\Omega$ ) were measured with a single frequency of 10kHz. Afterwards the 10k $\Omega$  resistor was measured with a sweep from 5kHz to 100kHz, with 1kHz increment. The measured values were then compared with the real value obtained with a standard multimeter.

The results for the single frequency measurement are shown in Table 15.

**Table 15 – Impedance measurement for a 10kHz single frequency point measurement.**

|                         | Resistance ( $\Omega$ ) |        |         |
|-------------------------|-------------------------|--------|---------|
| Real value (multimeter) | 10k                     | 56k    | 100k    |
| Measured value (AD5933) | 10.128k                 | 55k    | 90.163k |
| Error                   | 1.28%                   | -1.78% | -9.8%   |

The graphic presented in Figure 79 shows the results of the sweep frequency experiment for the 10k ohm resistor.

**Figure 79 – Impedance measurement of a 10K resistor from 5KHz to 100KHz.**

The results show that the AD5933 can be used to measure impedance values with a limited precision. In addition it can only be used in a restricted frequency range: theoretically from 1KHz to 100KHz. However the results showed that for higher frequencies the error increased strongly. Moreover as the system must be calibrated with a known resistor before measuring, impedances much far from the calibration value can also make the measurement error higher.

The second test was carried out with the human skin as load. It is known that the impedance varies a lot with the frequency, as already described in the theoretical foundations. Furthermore the AD5933 uses a sinusoidal voltage signal with

frequencies higher than 1kHz to perform the measurement, which is different than the low-frequency pulsed current signal used in the stimulation experiments.

Therefore the idea of this test was to find out the relationship between the skin impedance measured with the AD5933 for a single frequency and its impedance for a typical low frequency pulsed stimulation signal. This result was important to calibrate the system since the skin impedance measured with the AD5933 is used to configure some parameters of the system such as the PGA gains.

The following graphic shown in Figure 80 shows the behavior of the skin impedance for a frequency sweep from 5kHz to 100kHz, with 1kHz increment.

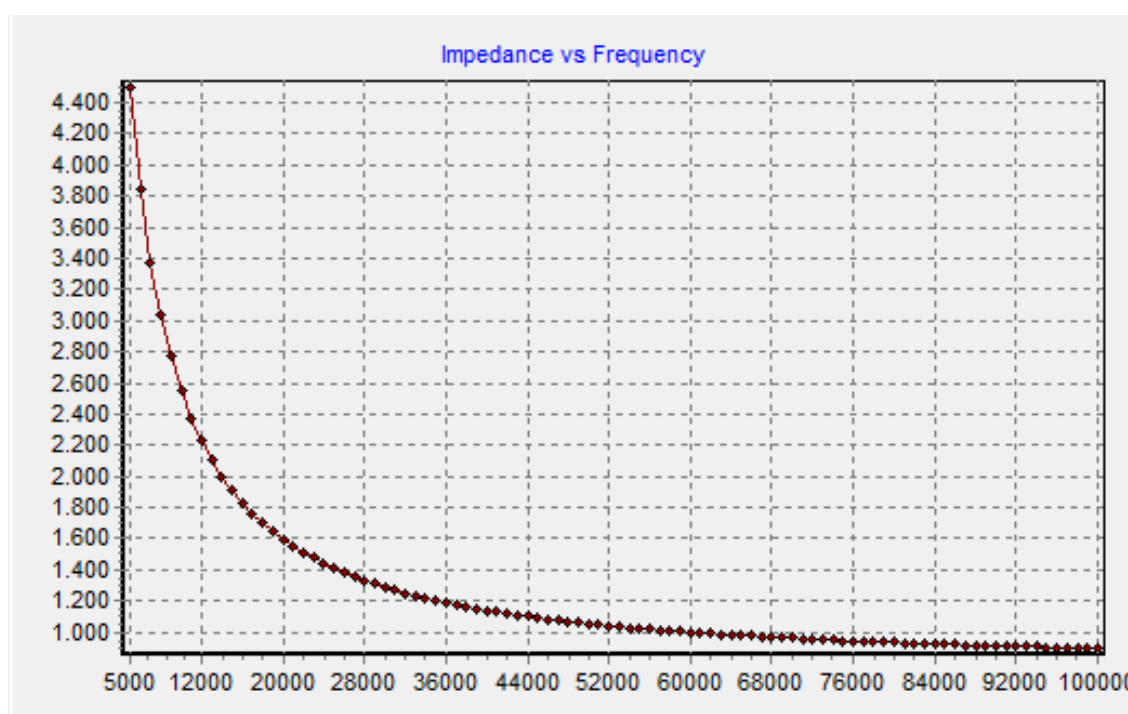


**Figure 80 – Forearm front skin impedance measurement (5KHz to 100KHz)**

It is clear to see that the skin impedance decays exponentially with the frequency. However the real value doesn't agree with the measured one. As a result the AD5933 should be used just to get an overall idea of the skin impedance magnitude (not precise) and the real value should be corrected with a correction factor.

For calibrating the system, a frequency of 10kHz was used when measuring with the AD50933. The real value for the stimulation pulse was then obtained by analyzing the skin voltage and current signals during the stimulation and calculating the absolute impedance.

The measurements were done using the standard electrodes, signal frequencies and amplitudes in the anterior forearm, where all the other tests were carried out.

**Table 16 – Skin impedance measurement for a 10kHz single frequency point measurement.**

|                         | Resistance ( $\Omega$ ) |
|-------------------------|-------------------------|
| Measured value (AD5933) | 2350                    |
| Real value (V/I)        | 40000                   |
| Ratio: Real/ Measured   | 17                      |

With these tests it was found that the measured absolute impedance value for a 10kHz sinusoidal signal corresponds to a fraction of the skin impedance for the 2-200Hz pulsed signal used in the stimulation, usually between 1/20 (5%) and 1/8 (12,5%). Therefore the impedance measured with the AD5933 should be multiplied by this factor before being used as a skin impedance value.

It is important to observe that this ratio can be different for other parts of the human body, methods and frequencies among other factors and therefore must be calibrated according to the test conditions.

#### 4.2.2 Signal Generation

To validate the signal generation block three signals were entered through the HMI and sent to the microcontroller. The waves at the DAC driver output and after the reconstruction filter at the system output were measured with the oscilloscope. The results are shown below in details.

##### 4.2.2.1 Symmetrical square wave

Designed signal was a symmetrical 1kHz, 1Vpp square wave. Figure 81 shows the output before and after the filter.



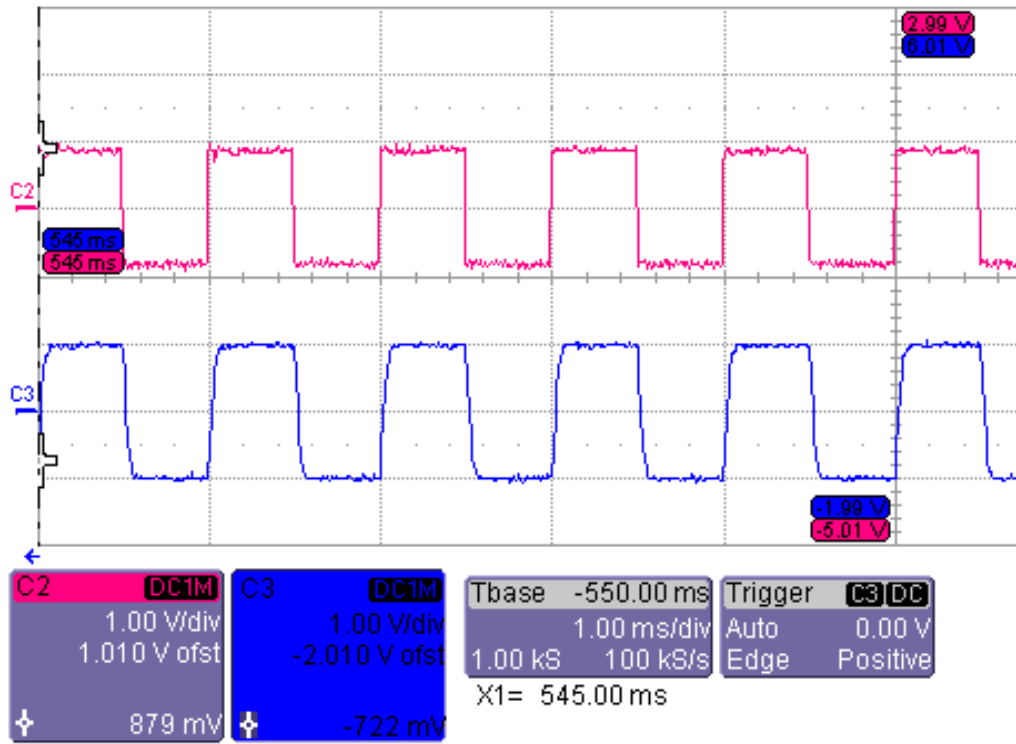


Figure 81 – 1KHz square wave before (red) and after (blue) the filter.

Figure 82 makes a comparison between the signals before and after the filter.

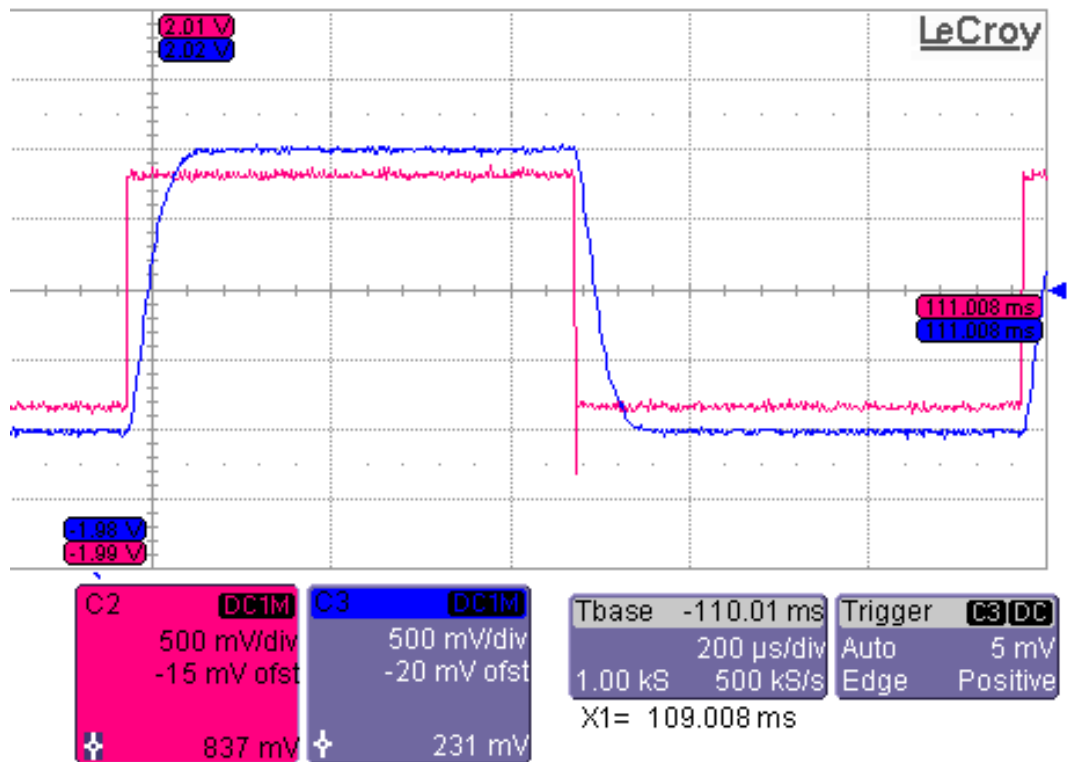


Figure 82 – Square wave in details.

#### 4.2.2.2 Pulsed square wave

Designed signal was a 20Hz, 1Vpp pulsed square wave with 750 $\mu$ s low and high time. Figure 83 shows one period of the signal before and after the filter.

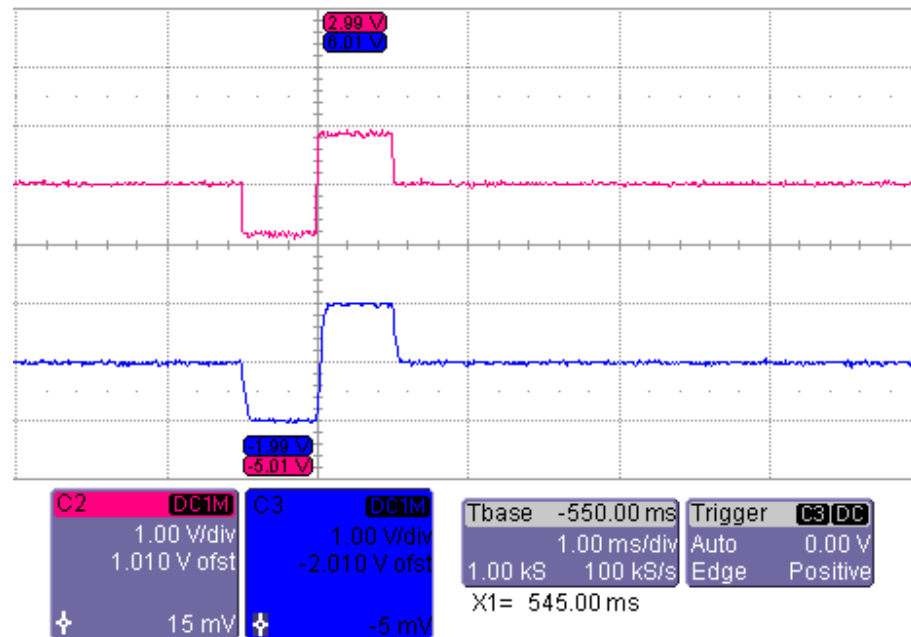


Figure 83 – Pulsed square wave before (red) and after (blue) the filter.

Figure 84 shows a comparison between the signals before and after the filter.

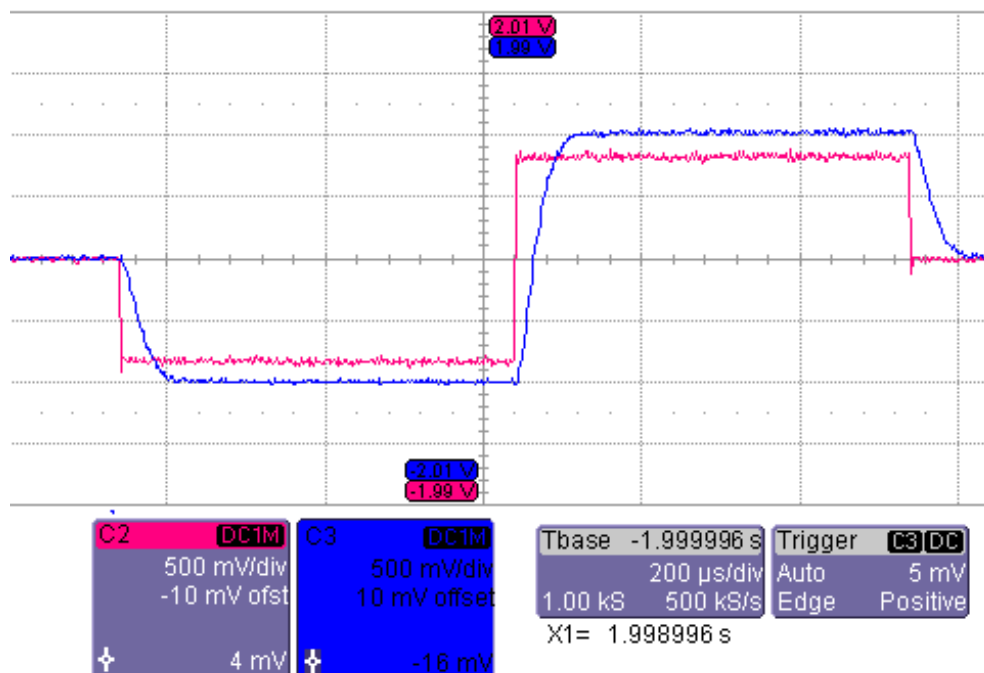


Figure 84 – Pulsed square wave in details.

Figure 85 shows the signals in a higher scale proving the 20Hz frequency.

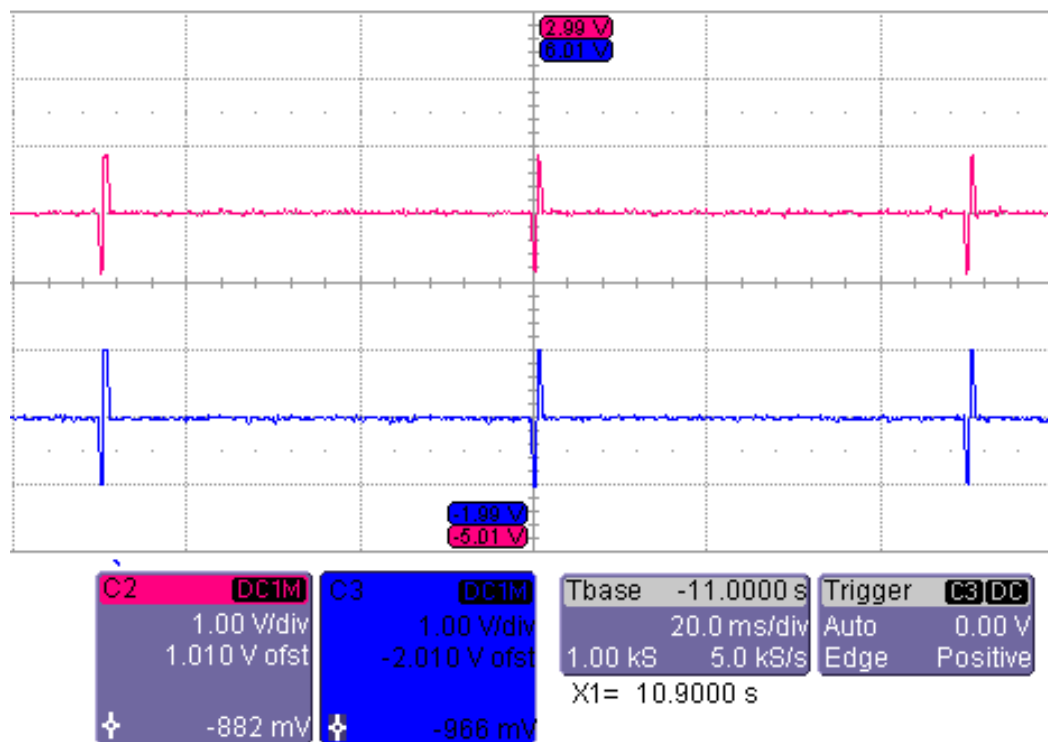


Figure 85 – 20 Hz pulsed square wave.

#### 4.2.2.3 Special QT-Signal

The designed signal was a 20Hz quasi-trapezoidal pulse as already described in the previous chapters: with -1V negative peak-amplitude, 100mV positive amplitude, 500μs low time and 500μs rise time. Figure 86 shows one period of the signals before and after the filter.

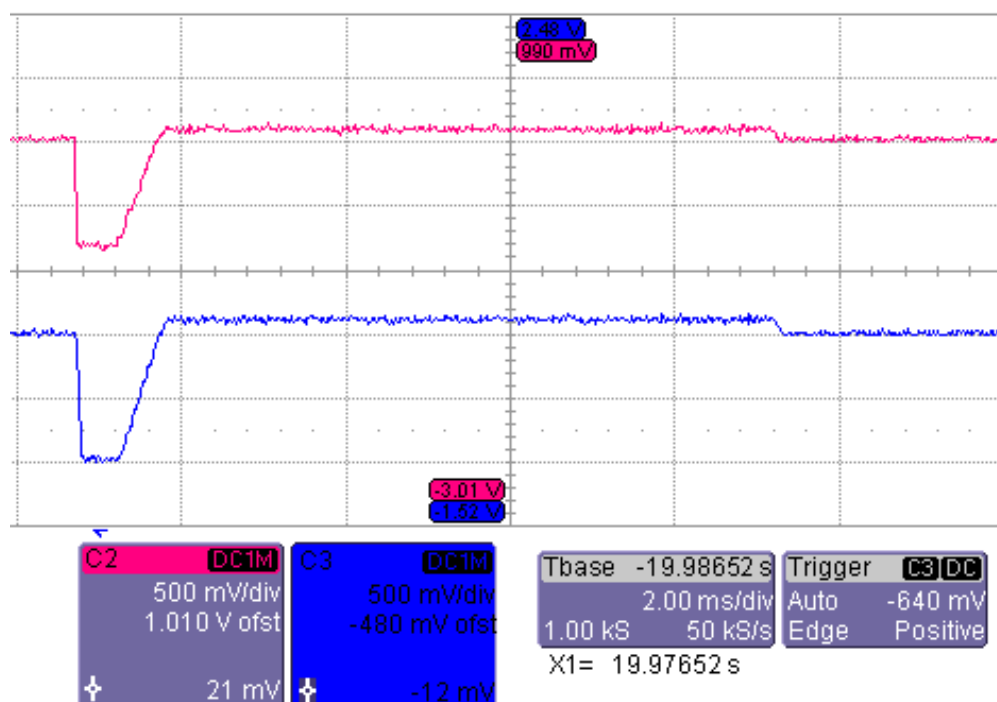


Figure 86 – QT-signal before (red) and after (blue) the filter

Figure 87 presents a comparison between the signals before and after the filter.

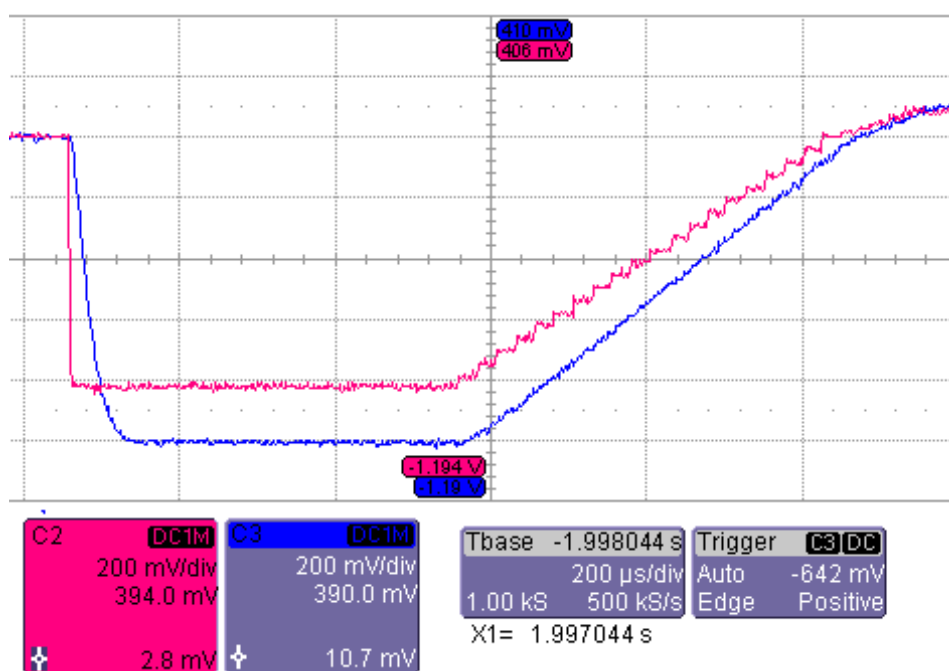


Figure 87 – QT-signal in details.

Figure 88 shows the signals in a higher scale proving the 20Hz frequency.

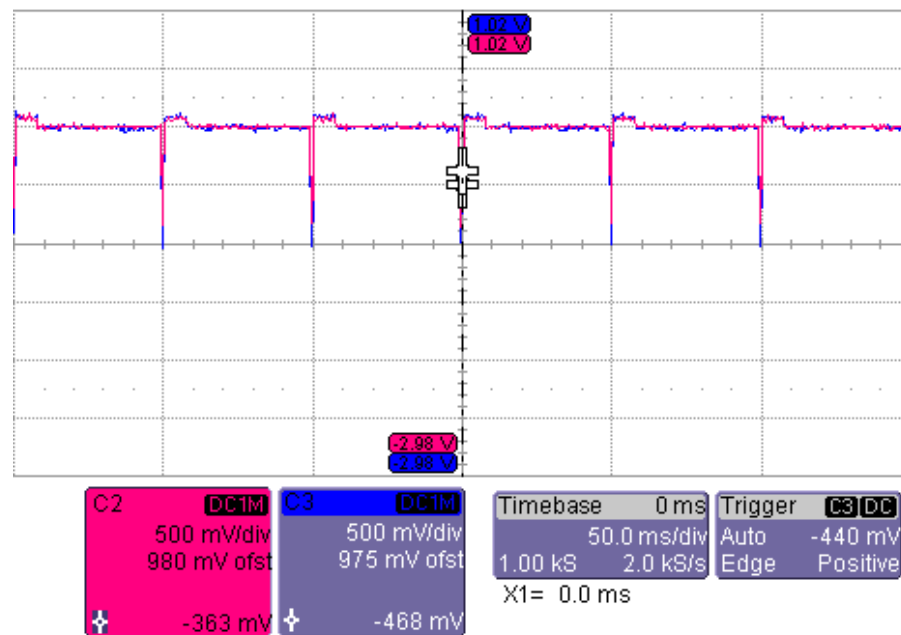


Figure 88 – 20Hz QT-signal.

The results show that the signal generation block worked as expected. It generated arbitrary signals with different shapes and amplitudes with sufficient quality and precision based on the information sent from the host computer.

The reconstruction filter's cutoff frequency can also be adjusted not to eliminate some high frequency components of the signal if necessary in order to achieve better rise/falling times.

#### 4.2.3 Signal Measurement

The signal measurement block could be validated by applying signals at the input and observing the system response.

The input signal was the stimulation current signal obtained from the DS5, which corresponds to 1V for each 10mA of current load.

On the stimulation a pulsed square wave of 1mA peak amplitude with a 10kΩ resistor as load was used. Therefore the input peak amplitude was 100mV and to the PGA gain was 8V/V.

The following items show the circuit operation in four steps: pre-amplifier and PGA, low-pass filter, offset compensation and the whole block.

a) .Pre-amplifier and PGA validation

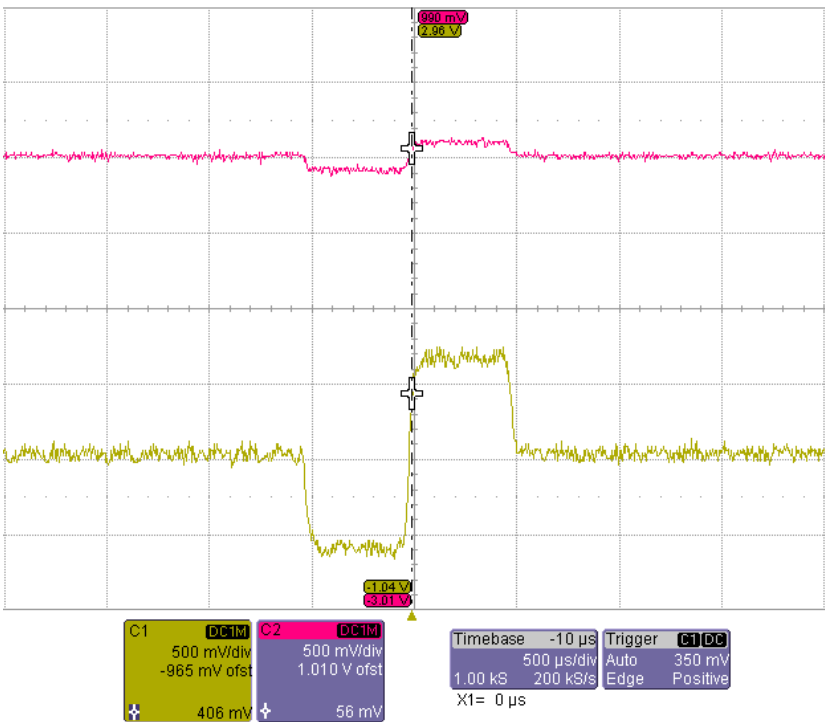


Figure 89 – Input signal (red) and after the unitary gain pre-amplifier and 8V/V gain PGA (yellow).

b) Low-Pass Filter validation

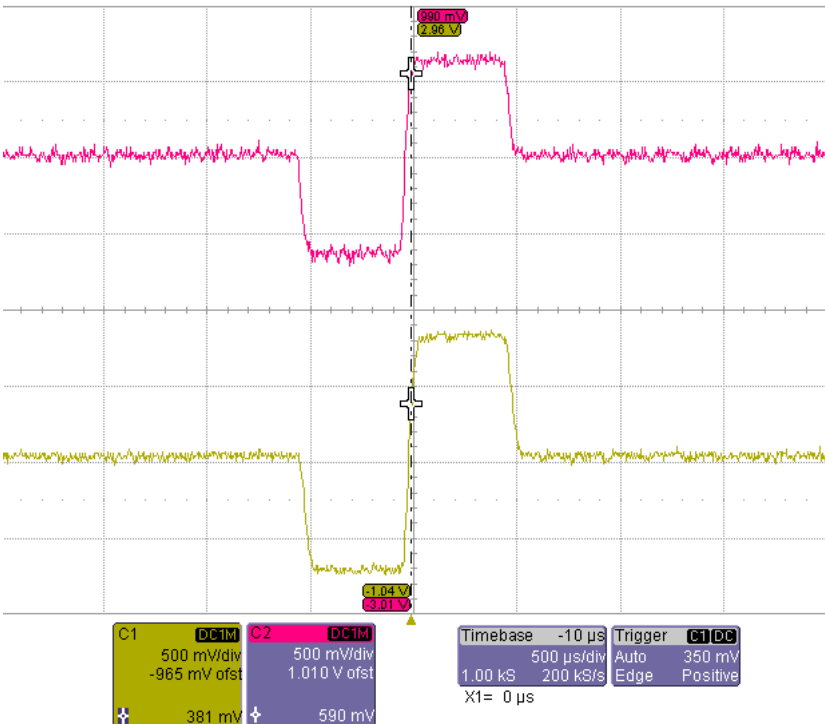


Figure 90 – Signal before (red) and after (yellow) the low-pass filter

## c) Offset compensation validation

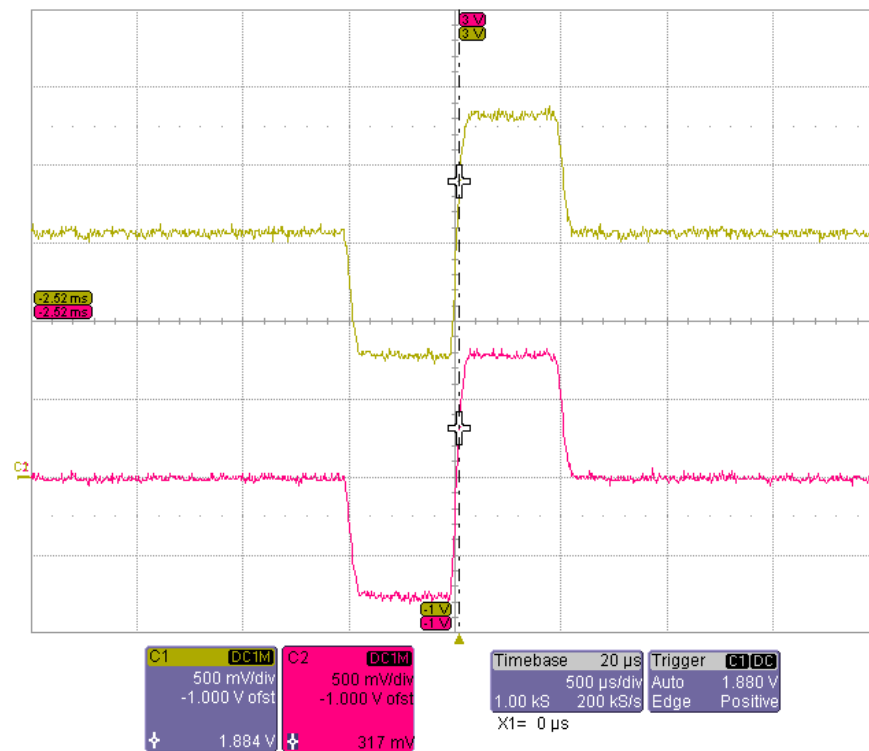


Figure 91 – Signal before the filter (red) and after the 1.65V offset compensation (yellow).

## d) Whole measurement block validation

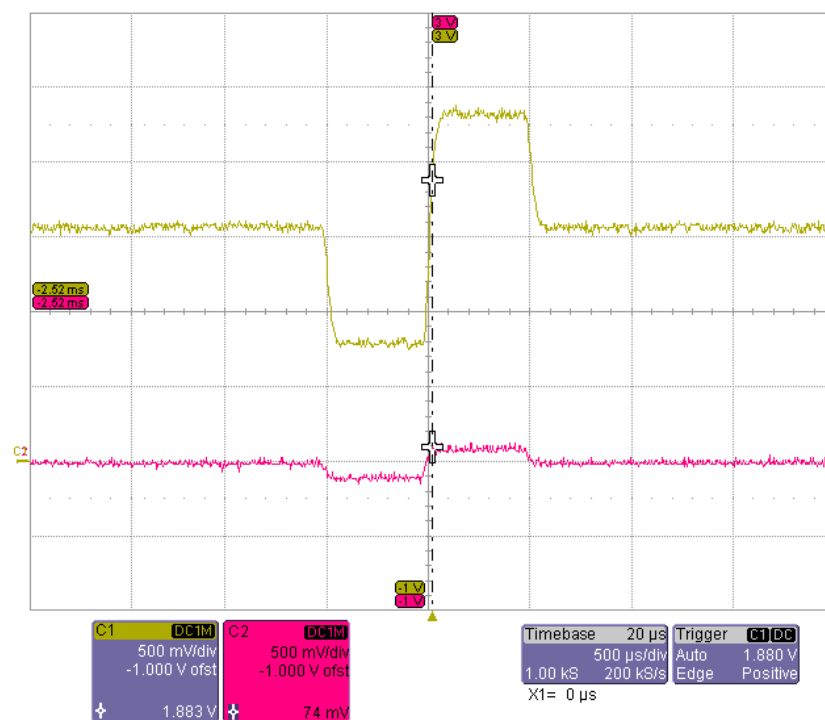
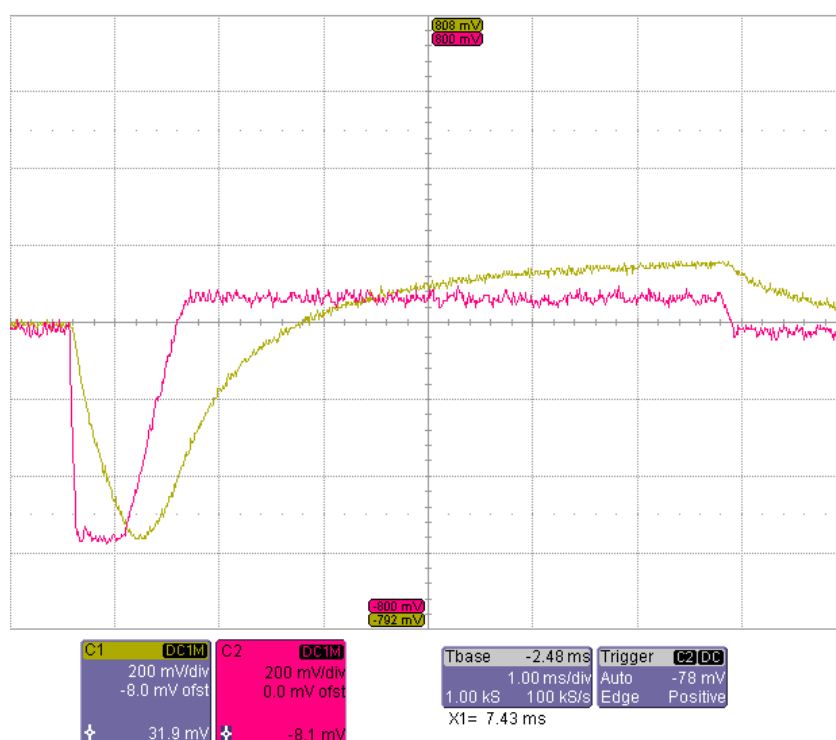


Figure 92 – Signal at the input (red) and output (yellow) of the signal measurement block

#### 4.2.4 Stimulation

The last validation was done by performing a complete stimulation process, with human skin as load. For this test the special QT-signal was used with 700 $\mu$ A peak current amplitude with 20Hz pulse period.

Figure 93 shows the skin current and voltage signals after the signal measurement block. It is possible to notice that the current signal has exactly the same shape as designed from the host computer. However the voltage signal is delayed and not as sharp as the current signal. It can be explained since the skin is not a pure resistive load but a complex capacitive model, as explained on the theoretical foundations.



**Figure 93 – Skin current (red) and voltage (yellow) signals during the stimulation process.**

During this test the skin impedance was also measured by the system, at first with the AD5933 and then online during the stimulation. The AD5933 gave as a result of the 10kHz single frequency measurement a value of 4.2k $\Omega$ . The real value obtained online during the stimulation resulted in 48k $\Omega$ . The relation between them was then 1/11.4 (8.8%). This ratio is between 1/20 (5%) and 1/8 (12,5%) as described in the item 4.2.1.



## CHAPTER 5

### TESTS AND RESULTS

After the design, development and validation the system could be used to perform some experiments. The idea was to analyze the best signal shape and amplitudes for selectively stimulating the human skin, as proposed in the objectives of this project. Simultaneously the average skin impedance was measured with help of the skin current and voltage signals acquired during the stimulation. A comparison of the impedance when applying different signal patterns was also performed. This chapter summarizes the methods and results of these tests.

Figure 93 shows a picture of the whole system being used during the tests.

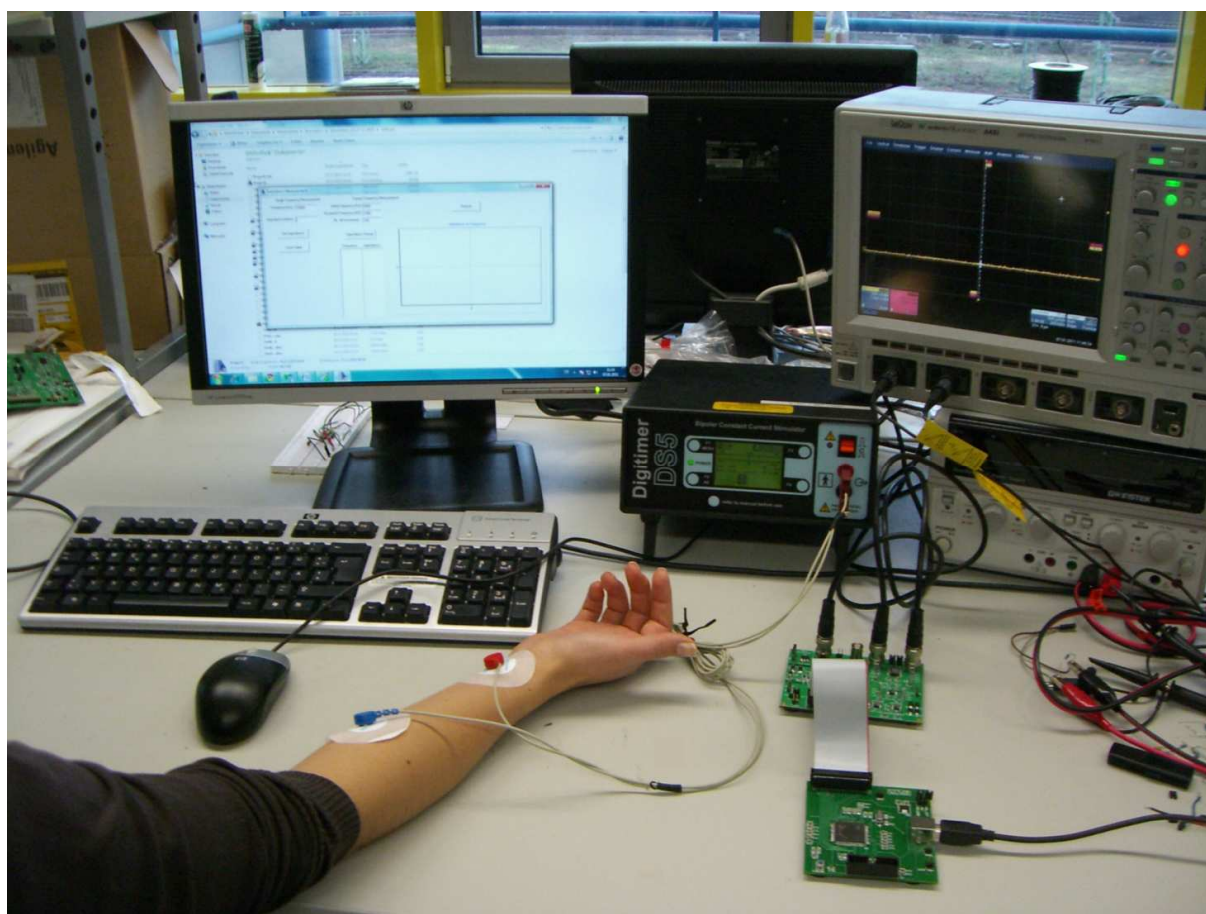


Figure 94 – Picture of the system operation during the tests

## 5.1 PAIN INTENSITY TEST

### 5.1.1 Methods

The first test consisted in stimulating the test subjects with two signals with same maximal amplitude and equal energy but with different shapes. The objective was to compare the effects of a regular pulsed square wave, mostly used in stimulation devices, with the proposed special QT-signal shape and verify if the selective stimulation of the C-Fibers could be achieved.

The feedback for the test was obtained in two ways based on the pain intensity. The subjective pain intensity was measured by asking the subject which signal was more/less painful or uncomfortable. The other was done through a high-sensitive device that measured the human body sensibility for external stimulus by measuring small variances on the skin superficial resistance. This device will be further referenced here as high-sensitivity device. If one signal shows to be more uncomfortable than the other with same desired effects it is probably because the A-delta fibers were less stimulated and the selective stimulation was achieved.

The subjects were stimulated with two 2mA peak amplitude on the inner forearm, 20Hz current pulses but different shapes and for a short time (5-10 second). The first signal was a pulsed square wave with 750 $\mu$ s on time and the second signal was the QT-signal with 500 $\mu$ s on time and 500 $\mu$ s rising time as described in topics 4.2.2.2 and 4.2.2.3 respectively.

Each pulse was applied three times with a one minute interval between them for six different people. The body reactions to the suddenly pain could then be measured with the high-sensitivity device. In a relative scale it could be seen the change between the still stand and the first reaction after the pulse injection. The short time was needed because after a while the body gets used to the new stimulus and the device can't register this feeling anymore.

### 5.1.2 Results of the Pain Intensity Test

The results are summarized in Table 17. The numbers correspond to the relative change on the high-sensitivity device's scale for the three experiments (N1, N2, N3) with six subjects. The higher the change the more uncomfortable was the pain sensation.

**Table 17 – Results of the pain intensity measurement.**

| Subject | Pulse Shape | N1  | N2  | N3  | Average |
|---------|-------------|-----|-----|-----|---------|
| 1       | Square      | 3   | 1   | 2   | 2       |
|         | QT-Signal   | 1.5 | 0.5 | 1   | 1       |
| 2       | Square      | 10  | 8   | 5   | 7.7     |
|         | QT-Signal   | 2   | 0.5 | 1   | 1.2     |
| 3       | Square      | 5   | 4   | 3   | 4       |
|         | QT-Signal   | 2   | 6   | 0.5 | 2.8     |
| 4       | Square      | 2   | 2.5 | 0.5 | 1.7     |
|         | QT-Signal   | 1   | 0.5 | 0   | 0.5     |
| 5       | Square      | 2.5 | 2.5 | 2   | 2.3     |
|         | QT-Signal   | 2   | 1.5 | 1.5 | 1.7     |
| 6       | Square      | 7.5 | 9   | 8   | 8.2     |
|         | QT-Signal   | 4   | 3   | 2   | 3       |

Afterwards the graphic shown in Figure 95 shows the average of the measurements for each of the six tested subjects. The vertical axis show the value from the sensibility measuring device and the horizontal axis presents the six measurements.

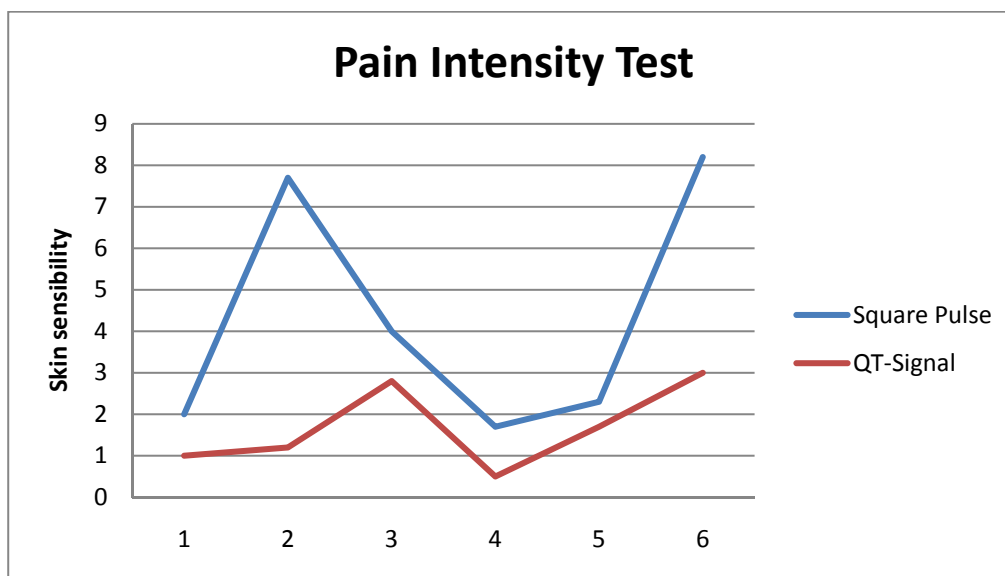


**Figure 95 – Average of the human body sensibility for the square and QT pulses**

The results show that the square pulse shape caused on the average a higher variation for all of the tested subjects. Moreover the magnitude of this variation also varies from person to person and therefore no absolute value should be used to compare the effects on different people. Concerning the subjective test, all six persons affirmed that the pulsed square wave was more uncomfortable than the special QT-signal shape.

## 5.2 IMPEDANCE VARIATION TEST

### 5.2.1 Methods

The second test was done by stimulating the subjects with the same signals used in the first experiment but for a longer time (around 2 minutes) and with 1mA peak current. Then the voltage and current signal were acquired in order to obtain the average skin impedance for each pulse shape. The idea was to compare if the skin impedance changes according to the applied signal shape.

### 5.2.2 Results of the Impedance Variation Test

For each subject the average skin impedance was calculated by dividing the skin voltage and current values during the stimulation. Furthermore the differences between the measured impedance for the two shapes were also calculated.

The results of the impedance variation test are shown in Table 18. The results indicate that the skin impedance for the QT-signal was on the average 4.7% lower than the impedance for the regular square pulse with same energy and peak-amplitude. Moreover the skin impedance value varied from 23k $\Omega$  to 50.8k $\Omega$  for different subjects, reinforcing the great variability of the human skin impedance with several factors and from person to person as described in the theoretical foundations.

**Table 18 – Results of the impedance variation test**

| Subject | Pulse Shape         | Impedance ( $\Omega$ ) | Difference ( $\Omega$ ) | Difference (%) |
|---------|---------------------|------------------------|-------------------------|----------------|
| 1       | Square<br>QT-Signal | 31.2k<br>29.8k         | 1.4k                    | 4.7            |
| 2       | Square<br>QT-Signal | 35.9k<br>33.5k         | 2.4k                    | 7.2            |
| 3       | Square<br>QT-Signal | 43.2k<br>42.4k         | 0.8k                    | 1.9            |
| 4       | Square<br>QT-Signal | 24.4k<br>23k           | 1.4k                    | 6.1            |
| 5       | Square<br>QT-Signal | 25.8k<br>24.9k         | 0.9k                    | 3.6            |
| 6       | Square<br>QT-Signal | 50.8k<br>48.3k         | 2.5k                    | 5.2            |
| Average | Square<br>QT-Signal | 35.2k<br>33.6k         | 1.6k                    | 4.7            |

Figure 96 shows the results of the skin measurement test in a graphic for each of the applied shapes. The vertical axis shows the ski impedance in k $\Omega$  for each one of the six tested subjects (horizontal axis).

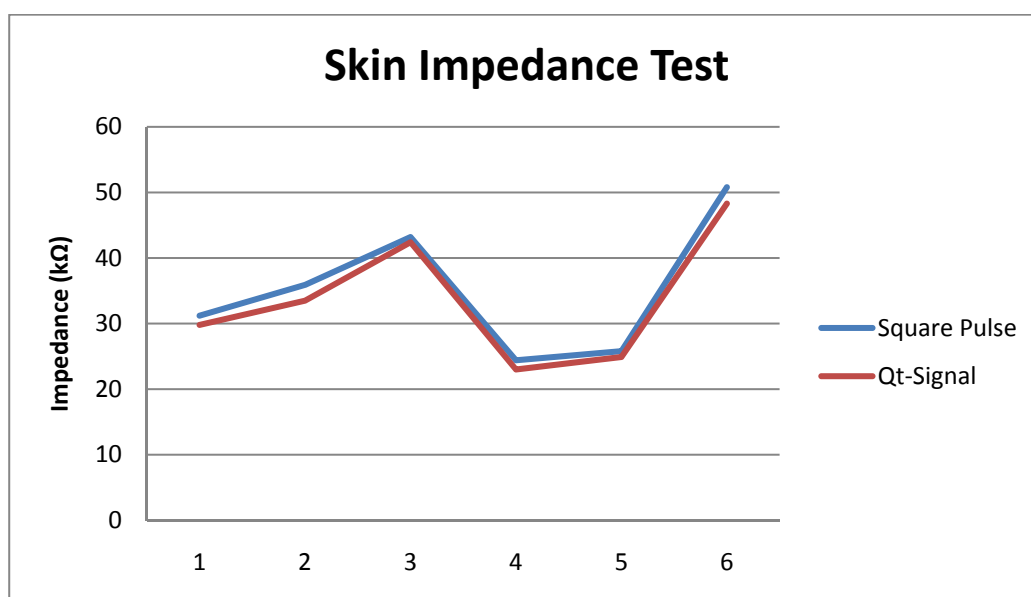


**Figure 96 – Skin impedance value measured during the stimulation.**

The differences on skin impedance between both signals were not high (1.9% to 7.2%). However for every subject the special QT-signal showed slight lower impedances than the square pulse. This result can be important to try to explain the selective stimulation and why this pattern doesn't stimulate the fast pain fibers.

### 5.3 DISCUSSION

After analyzing the experiments' results it is clear to see that the special proposed QT-signal and the regular square pulse cause different reactions on the human body.

The pain intensity test showed that the use of the quasi-trapezoidal shape makes the stimulation process more comfortable and less painful for the patient. This result indicates that the QT-signal doesn't stimulate the fast pain fibers so intensively as the square pulse. For this reason it is possible to conclude that a selective stimulation can be achieved by varying the pulse shape and that the developed system can be used as a tool for further experiments about this subject.

Furthermore the second test showed that the skin impedance tends to be a little lower when applying the QT-pulse. Although not really significant, this difference could indicate that the human skin impedance depends also on the pulse shape. In

addition this impedance difference could be related to the selective stimulation and therefore used to explain why different shapes cause different effects on the human skin.

## CHAPTER 6

### CONCLUSIONS

This document presented the development of an electronic system for controlling the selective stimulation of the human skin and simultaneously measuring the skin impedance. The system was developed to be a tool for studying the human neuronal system and the effects of the electrical stimulation on the human body. These studies have a promising future in the medicine field since the selective stimulation of the skin can be used to diagnose diseases, such as diabetes, in a fast and non invasive way.

In this context all initially proposed objectives were achieved. A microcontroller based application was developed to generate arbitrary signals based on the data received from a host computer as well as to acquire analog signals and to transmit them back to the host. Moreover an analog board was designed with electronic circuits to convert the digital stimulation pulse to analog and transmit it to an external voltage controlled current source. In addition another electronic circuit was developed to measure the skin voltage and current signals during the stimulation in order to obtain the real-time skin impedance during the stimulation. The system was later integrated in a final solution, including the design of a remote software for the host computer, which controlled all the parameters of the stimulation and impedance measurements through the USB interface.

Using the integrated system several tests could be carried out in order to compare the skin impedance and the pain intensity caused by signals with same amplitude and energy but different shapes. This comparison was made between a pulsed square wave and a proposed quasi-trapezoidal special pulse and the results showed that the pain intensity during the stimulation can be potentially minimized by changing the pulse shape while keeping the same amplitude and energy of the signal. The QT-signal showed a better response from the tested subjects than the regular square shape and a slight difference in the skin impedance was observed when applying both shapes. Although the difference was not significant, the skin impedance when applying the quasi-trapezoidal pulse was lower than when applying the square one, for all subjects. This fact could indicate that the electrical features of



the human skin are not constant and vary with the shape of the applied pulse. These results could be further investigated and may be used to better explain the selectivity properties of this shape.

## 6.1 FUTURE WORK

The most important future work within this project scope is the integration with another system being developed in the Institute of Biomedical Engineering at the Hochschule Mannheim. The new system should be able to acquire several human signals such as EEG, ECG among others, at the same time that the stimulation occurs.

Considering this integration one important step is the improvement of the signal acquisition block. Because not only the skin voltage and current but also other signals will be acquired at the same time, it is necessary to use a more powerful analog to digital converter than the 1Msps integrated in the microcontroller. One solution could be an external ADC such as the ADS1298 from Texas Instruments, which are already being used in other projects in the institute. Another important change concerns the firmware. It should be used the available feature of direct memory access (DMA) to improve the speed performance for the analog data acquisition. This feature is already being used to the USB transmission and should be extended to the ADC or SPI communication for external ADCs.

Regarding the hardware of the analog board, it is important to notice that the offset error of the LT6910 PGAs for high gain could be compensated by hardware. One option would be the use of a more expensive PGA with less output offset error such as the LT6915, also from Linear Technologies. However this integrated circuit is more expensive and more complex to control since it uses a serial interface instead of a simple parallel one, as used by the LT6910. Another option is to use an extra hardware for offset compensation, based on op amps for example.

In a longer term one possible extension of the system would be the improvement of the own voltage controlled current source, applying all the safety features necessary in a commercial medical device. This would discard the need of the external current source making the system complete, cheaper and modular.

Another topic for further study is the analysis of the complex skin impedance during the stimulation for several pulse shapes and amplitudes. This study could be used to propose an electrical model of the human skin for the pulse and to find the relation between the pain intensity and the electrical properties of the human skin.

## REFERENCES

CHRONI, E., et.al. The effect of stimulation technique on sympathetic skin responses in healthy subjects. **Clin Auton Res.** 16:396-400, 2006.

COLE, K. S. Permeability and impermeability of cell membranes for ions. Proc. Cold Spring Harbor Symp. **Quant. Biol.** 8:110-122, 1940.

GRIMNES, S. Impedance measurement of individual skin surface electrodes. **Med Biol Eng Comput.** 21:750-755, 1983.

GRIMNES, S.; MARTINSEN, O. G. Cole electrical impedance model - a critique and an alternative. **IEEE Trans. Biomed. Eng.** 52:132-135, 2005.

GRIMNES, S.; MARTINSEN, O. G. Bioimpedance and bioelectricity basics. **Oxford: Academic Press.** 2<sup>nd</sup> ed., 2008.

LOCHNER, G. P. **The voltage current characteristic of the human skin.** University of Pretoria, 2003.

MCNEAL, D. R. 2000 years of electrical stimulation. In: Functional Electrical Stimulation: Applications in Neural Protheses. 3-45, 1977.

PEASE, R. A. A comprehensive study of the howland current pump. **Application Note 1515, National Semiconductor**, 2008.

PETROFSKY, J. S.; RAMD, S.; ZIMMERMAN, G. Diabetes: sweat response and heart rate variability during electrical stimulation in controls and people with diabetes. **J App Res.** 8:48-54, 2008.

PURVES, D., et.al. Neuroscience. **Massachusetts: Sinauer Associates, Inc.** 2004.

QUATTRINI, C.; JERIOBSKA, M.; MALIK, R. A. Small fiber neuropathy in diabetes: clinical consequence and assessment. **Int J Low Extrem Wounds.** 3:16-21, 2004.  
ROSELL, J., et.al. Skin impedance from 1Hz to 1MHz. **IEEE Trans. Biomed. Eng.** 35:649-651, 1988.

SCHUETTLER, M., et.al. A voltage-controlled current source with regulated electrode bias-voltage for safe neural stimulation. **J Neurosci Methods**. 171:248-252, 2008.

SEDRA, A. S.; SMITH, K. C. Microelectronic circuits. **Oxford University Press**. 5<sup>th</sup> ed., 2004.

SEIF, C. Entwicklung zur Reizparametern zur selektiven urethralen Sphinkterblockade und simultanen Detrusorstimulation. **Urologischen Klinik**, Mannheim, 2001.

SIMPSON, R. E. Introductory electronics for scientists and engineers. **Allyn and Bacon**. 2<sup>nd</sup> ed., 1987.

TAKAGI, K., et.al. Sweating and the electric resistance of the skin. **J Neural Transm**. 24:405-412, 1962.

VAGLICA, J. J.; GILMOUR, P. How to select a microcontroller. **IEEE Spectrum**. 106-109, 1990.

VERLE, M. PIC Microcontrollers. **mikroElektronika**. 1<sup>st</sup> ed., 2008.  
Available at <<http://www.mikroe.com/eng/products/view/11/book-pic-microcontrollers>>.  
Accessed on: 3/10/2010.

WANG, W., et.al. A comprehensive study on current source circuits. **ICEBI, IFMBE Proceedings**. 17:213-216, 2007.

WHO. *World Health Organization Department of Noncommunicable Disease Surveillance*. **Definition, diagnosis and classification of diabetes mellitus and its complications**. 1999.

WILKINS, R. W.; NEWMAN, H. W.; DOUPE, J. The local sweat response to faradic stimulation. **Brain**. 61:290-297, 1938.

DIGITIMER DS5. Isolated bipolar constant current stimulator – Operator's Manual 6.0.

DATASHEET Atmel AT91 ARM Cortex-M3 based Microcontrollers – SAM3U series.

DATASHEET Linear Technologies LTC1666/LTC1667/LTC1668 DACs.

DATASHEET Linear Technologies LT1124 Dual high speed precision op amps.

DATASHEET Linear Technologies LT1001 Precision operational amplifiers.

DATASHEET Linear Technologies LT1006 Precision, single supply op amp.

DATASHEET Linear Technologies LT1113/14 Dual/Quad precision operational amplifiers.

DATASHEET Linear Technologies LTC6910 Digital controlled programmable gain amplifiers in SOT-23.

DATASHEET Linear Technologies LT1931 1.2MHz/2.2MHz Inverting DC/DC Converters.

DATASHEET Analog Devices AD5933 1MBPS, 12-Bit Impedance Converter, Network Analyzer.



Ministério da Educação  
Universidade Tecnológica Federal do Paraná  
Gerência de Ensino  
Departamento de Apoio as Atividades de Ensino  
Divisão de Biblioteca – Biblioteca de Pós-Graduação

**TERMO DE AUTORIZAÇÃO PARA PUBLICAÇÃO DE TESES E DISSERTAÇÕES ELETRÔNICAS NA BIBLIOTECA DIGITAL DA UTFPR**

Na qualidade de titular dos direitos de autor da publicação, autorizo a UTFPR disponibilizar através do site da Biblioteca Digital desta Instituição, sem ressarcimento dos direitos autorais, de acordo com a lei n. 9610/98, o texto integral da obra abaixo citada, conforme permissões assinaladas, para fins de leitura, impressão e/ou download, a título de divulgação da produção científica brasileira, a partir desta data 02/04/2009.

1. Identificação do material bibliográfico ☐ Teses ☒ Dissertação

2. Identificação da Tese ou Dissertação:

Autor: Eduardo Mussoi Esser

RG: 7.868.061-0

CPF: 053.622.669-50

Telefone: (41) 3336-6193

e-mail: eduesser@gmail.com

Programa de Pós-Graduação: Programa de Pós-Graduação em Engenharia Elétrica e Informática Industrial (CPGEI)

Orientador: Humberto Remígio Gamba

Co-orientador: Phuc Nguyen

Membros da Banca: Prof. Humberto Remígio Gamba, Dr. (Presidente - UTFPR); Prof. Albrecht Zwick, Dr. (University of Applied Sciences of Mannheim); Prof. Carlos Amaral, Dr. (UTFPR); Prof. Fábio Kurt Schneider, Dr. (UTFPR)

Data de defesa: 11/02/2011

Titulação: Mestre em Ciências

Título/subtítulo (português): Projeto e desenvolvimento de um sistema eletrônico para estimulação seletiva e medição simultânea da impedância da pele.

Título/subtítulo (inglês): Design and development of an electronic system for the selective stimulation and simultaneous measurement of the skin impedance.

Instituição de defesa: Universidade Tecnológica Federal do Paraná (UTFPR)

Afiliação (Instituição de vínculo empregatício do autor): \_\_\_\_\_

Área de conhecimento: Engenharia Biomédica

Palavras-chave: Estimulação elétrica da pele. Medição da impedância da pele. Geração e aquisição de sinais. Sistemas de diagnóstico.

3. Agência(s) de fomento: \_\_\_\_\_

4. Informações de acesso ao documento:

Liberação para publicação: ☒ Total ☐ Parcial

Em caso de publicação parcial, especifique o(s) arquivo(s) restrito(s):

Arquivo(s) Capítulo(s). Especifique: \_\_\_\_\_



Assinatura do autor

19.07.2011

Data

A restrição (parcial ou total) poderá ser mantida por até um ano a partir da data de autorização da publicação. A extensão deste prazo suscita justificativa junto à UTFPR. Todo o resumo e os metadados ficarão sempre disponibilizados.

Havendo concordância com a publicação eletrônica, torna-se imprescindível o envio do(s) arquivo(s) em formato digital PDF da tese ou dissertação.